STUDIES ON NANOMATERIALS AND A BIOMATERIAL AS CHOLESTEROL OXIDASE-IMMOBILIZATION SUPPORTS FOR DEVELOPING CHOLESTEROL BIOSENSOR

Thesis submitted by

URMILA SAXENA

For the award of the degree

of

Doctor of Philosophy

DEPARTMENT OF BIOTECHNOLOGY

INDIAN INSTITUTE OF TECHNOLOGY GUWAHATI

GUWAHATI-781039, ASSAM, INDIA

December 2011

Dedicated to my most precious possession-
My family

Department of Biotechnology

Indian Institute of Technology Guwahati

STATEMENT

I do hereby declare that the matter embodied in this thesis is the result of investigations carried out by me in the Department of Biotechnology, Indian Institute of Technology Guwahati, Guwahati, Assam, India, under the guidance of Prof. Pranab Goswami.

In keeping with the general practice of reporting scientific observations, due acknowledgements have been made wherever the work described is based on the findings of other investigators.

December, 2011 Urmila Saxena

Acknowledgments

I take this opportunity with much pleasure to express my sincere gratitude to all those who have supported me through the course of my journey towards producing this thesis. First of all, I am thankful to Indian Institute of Technology Guwahati for giving me the opportunity to carry out Ph.D. in this esteemed Institute and providing me the financial support. I am deeply indebted to my supervisor, Prof. Pranab Goswami for his enthusiastic guidance during my Ph.D. from its conception to its completion and most importantly, for the conviction he has shown in my abilities.

I am thankful to my doctoral committee members, Dr. Vikash Kumar Dubey, Dr. Utpal Bora and Dr. Anil Verma for their constructive criticism and helpful suggestions during my various progress seminars. I am gratified to Prof. Pranab Goswami, Dr. Biplab Bose, Dr. S. S. Ghosh, Dr. A. Ramesh and Dr. L. Sahoo for providing excellent lab facilities. I am also grateful to other faculty members, office staff and my colleagues from Department of Biotechnology for their inestimable support and help.

I would like to thank Central Instruments Facility, IIT Guwahati for providing the access to various instruments without which this study would not be feasible. I am also thankful to Prof. B. P. Asthana, Department of Physics, BHU for his help in FTIR studies.

I am especially appreciative to my former colleagues Dr. A. Kiran Kumar and Dr. Preety Vatsyayan for their inspired support at the time of my acclimatization in the lab and guidance in learning various experimental techniques. I would like to mention my special thanks to my amazing fellow lab members, Seraj, Madhuri, Vishwa, Mitun, Ankana, Reddy, Babina, Santhosh, Lipakshi di, Anupa, Priyanki, Priyamvada and Mrinal who have shared their struggles so intimately and trusted my assistance in their various endeavors.

Beauty of Assam, beauty of IITG campus never let me feel bore. Memories of this place and time spent together with friends (especially our tea breaks) will always be remembered by me in my later life. I feel much fortunate to have a wonderful friend, Asim who has shared the journey of Ph.D with me. I am deeply indebted to him for the transformation he has brought in me in these years which gave me a completely different vision to see things. I am also thankful to my friends Rachna, Pojul, Vinod,

Mithilesh di, Vigya di, Ashok, Manab, Seema, Nandini and Vijay with whom I share tons of fond memories. I also thank Manisha, Amit and Shraddha for their unconditional love and trust.

Most of all, I would like to dedicate this work to my papa and mummy whose love, teachings and unconditional support have brought me this far. I thank my didi for all the long and refreshing conversations we had on phone and for her brilliant ideas, from which I always benefit. Last but not the least I owe a special thanks to my sweet and wonderful bhai Shibu for teaching me being responsible and always reminding me that life is beautiful.

Urmila Saxena

December 2011

Abstract

This study aims at fabricating different kinds of cholesterol biosensors where cholesterol oxidase (ChOx) from *Pseudomonas fluorescens* has been used as the biorecognition element. Preliminary characterization of the ChOx has been carried out in terms of molecular weight, kinetic parameters, optimum working parameters etc. The molecular weight of the ChOx was found to be ~57 kDa. The N-terminal sequencing of the *P. fluorescens* ChOx was carried out and the obtained N-terminal sequence was found to be similar to the N-terminal sequence of ChOx protein from *Burkholderia cepacia.* Product analysis demonstrated that *P. fluorescens* ChOx produces 6β-hydroperoxycholest-4-en-3-one (HCEO) upon cholesterol oxidation. This *P. fluorescens* ChOx was first covalently immobilized onto woven silk-mat using N-ethyl-N'-(3-dimethylaminopropyl) carbodimide (EDC) and N-hydroxysuccinimide (NHS) ligand chemistry. The silk-mat with immobilized ChOx was assembled on the surface of an oxygen electrode to fabricate the bioelectrode. The enzyme loading and the enzyme loading efficiency of the silk-mat were found to be 0.046 U cm^{-2} silk-mat and 70 %, respectively. The biosensor response (depletion of µmol O_2 min^{-1}) was linearly related to the cholesterol concentration in the range of 20 to 90 µM with a detection limit of 8.5 µM and response time of 20 s. The ChOx immobilized silk-mat was not found to pose any obstacle for the diffusion of oxygen to the oxygen electrode during the assay. The silk-mat based bioelectrode retained ~70% of its initial response till 60 days. Apart from silk-mat, two types of nanomaterials, multiwalled carbon nanotubes (MWCNTs) and gold nanoparticles (AuNPs) were also exploited as the ChOx immobilizing support matrices. For the fabrication of MWCNTs based bioelectrode, the gold electrode was first modified with

MWCNTs uniformly dispersed in nafion (Nf) matrix. ChOx and cholesterol esterase (ChEt) were then immobilized into this Nf-MWCNTs film modified gold electrode using layer-by-layer technique to fabricate the final bioelectrode. On the other hand, fabrication procedure of AuNPs based bioelectrode is based on the deposition of AuNPs on the 1, 6-hexanedithiol modified gold electrode, functionalization of the surface of deposited AuNPs with carboxyl groups using 11-mercaptoundecanoic acid and then covalent immobilization of ChOx in the surface of AuNPs film using the EDC and NHS ligand chemistry. Morphological characterization of the electrodes was done using either scanning electron microscopy (SEM) or atomic force microscopy (AFM). Both the MWCNTs and AuNPs based bioelectrodes were electrochemically characterized using cyclic voltammetry (CV) and electrochemical impedance spectroscopy (EIS). The MWCNTs based bioelectrode showed linear response range of 0.080 to 0.950 mM cholesterol with a detection limit of 10 μM and a sensitivity of 690.13 μA mM^{-1}. Where as, the AuNPs modified electrode exhibited a linear response towards cholesterol in the range of 0.04 to 0.22 mM with a detection limit of 34.6 μM and a sensitivity of 9.02 μA mM^{-1}. The heterogenous electron transfer rate constant (k_s) in case of MWCNTs based bioelectrode was found to be 0.189 s^{-1} while in case of AuNPs based bioelectrode it was found to be 0.35 s^{-1}. The fabricated bioelectrodes were also found to efficiently exclude interference by the commonly coexisting electroactive species in blood such as ascorbic acid, uric acid, lactic acid, glucose and urea and thus, can be used as biosensors for highly selective analysis of total cholesterol in serum samples. The MWCNTs based bioelectrode retained ~90 % of its original response even after 3 weeks while AuNPs based bioelectrode retained ~95% of its initial response even after 1 month. Finally, the

electronic coupling of ChOx and AuNPs was studied with spectrophotometric technique using a redox dye 2,6-dichloroindophenol (DCPIP), where AuNPs were found to increase the electron transfer rate between ChOx and DCPIP by ~1.68 fold. This study demonstrated AuNPs as efficient electron transfer mediator for ChOx based electrochemical cholesterol biosensors. In addition, the optocatalytic property of AuNPs was also used in the AuNPs seed mediated enlargement system to develop an optical detection path for cholesterol. The effect of AuNPs size (13 to 21 nm) on the catalytic properties of AuNPs was also studied. Spectrophotometric analysis of the electron transfer process between ChOx and DCPIP with different sized AuNPs showed highest electron transfer efficiency with smaller (13 nm) AuNPs. The electrochemical bioelectrode fabricated with AuNPs and ChOx gave consensus results. Contrastingly, AuNPs size did not affect its optocatalytic activity and eventually the performance of the optical method based on the growth of AuNPs.

Contents

List of Figures

List of Tables

List of Schemes

List of Acronyms

4-AAP	4-Aminoantipyrine
AA	Ascorbic acid
AFM	Atomic force microscopy
APZ	4-Aminophenazone
AuE	Gold electrode
AuNPs	Gold nanoparticles
BA	Boronic acid
BLAST	Basic local alignment search tool
BOM	Biological oxygen monitor
BSA	Bovine serum albumin
CBB	Coomassie brilliant blue
CEO	Cholest-4-en-3-one
ChEt	Cholesterol esterase
CHIT	Chitosan
Chol	Cholesterol
ChOx	Cholesterol oxidase
CNTs	Carbon nanotubes
CPs	Conducting polymers
CV	Cyclic voltammetry
Cys	Cysteamine
DCPIP	2,6-Dichlorophenol indophenol
df	Dilution factor
DI	Deionized
DL	Detection limit
EC	Enzyme commission
EDC	N-ethyl-N'-(3-dimethylaminopropyl) carbodimide
EIS	Electrochemical impedance spectroscopy
FAD	Flavin adenine dinucleotide
$FADH_2$	Flavin adenine dinucleotide (reduced)

FC	Free cholesterol
FNAB	4-Fluoro-3-nitro-azidobenzene
FTIR	Fourier transform infrared spectroscopy
GC	Gas chromatography
Glu	Glucose
HCEO	6β-hydroperoxycholest-4-en-3-one
HPLC	High performance liquid chromatography
HRP	Horseradish peroxidase
IL	Ionic liquid
ITO	Indium tin oxide
LA	Lactic acid
MPA	Mercaptopropionic acid
MUA	11-mercaptoundecanoic acid
MWCNTs	Multiwalled carbon nanotubes
NCBI	National center for biotechnology information
Nf	Nafion
NHS	N-hydroxysuccinimide
NiNP	Nickel nanoparticle
NPs	Nanoparticles
ODA	*o*-dianasidine
P3HT	Poly(3-hexylthiophene)
PANI	Polyaniline
PBS	Phosphate buffer solution
PEG	Polyethylene glycol
pHEMA	Poly(hydroxymethyl methacrylate
PPy	Polypyrrole
PQQ	Pyrroloquinoline quinone
PtNPs	Platinum nanoparticles
RSD	Relative standard deviation
RT	Room temperature
SAM	Self assembled monolayer

SC	Selectivity coefficient
SD	Standard deviation
SDS-PAGE	Sodium dodecyl sulfate polyacrylamide gel electrophoresis
SEM	Scanning electron microscopy
S.E.M.	Standard error mean
SPR	Surface plasmon resonance
TC	Total cholesterol
TEM	Transmission electron microscopy
TEOS	Tetraethylorthosilicate
TLC	Thin layer chromatography
TMOS	Tetramethoxysilane
U	Urea
UA	Uric acid
UV-Vis	UV-Visible
kDa	Kilo dalton
U	Units of enzyme

List of Symbols

k_s	Electron transfer constant
K_m^{app}	Apparent Michaelis-Menten constant
A	Electrode surface area
$E^{o'}$	Apparent standard potential
E_p	Peak potential
E_{pa}	Anodic peak potential
E_{pc}	Cathodic peak potential
F	Faraday constant
I_{pa}	Anodic peak current
I_{pc}	Cathodic peak current
K_{cat}	Turnover number
K_m	Michaelis-Menten constant
R	Thermodynamic rate constant
R^2	Regression coefficient
R_{et}	Electron transfer resistance
Rf	Retention factor
$t_{1/2}$	Half life
Z	Impedance
α	Charge transfer coefficient
ΔE_p	Peak separation
ε	Extinction coefficient
λ	Wavelength
ν	Potential scan rate
Γ	Surface concentration of ionic species

Introduction

Hypercholesterolemia is a major risk factor for many life-threatening diseases such as hypertension, coronary heart disease, arteriosclerosis, lipid dysfunction etc. (Rose and Shipley 1980; Zicha et al. 1999). The need for rapid and reproducible clinical measurement of cholesterol in biological samples has been continuously stimulating interest of the researchers for developing efficient cholesterol estimation methods. Among various cholesterol estimation methods, biosensors are extremely attractive because of their advantages in direct real time procedures, cost effectiveness, high selectivity etc. From the past few decades a variety of cholesterol biosensors have been developed, which generally employ cholesterol oxidase (ChOx) as the biorecognition element (Arya et al. 2008). Among various kinds of biosensors, majority of the cholesterol biosensor research is focused on amperometric technique with a few reports on optical cholesterol biosensors.

In the current state of affairs, the major challenge faced during the fabrication of commercially viable amperometric cholesterol biosensors, is the low stability and

sensitivity as well as high interference that impairs the overall performance of the biosensor. The stability of the biosensor usually gets impaired due the mutilation of enzyme activity upon immobilization. The focus of current cholesterol biosensor research has been laid on the direct electron transfer between redox active site of ChOx (FAD) and electrode surface (Willner et al. 2002) to increase the electron transfer kinetics and reduce the interference. But deep embedment of FAD in the protein core prevents this direct electrical communication with the electrode (Willner and Katz 2000). As a result, cholesterol biosensors based on ChOx do not exhibit high signals leading to low sensitivity. Moreover, the random orientation of enzyme molecules upon immobilization reduce the total number of catalytically active immobilized enzyme units on sensing surface which further reduce the sensitivity of the biosensor.

It has been noted that the matrix and method for enzyme immobilization on the sensing surface are the most critical factors that govern the overall performance of the biosensors (Sarma et al. 2009). The choice and proper selection of these elements along with appropriate instrument design may facilitate the designing of a cholesterol biosensor with improved performance in terms of shelf life and sensitivity towards estimation of cholesterol. Various matrices and methods for immobilization of ChOx on different electrode systems for the construction of amperometric cholesterol biosensor have been reported (Arya et al. 2008). Continuous efforts are being made for developing suitable support matrix employing novel materials that offer promise to solve the problem of impairment of enzyme activity and stability on immobilization and also provide better electrical communication between enzyme and the electrode.

One possible and effective way of improving the stability of the biosensor is to incorporate the enzyme into suitable biomaterial matrix that is more biocompatible. Also, proper electronic communication between the enzyme and the electrode can be established using the concept of molecular wiring and nanobiosensing. The unique and attractive properties of nanomaterials have paved the way for the development of nanomaterial-biomolecule hybrid systems that exhibit attractive and promising analytical behaviors (Willner et al. 2007a). Varieties of nanomaterials have been widely used in constructing electrochemical biosensors with improved performance where the former act as hoping bridge of electrons between the enzyme's redox active site and the electrode (Willner et al. 2006a). These properties of nanomaterials make them excellent candidate for replacing potentially harmful mediators in the construction of biosensors.

Objectives of the study

In view of the above challenges, the overall objective of the present investigation is to assemble cholesterol oxidase with suitable biomaterials and nanomaterials with the focal visualization of developing cholesterol biosensors with improved sensitivity and overall performance that can be efficiently used for cholesterol estimation in real samples. The specific objectives of the work are:

1. Immobilization of cholesterol oxidase on a suitable biomaterial support system for the construction of an oxygen electrode based cholesterol biosensor.

2. Development of amperometric cholesterol biosensors based on potential nanomaterials: multiwalled carbon nanotubes and gold nanoparticles.

3. Studies on cholesterol oxidase-nanomaterial interactions to understand the electronic coupling of the redox center of the enzyme with the nanomaterials for signal transduction.

Significance of the study

The present investigation has been aimed to study biomaterials and nanomaterials as the cholesterol oxidase immobilization matrices for developing cholesterol biosensors. Most of the cholesterol biosensors reported till date face the problem of loss of enzyme activity upon immobilization due to the poor biocompatibility of the matrix with the enzymes. In this regard, use of a biomaterial for immobilizing cholesterol oxidase may maintain the enzyme's activity upon immobilization and therefore may result into a stable cholesterol biosensor. Apart from biocompatibility, another major challenge is the lack of proper electrical communication between active site of ChOx and the electrode which is a bottleneck in developing sensitive and interference free amperometric cholesterol biosensors. The use of nanomaterials in developing amperometric biosensors is an emerging area. For the development of cholesterol biosensors, nanomaterials are less explored matrix materials as compared to other materials like conducting polymers. In our study carbon nanotubes and gold nanoparticles have been used to immobilize cholesterol oxidase on the electrodes surface with the aim to improve the analytical performance of the biosensor. The use of nanomaterials as alternative immobilization matrix would reduce the overpotential and thus replace the need for harmful chemical mediators and would result into sensitive and interference free cholesterol biosensors. The biophysical studies of the electronic coupling of cholesterol oxidase with nanomaterials will further explicate the influence of these materials on the performance

of the biosensor. These findings may give a proper insight into the working and designing of nanomaterials based bioanalytical devices.

The study embodied in this thesis is categorized into the following chapters:

Chapter 1: Literature Review

The objective of this chapter is to summarize the current status and progress in the area of cholesterol biosensors. The chapter highlights the general principles governing electrochemical cholesterol biosensors that specifically utilize immobilized enzymes. Special emphasis has been given on discussing technical importance, performance, benefits and limitations of different types of materials and techniques currently used for cholesterol biosensors design and construction.

Chapter 2: Cholesterol Oxidase from *Pseudomonas fluorescens*

In this chapter, preliminary characterization of cholesterol oxidase from *Pseudomonas fluorescens* has been described. The analysis of ChOx molecular weight, its oxidation product and its N-terminal sequence is carried out. The optimum physical parameters for enzyme activity are also studied and presented.

Chapter 3: Silk-mat based Cholesterol Biosensor

This chapter describes the fabrication of a highly stable and reproducible bioelectrode based on the immobilization of cholesterol oxidase onto woven silk-mat. The assembly process of the silk-mat with immobilized ChOx onto an oxygen electrode is portrayed. The estimation of various response parameters of the fabricated bioelectrode and optimization of its working conditions are also reported.

Chapter 4: Carbon Nanotubes based Cholesterol Biosensor

In this chapter, multiwalled carbon nanotubes (MWCNTs) along with nafion (Nf) have been used as immobilization support for cholesterol oxidase and cholesterol esterase for developing amperometric cholesterol biosensor. The morphological and electrochemical characterization of the fabricated bioelectrode is discussed in detail. The response of the biosensor is checked with cholesterol and various response parameters are estimated. The application of the biosensor for real sample analysis is also demonstrated.

Chapter 5: Gold Nanoparticles based Cholesterol Biosensor

The studies in this chapter include the fabrication of an amperometric bioelectrode based on the covalent immobilization of ChOx on the surface of a layer of gold nanoparticles self-assembled on a gold electrode. Detail electrochemical and morphological characterization of the fabrication procedure is presented. Further characterization of the fabricated bioelectrode in terms of sensitivity, detection limit, and stability is discussed. Ultimately the application of the AuNPs based bioelectrode for the real sample analysis is also shown.

Chapter 6: Biochemical and Biophysical Studies of Cholesterol Oxidase and Gold Nanoparticles Interactions

This chapter includes the detailed biophysical study of two kinds of AuNPs-ChOx hybrid systems (electrochemical and optical). The electrocatalytic and optocatalytic activities of AuNPs in conjunction with ChOx are examined. The relationship between the catalytic activities of AuNPs with their size is also studied and detail findings are described in this chapter.

CHAPTER 1

Literature Review

1.1. Overview

Cholesterol and its fatty acid esters are essential to human body as they are one of the major components of protein and lipid assemblies in mammalian cell plasma membranes that are involved in signal transmission among cells, cell infection and immune response (Devadoss and Burgess 2004). It is essential for the maintenance of cell membrane structure and phase. Furthermore, cholesterol is also a precursor of other vital biological materials, such as bile acid and steroid hormones. Normal concentration of cholesterol in human serum is in the range of 150-250 mg dL^{-1} (3.87-6.46 mM) of which 30% is present as sterol and 70% is esterified with fatty acids (Wong et al. 1994; Zicha et al. 1999). Although, cholesterol is important in small amounts for physiologic functions of an organism, improper maintenance of its concentrations can have severe effects. Elevated level of plasma cholesterol concentrations (hypercholesterolemia) may lead to an increased chance of developing various clinical disorders such as coronary heart diseases, hypertension, arteriosclerosis, myocardial infarction, cerebral thrombosis, lipid

metabolism dysfunction etc. (Rose and Shipley 1980; Wong et al. 1994; Zicha et al. 1999).

This correlation of blood cholesterol levels with life threatening diseases aroused the need for determining cholesterol levels in blood for the diagnosis of these diseases (Aravamudhan et al. 2007b). Also, as cholesterol is a constituent of animal foods such as eggs, meat and dairy products, determination of the cholesterol content in food is of primary importance to select a diet for low intake of cholesterol. The requirement for accurate determination of cholesterol in blood and food samples stimulated a large amount of work in the past few decades on the development of methods for its selective, rapid, cost-effective and reliable assay (Arya et al. 2006; Kumar et al. 2006; Wong et al. 1994; Zicha et al. 1999). Sensitive and selective detection of a particular bio-marker in a multi-component blood system is a challenging task in clinical analysis/diagnosis. Numerous methods exist for the determination of cholesterol and have been reviewed by different authors (Newman 1989). The conventional methods for cholesterol determination are gas chromatography (GC), high performance liquid chromatography (HPLC) and non-enzymatic spectrophotometric techniques using colored substances (Wong et al. 1994). These methods however, are labor-intensive as they involve complex procedures for precipitation of lipoprotein fractions and suffer from various drawbacks, such as low specificity, instability of reagents, susceptibility to interference and high cost.

Since their introduction about three decades ago (Allain et al. 1974), enzymatic assays for serum cholesterol have principally replaced the non-enzymatic methods since the former offer improvements in terms of specificity and selectivity (Arya et al. 2006; Kumar et al. 2006). Serum cholesterol analysis is now, generally accomplished using a three-enzyme

assay and indicator method as originally devised by Richmond (Richmond 1973). The three enzymes used for this purpose are cholesterol oxidase (ChOx), cholesterol esterase (ChEt) and horseradish peroxidase (HRP). Firstly, ChEt hydrolyzes the esterified cholesterol into free cholesterol. In the subsequent oxidation of free cholesterol by ChOx, hydrogen peroxide (H_2O_2) is liberated. The liberated H_2O_2 under the catalysis of HRP generates a free radical, which reacts with an indicator molecule and produces a chromogen which is when measured facilitates the indirect estimation of total serum cholesterol. This coupled assay has been in clinical use for over 20 years and several versions of this procedure exist (Omodeo Sale et al. 1984).

Although enzymes have several advantages in the clinical diagnosis of cholesterol, their high cost makes the overall process less economic. This can be overcome through immobilization of enzymes which is a promising way for enhancing the enzyme reuse and stability and reducing the overall cost of biocatalytic processes (Amine et al. 2006). Biosensors have the exquisite selectivity of the biological molecule and the processing power of modern microelectronics and optoelectronics to offer powerful new analytical tools with applications in medical diagnostics. Enzyme biosensors based on immobilized enzymes on a suitable solid matrix are rapidly gaining interest in the field of analytical technology (D'Orazio 2003). Since the invention of the first enzyme electrode was disclosed (Clark and Lyons 1962; Updike and Hicks 1967) about half-a-century ago, research in this area has been intensified that generates a large base of literature in this area.

A biosensor is commonly described as an analytical device incorporating a biological or biologically derived recognition element, either intimately associated or integrated within

a physiochemical transducer. The basic concept of a biosensor's operation can be illustrated with the help of Scheme 1.1. The biological component recognizes a specific target analyte and the physiological change produced by their specific interaction is processed and transduced by the sensor element into an analog or digital format. The concentration of the analyte is directly proportional to the amount of signal generated, allowing for both quantitative and qualitative measurements. Depending on the transducing mechanism used, biosensors can be electrochemical, optical, thermometric, piezoelectric, and magnetic. Majority of the current cholesterol biosensors are of the electrochemical type, because of their better sensitivity, reproducibility, and easy maintenance as well as their low cost. Apart from electrochemical cholesterol biosensors, cholesterol biosensors based on optical detection techniques have also been reported.

1.2. Electrochemical Cholesterol Biosensors

The high demand for rapid, reproducible and accurate measurement of cholesterol in biological samples in clinical and health care sectors has been continuously stimulating interest of the researchers for developing efficient cholesterol biosensors. Over the past decade, there has been a huge increase in the development of different cholesterol biosensors as reviewed by Arya and his group (Arya et al. 2008).

Among various methods of cholesterol determination, enzymatic electrochemical cholesterol biosensors are the most widely studied over the last few decades because of their unbeaten sensitivity and selectivity. Additionally, electrochemical techniques show lower detection limit, faster response time, better long term stability and inexpensiveness.

There has been a huge interest in the development of different electrochemical cholesterol biosensors based on either ChOx (Ram et al. 2001; Tan et al. 2005; Torabi et al. 2007; Vidal et al. 2004a; Vidal et al. 2004b) or both ChOx and ChEt (Li et al. 2005; Malhotra and Chaubey 2003). Most of the electrochemical cholesterol biosensors developed so far relies on the amperometric detection method where currents generated resulting from the exchange of electrons directly or indirectly between the biological system and the electrode. The number and types of ChOx-based amperometric biosensors have been increasing recently (Basu et al. 2007; Ram et al. 2001; Situmorang et al. 1999; Yang et al. 2006b; Yang et al. 2006c) (Aravamudhan et al. 2007a). For electrochemical determination, electrodes are conventionally made of gold (foil and rod), platinum (foil and rod), or carbon-based materials (paper, rod, paste, materialized carbon, glassy carbon, carbon fiber). These materials are preferred due to their excellent electrical and mechanical properties. Also, they have a high chemical inertness and provide a wide range of anode working potentials with low electrical resistivity. In electrochemical detection of cholesterol, cyclic voltammetry (CV) and amperometric technique are most widely employed (Kumar et al. 2001; Zhou et al. 2006). There may be different transduction mechanism involved in the amperometric cholesterol biosensor.

The complete configuration of cholesterol biosensor includes selection of biomolecules, matrix for immobilization and immobilization method for biomolecules and transduction mechanism. The choice and combination of all these individual components decide the overall performance of the biosensor.

During the fabrication of amperometric cholesterol biosensor, selection of biorecognition element specific to the target analyte is the first and the most critical step. After the

proper selection of the biomolecule, the next important step is the coupling of the biological sensing element with the transducer. The two crucial components of the biosensor are usually integrated by the immobilization of the biorecognition molecule onto the surface of the transducer. Immobilization of the biological molecule is a particularly demanding aspect of the fabrication of biosensors as the immobilization procedure should maintain the biorecognition molecule close to the transducer surface, while retaining its biological activity, in a reproducible manner. It is also desirable that the immobilization layer provides enhanced stability to the biological molecule and it should be applicable to many different biological molecules. Furthermore, the immobilization layer should be chemically resistant to the reactants and products of the biochemical reaction and gives some control over the distribution and orientation of the immobilized species. The choice of material and the method for enzyme immobilization is the most critical step of the biosensor construction.

1.2.1. Biomolecules for electrochemical cholesterol biosensors

A reliable biosensor should respond selectively to an analyte of interest among a range of analytes. The biological component is mainly responsible for the high selectivity of the biosensor in recognizing its target analyte. Owing to the substrate specificity of cholesterol oxidase, it is the most commonly used enzyme in the fabrication of cholesterol biosensor. ChOx is a bi-functional flavin adenine dinucleotide (FAD)-containing flavoenzyme that catalyzes the oxidation and isomerization of 3β-hydroxysteroids having trans double bond Δ^5– Δ^6 of the steroid ring and yields the corresponding Δ^4-3-ketosteroid and hydrogen peroxide (H_2O_2) (Smith and Brooks 1976).

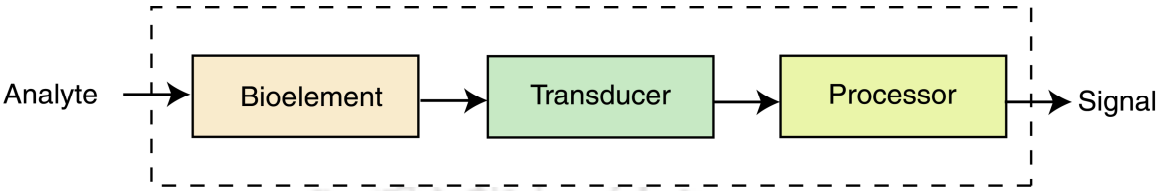

Scheme 1.1 Schematic representation of a biosensor

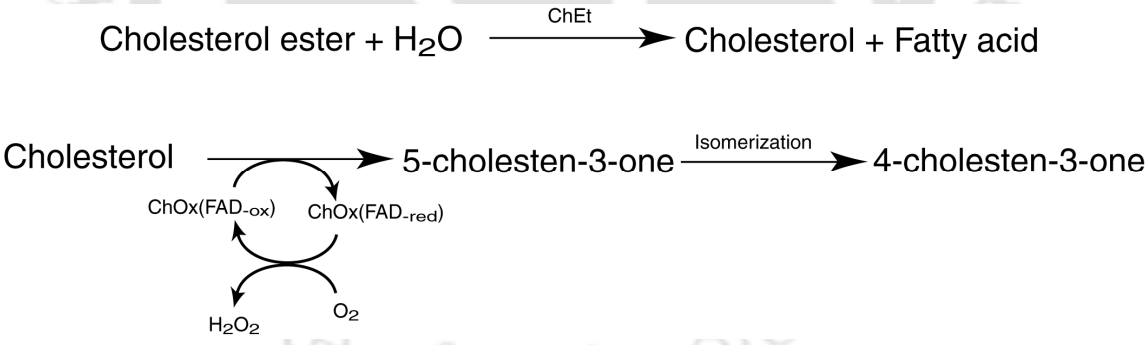

Scheme 1.2 Reaction catalyzed by cholesterol esterase and cholesterol oxidase

The oxidized FAD is a primary acceptor of hydride from alcohol. Upon oxidation of substrate, the FAD is reduced to $FADH_2$. The reduced FAD then transfers the redox equivalents to dioxygen as the final acceptor. Most of the cholesterol biosensors reported till date employ ChOx for free cholesterol (FC) determination cholesterol. For total cholesterol (TC) determination, ChEt is used along with ChOx (Scheme 1.2). Besides these enzymes, Shumyantseva et al. and few others have shown that flavocytochrome P450scc and its modified forms can also be utilized for amperometric determination of cholesterol (Antonini et al. 2004; Paternolli et al. 2004; Shumyantseva et al. 2004; Shumyantseva et al. 2005). In few cases, HRP is also used in the fabrication of photometry based cholesterol biosensors (Law et al. 1997; Malik and Pundir 2002).

1.2.2. Detection techniques in electrochemical cholesterol biosensors

The stochiometric consumption of O_2 and production of H_2O_2 upon catalysis of cholesterol by ChOx as well as the transfer of electrons during the reaction (or redox nature of ChOx) has laid the basis of cholesterol biosensors. The general strategies used for the electrochemical sensing of cholesterol are the measurement of oxygen consumption or H_2O_2 production, use of a diffusible or immobilized mediator, or by using direct electron transfer the electrons from the ChOx to the electrode.

Amperometric measurements can be made based on the monitoring of oxygen consumed using a polarographic oxygen probe. A negative potential (-0.7 V) is applied to the platinum cathode of the probe for a reductive detection of oxygen consumption. Detection of H_2O_2 produced during enzymatic reaction is also an efficient method for indirect measurement of cholesterol. Measurement of peroxide formation has the advantage of being simpler, especially when miniaturized devices are concerned. Such

measurements are commonly carried out on a platinum electrode at an anodic potential of around +0.6 V (vs Ag/AgCl). Majority of electrochemical cholesterol biosensors developed till date relies on the amperometric detection of H_2O_2 (Brahim et al. 2002; Ram et al. 2001; Umar et al. 2009). Cholesterol biosensors which involve detection of O_2 or H_2O_2 come under first generation of biosensors (Scheme 1.3A).

During the amperometric (anodic) measurement of H_2O_2, the anodic potential applied is sufficient to induce simultaneous oxidation of other electrochemically active species present in samples leading to false positive signals (Iannello and Iacynych 1981). Therefore, in recent years, the focus of cholesterol biosensor research is focused on the direct electron transfer between ChOx redox active site (FAD) and electrode surfaces (Willner et al. 2002). The direct electron transfer results into the flow of current that is proportional to cholesterol concentration in the sample. The electron transfer between the active site of ChOx and the electrode is the limiting factor in the operation of amperometric cholesterol biosensors. The electronic communication between cholesterol oxidase and conventional electrodes is poor because of the deep embedment of FAD redox center in the protein shell that act as an intrinsic barrier to direct electron transfer (Willner and Katz 2000; Willner and Willner 2001). Consequently, for establishing better electrical contact between the ChOx redox center and the electrode surfaces, different approaches have been proposed. One useful technique is the use of artificial redox mediators that can shuttle electrons between the enzyme redox center and the surface of the electrode. In case of cholesterol biosensor, these mediators accept electrons from the active site of enzyme during the substrate catalysis and get reduced itself. The reduced

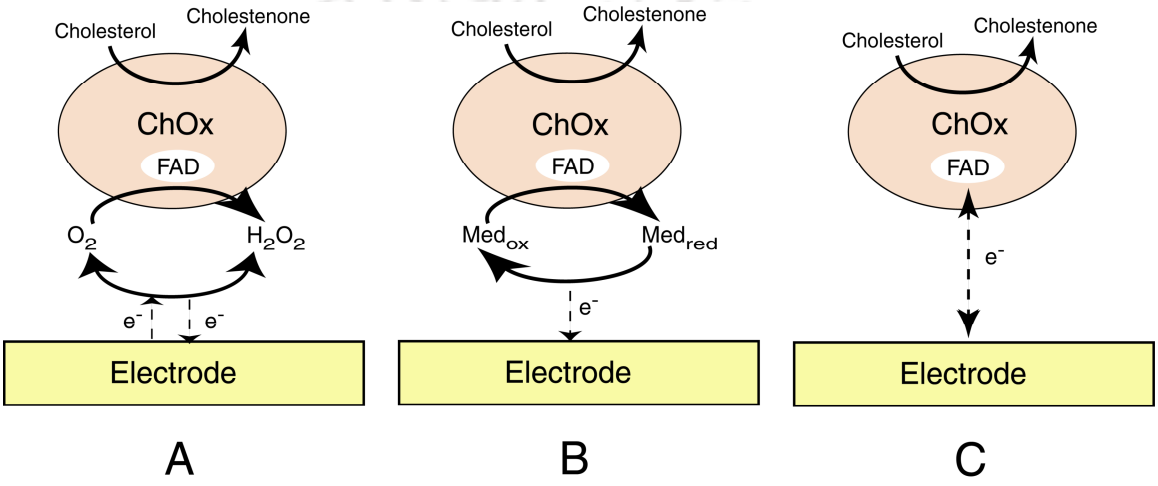

Scheme 1.3 Three generations of amperometric enzyme electrodes for cholesterol: Use of **A**: natural oxygen cofactor, **B**: artificial redox mediators, and **C**: direct electron transfer between ChOx and the electrode

form is reoxidized at the electrode, giving a current signal (proportional to the cholesterol concentration) while regenerating the oxidized form of the mediator. Such mediation cycle is displayed in Scheme 1.3B. Mediators can be either diffusional or wired to the enzyme. It was shown that redox species like phenazene derivatives, thionine, and ferricyanide derivatives work as good electron acceptors for ChOx and are commonly used as the electron transfer mediators for the generation of amperometric cholesterol biosensors (Motonaka and Faulkner 1993; Nakaminami et al. 1999; Nakaminami et al. 1997). Another advantage of use of these mediators is that these mediators have low redox potentials and therefore there are fewer chances of interferring reactions from coexisting electroactive species. In order to function effectively, the mediator should be insoluble, nontoxic, chemically stable and should posses good electrochemical properties. However, in few cases, oxidation of the reduced ChOx by oxygen can occur even in the presence of mediator (particularly as oxygen is freely diffusing), hence limiting the accuracy. In addition, the low potential of most mediators minimizes but does not eliminate the oxidation of endogenous species (particularly ascorbate). Such endogenous electroactive compounds can also consume the mediator, leading to additional errors. Moreover, leaching of these toxic mediators make them incongruous for use in *in vivo* detection systems. However, this problem is likely to overcome by wiring the ChOx with the electron mediators. Wiring of the enzyme with the electron mediator has been reported in the case of glucose oxidase (GOx) (Bartlett et al. 1991; Battaglini et al. 2000). However, wiring may cause conformational change of the enzyme that may impair the stability of the enzyme.

Ultimately, these mediators can be eliminated to develop a reagentless cholesterol biosensor, with a low operating potential, close to that of the redox potential of the enzyme. In this case, the enzyme itself acts as molecular transducer and the electron is transferred directly from cholesterol to the electrode via the active site of the enzyme (Scheme 1.3C). The absence of mediators is the main advantage of such third generation biosensors, leading to a very high selectivity (owing to the very low operating potential). However, critical challenges must be overcome for the successful realization of this direct-electron transfer route owing to the spatial separation of the donor-acceptor pair.

1.2.3. Matrix for immobilization

The first and the most crucial step in the fabrication of any enzyme based biosensor is the immobilization of the enzyme molecules on the sensing surface (electrode in case of amperometric technique). As a consequence, immobilization strategies for biomolecules are of paramount importance in order to preserve their biological activity. This is done with the help of an immobilizing material that is called a matrix whose function is to hold the enzyme molecules on the electrode. The properties of the matrix used, govern the efficiency of the fabricated biosensor in terms of sensitivity, selectivity and stability (Sarma et al. 2009). There are various properties of the matrix that are desirable for the successful immobilization of biomolecules on the surface of these electrodes. First of all, it is the prime requisite that the support matrix have good mechanical stability, rigidity and good flow properties for enzyme stability and activity on storage (Park et al. 2010). Also it should be adaptable to different environments like different pH, temperature, ionic strength and chemical composition of the solvents. Apart from this, a good support

material should be non-degradable and biocompatible without altering the native structure of the enzyme and affecting its biological activity.

Different types of matrix materials have been utilized to immobilize enzyme towards the construction of cholesterol biosensor over the years. Conducting polymers, nanomaterials, sol–gel/hydro-gels and self-assembled monolayer (SAM) are the most common materials. Each of the matrix material has its advantages and disadvantages. The final support matrix may consist of either a single component or multi components. Intensive research activities are continuously pursued to develop new matrices for immobilization of enzymes.

1.2.3.1. Conducting polymers

In the construction of amperometric enzyme electrodes, it is important to have efficient charge transfer produced by the biochemical reactions to electronic circuit. To some extent, this can be controlled by applying suitable potential. However, some reactions, specifically those which involve biomolecules endure rather slow interfacial electron transfer even with large electrochemical driving forces. This problem can be eliminated by modifying a given electrode with a thin film of an electro-active polymer. These electroactive polymers or conducting polymers (CPs) have become the materials of choice for the amperometric biosensor fabrication as they can play both as a binding matrix and as electron transfer mediator for the signal amplification of the biosensors (Ahuja et al. 2007; Nambiar and Yeow 2011). Other than their conducting nature, they have other features like optical transparency, flexibility in chemical structure, biocompatibility, ion selectivity and ease of handling. Also, their chemical and physical properties may be tailored according to the particular needs. A number of CPs such as

polyaniline (PANI), polythiophene, polyphenylene and polypyrrole (PPy) have been utilized for the development of biosensors for application in clinical diagnostics. Among different techniques, electrochemical polymerization method is one of the most frequently used methods for fabrication of CPs based electrodes that can yield uniform, dense and porous CPs films (Kowalski and Schmuki 2010; Lu and Li 2008) and also simultaneous immobilization of enzymes can be achieved. Many researchers have used CPs to provide stability to a biosensor and to selectivity toward interferents.

Under the application of CPs for the fabrication of cholesterol biosensors, the largest part employs polypyrrole (PPy) which have been extensively studied by Vidal and his group (Vidal et al. 2004b; Vidal et al. 2002; Vidal et al. 2000; Vidal et al. 2003). Apart from PPy, polyaniline (PANI) has also been widely used for cholesterol biosensors (Barik et al. 2010; Dhand et al. 2010; Matharu et al. 2007; Singh et al. 2006). Muhammet and his group have immobilized ChOx in a composite film of PPy-PANI via crosslinking (Muhammet et al. 2009). In all these reported studies, ChOx alone or in combination with ChEt is immobilized in the CPs matrices via, adsorption, covalent binding, crosslinking, entrapment and encapsulation.

Besides their various advantages, certain major challenges have to be overcome for the successful use of conducting polymers in the fabrication of biosensors. The polymeric layer may create diffusional limitations for the proper transport of substrate to the enzyme which can reduce the overall performance of the biosensor. Enzyme leakage is another setback of entrapment of enzymes in polymeric materials that can lead to reduction of biosensor stability.

1.2.3.2. Sol-gels and hydro-gels

Sol-gel and hydrogel derived materials are another class of materials that have emerged out as promising matrices for enzyme immobilization in biosensor fabrication (Tan et al. 2005; Yao and Takashima 1998). Sol-gel based materials possess physical rigidity, chemical inertness, thermal and chemical stability etc. They also show good biocompatibility by allowing immobilization of large amount of enzymes with stable tertiary structures without denaturation (Lei et al. 2004). Tetraethylorthosilicate (TEOS) and tetramethoxysilane (TMOS) are effective precursors for the formation of sol-gels, which have been used for the estimation of glucose (Hussain et al. 2005), alcohol (Xu et al. 2005) etc. Hydrogels are polar, uncharged water swellable, flexible materials which are also considered favoring biocompatibility, particularly due to their high water content (Brahim et al. 2002). When coated on electrodes surface, these hydrogels act as antifouling agents and produce a hydrophilic interface from which water-soluble analytes can readily diffuse from the aqueous bulk to the solid surface. The most widely used hydrogels are cross-linked polymers of either poly(hydroxymethyl methacrylate) (pHEMA) of polyethylene glycol (PEG). Apart from these use of sol-gel and hydrogel based matrices have other benefits like their simple construction procedures and flexibility of controlling pore size and geometry. As such, they pose as attractive outer membrane coatings for biosensors. Their optical transparency also makes them ideal for optical biosensors. They can easily be modified with various mediators, polymer additives etc. to furnish electrical conductivity to them so that they can be used in electrochemical biosensors (He et al. 2011).

Sol-gel and hydrogel based materials have been successfully applied in fabrication of various cholesterol biosensors. TEOS derived sol-gel matrices have been used to entrap ChOx either individually or along with ChEt or HRP to develop amperometric or optical cholesterol biosensors (Kumar et al. 2006; Singh et al. 2007). Yao and Takashima have entrapped ChOx in TMOS sol-gel/poly(1,2-diaminobenzene) matrix and used gluteraldehyde cross-linking to improve the stability of the biosensor (Yao and Takashima 1998). Composite materials of sol-gels and hydrogel based materials along with other matrices like polymers, CPs and nanomaterials have also been used in developing cholesterol biosensors (Brahim et al. 2002; Tan et al. 2005; Wu and Choi 2003).

Although sol-gel and hydrogel based materials are proved to be promising but they often face several drawbacks. The problems of diffusional limitations through the porous network and poor reproducibility are the most disconcerting. The encapsulated enzyme may lose its catalytic efficiency due to the reduction of substrate binding and release rate by mass transport barrier of the sol-gel. Moreover, the biosensor based on these matrices may face unfavorable problem of enzyme leakage. These setbacks can reduce the overall stability of the biosensor. For better confinement of enzyme, the matrix pore size has to be controlled. The concentration of a polymer solution for making a membrane should be optimized to have pore size large enough to prevent the diffusion barrier and small enough to prevent enzyme leakage (Smith et al. 2002). Also, sometimes enzymes or matrix have to be functionalized with cross-linkers such as gluteraldehyde for better immobilization of enzymes which may require complex processing steps. These issues

should be taken into consideration while using sol-gel and hydrogels based matrices for developing biosensors.

1.2.3.3. Self-assembled monolayers

Self-assembled monolayer (SAM) is a layer of molecular thickness formed by chemisorption of selected organic molecules on solid metal surfaces (Chaki and Vijayamohanan 2002). The organic molecules used to generate SAMs are generally bi-functional molecules of different terminal functional groups (sulfides, thiols amines, etc.) which can be tailored using various chemistries making them compatible for desired applications (Arya et al. 2009). Self-assembly technique offers several interesting perspectives in the filed of biosensors. Functionalized SAMs can provide a reproducible and robust method of immobilizing desired biomolecules in the near vicinity of the electrode where some control over the orientation and distribution of the enzyme is afforded (Wink et al. 1997). Besides this, there are other numerous benefits of using SAMs in biosensor systems. Immobilization over SAMs modified surface can be achieved using either covalent or noncovalent coupling techniques requiring only minimal amount of biomolecule. The high degree of ordered and dense nature of SAMs mimics the membrane like cellular microenvironment and shield biomolecules from the sensor surface, preventing possible denaturation (Chaki and Vijayamohanan 2002). The improvements of detection limits and stability, the ability to regenerate the sensor, prevention of aspecific adsorption are other features using SAM (Nakaminami et al. 1999). SAM technology can be used with electrochemical, optical or piezoelectric sensors. In electrochemical biosensors, SAMs can be used for obtaining electroactive surface and can act as molecular wire between the biomolecule and the electrode surface.

Several reviews are available on the application of SAMs for biosensors (Chaki and Vijayamohanan 2002; Samanta and Sarkar 2011; Vijayamohanan and Aslam 2001).

There are numerous reports where SAMs have been used in fabricating electrochemical or optical (based on surface plasmon resonance) cholesterol biosensors. Arya and coworkers have used covalently immobilized ChOx on 4-fluoro-3-nitro-azidobenzene (FNAB) modified SAM of octadecanethiol (Arya et al. 2006) and poly(3-hexylthiophene) (P3HT) (Arya et al. 2007d) in combination with surface plasmon resonance (SPR) technique for the fabrication of a cholesterol biosensor. The same group has used aminosilane SAM modified indium tin oxide (ITO) surface for fabricating optical cholesterol biosensor (Arya et al. 2007c) wherein the electrode shows detection limit of 25 mg/dl and stability of approximately 10 weeks. They have also used N-(2-aminoethyl)-3-aminopropyl-trimethoxysilane SAM for co-immobilizing ChOx, ChEt and HRP to develop an amperometric cholesterol biosensor (Arya et al. 2007a). Solanki and coworkers have also fabricated SPR based cholesterol biosensor using 11-amino-1-undecanethiol SAM (Solanki et al. 2007). Vidal and group have used a cysteamine SAM to covalently bind pyrroquinoline quinine (PQQ) on the Au electrode. The PQQ was subsequently modified with FAD which was used to reconstitute apo-ChOx on the electrode surface. The resulting electrode was subsequently used for the highly sensitive detection of cholesterol (Vidal et al. 2004a). Several other SAMs like dithiobissuccinimidyl propionate (Arya et al. 2007b), 2-aminoethanethiolate (Nakaminami et al. 1999) etc. have been used for immobilization of ChOx for fabricating cholesterol biosensor with improved sensitivity and selectivity.

Inspite of several advantages of using SAM, there are some limitations also. Firstly, SAMs can decrease electron-transfer rates. Enzymes immobilized on SAMs are very much sensitive towards changes in pH, ionic strength and temperature: a minor change in one of these parameters can sometimes responsible to loose the biological activity. The chemical stability of some of the SAMs is not very good as monolayer can be chemically oxidized during the course of investigations. Electric field induced and thermal desorption of monolayers is detrimental to biosensor applications. Due to high surface energy, hydrophobic SAM surface can accumulate several contaminants and hence unwanted impurities can adsorb and block the analyte recognition sites.

1.2.3.4.. Nanomaterials

Nanotechnology has recently attracted extensive interest in the area of bioanalytical chemistry. Owing to their nanoscale dimensions, nanomaterials like nanoparticles (NPs), nanorods and nanotubes exhibit unique chemical, physical and electronic properties that are different from their bulk counterparts. The dimensional similarity between various nanomaterials and biomolecules made it possible to conjugate them into novel functional biomolecule-nanomaterial hybrid systems. These hybrid systems have synergistic properties originating from highly selective, catalytic and recognition properties of biomolecules and unique electronic, photonic, and catalytic features of nanomaterials (Guo and Dong 2009). This brings endless opportunities for interfacing biological recognition events with electronic signal transduction so as to design a new generation of bioelectronic devices. Different kinds of nanomaterials, and sometimes the same kind of nanomaterials can play different roles in different electrochemical sensing systems (Katz et al. 2004). Due to their high surface area, favorable electronic properties and

electrocatalytic effect, nanomaterials modified electrodes provide a larger electroactive surface area for higher biomolecule loading (Asefa et al. 2009; Kim et al. 2008) and increased flow of electrons between the electrode and the biomolecules that probably help in decreasing the overpotential, amplifying biorecognition signal and increasing overall sensitivity of the biosensor. Also, due to their biocompatibility, they help in retaining the bioactivity of biomolecules on their surface which otherwise frequently lost when biomolecules are directly immobilized on naked surfaces of bulk materials (Pingarron 2008). These properties of nanomaterials make them attractive immobilization matrix for construction of electrochemical enzyme biosensors. Metal nanoparticles (gold and platinum), oxide nanoparticles (zinc oxide), carbon nanotubes are among the most widely used nanomaterials in the area of biosensors. There has been substantial progress in the past decade in biomolecule-NP hybrids for electrochemical biosensors that has established nanobioelectrochemistry as a mature scientific discipline. Several comprehensive reviews have summarized important achievements the field of electrochemical nanobiosensors (Hyun and Park 2011; Mi et al. 2009; Vaddiraju et al. 2010; Wang 2005).

Nanomaterials have also found application in the development of cholesterol biosensors. Carbon nanotubes (CNTs) and their composite with nanoparticles, owing to low potential detection of cholesterol, high sensitivity and fast response, have gained much interest for application to cholesterol biosensor (Gopalan et al. 2009; Li et al. 2005; Yang et al. 2006c). Carrara and group have investigated the electron transfer between cytochrome P450scc immobilized on MWCNTs modified nanostructured rhodium-graphite electrode (Carrara et al. 2008). Wisitsoraat and coworkers reported a new cholesterol detection

scheme using functionalized carbon nanotube (CNT) electrode in a polydimethylsiloxane/glass based flow injection microfluidic chip. The proposed system showed high sensitivity, low interference and good stability (Wisitsoraat et al. 2010). Aravamudhan and group have used thioctic acid modified aligned nanowires of gold as a matrix for biomolecules immobilization. They have shown that the large conductivity and aligned nature with large surface to volume ratio, gold nanowires help in better electron transfer between enzyme and electrode (Aravamudhan et al. 2007a). The fabricated bioelectrode exhibits a sensitivity of 69 mM^{-1}. Ahmadalinezhad and Chen have reported a highly sensitive electrochemical cholesterol biosensor fabricated by co-immobilizing ChOx, ChEt and HRP on nanoporous gold networks directly grown on titanium substrate (Ahmadalinezhad and Chen 2011). ZnO nanoparticles uniformly dispersed in chitosan have been used to fabricate a hybrid nanocomposite film onto ITO glass plate. ChOx was immobilized in this nanocomposite to develop a cholesterol biosensor (Khan et al. 2008). Safavi and Farjami applied an electrodeposition method to form gold-platinum alloy nanoparticles on the glassy carbon electrode modified with a mixture of an ionic liquid and chitosan. ChOx was then immobilized on the surface of the electrode by cross-linking ChOx and chitosan using gluteraldehyde (Safavi and Farjami 2011). The fabrication of a highly-sensitive cholesterol biosensor was reported based on ChOx immobilization on well-crystallized flower-shaped ZnO structures composed of perfectly hexagonal-shaped ZnO nanorods grown by low-temperature simple solution process. The fabricated cholesterol biosensor reported a very high and reproducible sensitivity (Umar et al. 2009). Besombes and group have shown that incorporation of laponite clay nanoparticles in the immobilization matrix improved the analytical performance and

stability of amperometric cholesterol biosensor. They have shown that incorporation of laponite nanoparticles within the electrogenerated polymer induces improvement in the analytical performance of amperometric biosensor. Further, their presence results in large improvement in the storage stability of the electrode (Besombes et al. 1997). The study reveals that addition of laponite nanoparticles increases the sensitivity of the cholesterol biosensor from 5.1 to 13.2 mA M^{-1} cm^{-2} for estimation of free cholesterol.

However, analytical validation for the control of the surface characteristics under similar conditions has been difficult. Small variations in the density of the metal nanoparticles or the biomolecules that are attached to them would cause large variations between batches of measurements. As modification of the surface became more sophisticated with various nanomaterials immobilized onto a single surface, the reproducibility and the repeatability of the measurements had to be sacrificed. The researchers are now working on automating surface- modification techniques using nanomaterials. Although electrochemical biosensors are a most promising system in life sciences, their potential applications using complex matrices as real samples remain the major challenges for point-of-care applications. Complementary strategies involving nanomaterials are therefore the subject of intense study. We are in the early days of the emerging technology of using nanomaterials to modify biosensors. Although many improvements are required in reproducibility and sensitivity, there is no doubt that a growing number of nanomaterial-based biosensors will soon be offered for diagnosis of diseases and monitoring following therapy.

1.2.4. Methods of immobilization

The success of a biosensor relies on how well an enzyme bonds to a desired biosensor surface and remains active during a desired application. The immobilization technique used to attach the biological material to a transducer surface is considered as one of the decisive steps that decide the operational behavior of a biosensor. Various factors influence the selection of immobilization method, such as biomolecule, transducer type, the nature of the analyte and the operating conditions of the biosensor. The method needs to be compatible with the biomolecule being immobilized and the matrix on which immobilization is to proceed. The immobilization method should bring about high enzyme loading to insure sufficient biocatalyst activities. The immobilized biomolecules must retain biological activity after immobilization, remain tightly bound to the surface and should not be desorbed during the use of the biosensor. The improper selection of immobilization technique can cause damage to the conformation of biomolecules leading to the deactivation of biomolecular activity. Generally the choice of the matrix material decides the choice of the immobilization method. Commonly used methods include physical adsorption, entrapment, covalent binding using activators or cross-linkers and chemical crosslinking with gluteraldehyde or other bifunctional agents.

1.2.4.1. Entrapment

The method of entrapment is based on the localization of an enzyme within the interstitial spaces of a crosslinked and water-insoluble polymer matrix or semi-permeable membranes. This localization is independent of formation of bonds or chemical coupling between the enzyme and gel matrix or membranes. The matrix used for the entrapment should be tight enough to prevent the leakage of the biocatalyst and permeable enough

for the substrate(s) or product(s) to diffuse into or out of the reaction medium. The advantages of the technique include extremely large surface area for contact between substrate and enzyme within a relatively small volume and the possibility of co-immobilizing different types of enzymes physically separated from each other in a single step. The technique does not alter the conformation of the enzyme where only aqueous solvents are used (Park et al. 2010).

In the fabrication of a cholesterol biosensor, entrapment of enzyme within a polymer or a membrane matrix has been widely used. In most cases entrapment of a biomolecule is accomplished during polymeric gel or sol-gel preparation in a solution containing biomolecules (Brahim et al. 2002; Tan et al. 2005; Vidal et al. 2000). The entrapment can also be achieved using layer-by-layer or electrochemical polymerization techniques (Ram et al. 2001; Vidal et al. 2002). The entrapment of ChOx has been carried out in various conducting polymers, sol-gel and hydrogels like polypyrrole (Vidal et al. 2004b; Vidal et al. 2002; Vidal et al. 2003), hydroxyethyl carboxymethyl cellulose (Wu and Choi 2003), etc. for cholesterol biosensor fabrication.

There are, however, some major drawbacks of the entrapment method. Firstly, the diffusional barriers as well as the steric hindrance to high molecular weight substrates make the method unsuitable for few enzymes acting on macromolecular substrates. This may slow down the reaction and the response time of the biosensor. Secondly, some loss of enzyme activity due to the production of free radicals during polymerization or leakage through the wide pores in the gel could occur.

1.2.4.2. Physical adsorption

Physical adsorption involves the direct adsorption of enzymes on the surface of matrix. This is a simple, economical, reversible and quick method for immobilizing an enzyme with the retention of its activity. In the immobilization method the interaction between enzyme and matrix is based on van der Waals forces, ionic binding or hydrophobic forces. Many substances adsorb enzymes on their surfaces, eg. alumina, charcoal, clay, cellulose, kaolin, silica gel, glass and collagen. The main advantage associated with direct adsorption onto solid surfaces is that it is simple and can be used under mild conditions with little or no conformational changes of the enzyme or destruction of its active center.

There are few reports where the immobilization based on physical adsorption method has been used for the development of cholesterol biosensors (Kumar et al. 2001; Li et al. 2005; Motonaka and Faulkner 1993). Kumar and group have carried out the immobilization of ChOx onto the dodecylbenzene sulphonate doped polypyrrole films exploiting physical adsorption technique (Kumar et al. 2001).

Physical adsorption has certain disadvantages. The amount and stability of the immobilized enzyme might be low with no formation of covalent bonds between the support and the amino acid residues on the enzyme surface. The immobilized enzyme may get desorbed from the matrix during operation due to changes in temperature, pH or ionic strength.

1.2.4.3. Covalent binding using activators or cross-linkers

The immobilization of biomolecules onto a matrix can also be achieved by binding of functional group of enzymes and matrix via covalent bonds. The bond is normally formed

between functional groups on the carrier and groups on the enzyme not essential for catalytic activity (Aravamudhan et al. 2007a; Yang et al. 2006c). The support materials must possess reactive groups. If they do not, then the support can be activated by chemical means using cyanogen bromide, carbodimide, gluteraldehyde, aminosilane, diazonium salts, acid chloride, isocyanate and isothiocyanate derivatives. Chemically reactive sites of a protein are usually amino (NH_2) groups from lysine or arginine, carboxyl (COOH) groups from aspartic acid, glutamic acid, hydroxyl (OH) groups from serine, threonine, phenol residues of tyrosine, sulfhydryl (SH) group from cysteine and the imidazole group of histidine. This method has several advantages like it leads to very stable preparations with no release of enzyme into the solution. The covalent bonding between enzyme and carrier not only stabilizes the enzyme during catalytic reactions at higher temperature, it also allows the enzyme to withstand denaturants and organic solvents better. The covalent bonding has been employed to improve uniformity, density and distribution of the bound proteins, as well as reproducibility on the surfaces. It overcomes the problems of instability, diffusion and aggregation of enzymes in entrapment or adsorption techniques.

Various cholesterol biosensors have been developed that exploit gluteraldehyde for the covalent immobilization of enzymes on a wide variety of matrices like polyaniline (Singh et al. 2006), cellulose acetate membrane (Wang et al. 2004), polyacrylonitrile hollow fiber (Lin and Yang 2003), and other matrices (Kumar et al. 2006; Nakaminami et al. 1999; Solanki et al. 2007; Song et al. 2007). Apart from gluteraldehyde, covalent binding using carbodimide have also been used to immobilize ChOx. Kouassi and group have used the carbodiimide coupling for the immobilization of ChOx onto the magnetic

nanoparticles (Kouassi et al. 2005). Carbodimide coupling has also been carried out using *N*-ethyl-*N*'-(3-dimethylaminopropyl) carbodiimide (EDC)/*N*-hydroxysuccinimide (NHS) ligand chemistry to immobilize ChOx onto SAMs (Arya et al. 2007c). Various other coupling methods involving 4-fluoro-3-nitroazidobenzene (Arya et al. 2006; Arya et al. 2007d), boronic acid (Vidal et al. 2004a), diazotization (Malik and Pundir 2002) have also been utilized for fabricating cholesterol biosensor.

Although the covalent binding offers stability however, the conditions for this immobilization method are much more complicated and less mild than in the case of physical adsorption and entrapment. A loss of enzymatic activity due to its conformational changes is encountered if amino acids essential for the catalytic activity are involved in the covalent linkage to the support. Therefore, the binding reaction must be performed under conditions that do not cause loss of enzymatic activity. To protect the active site, the enzyme can be immobilized in the presence of a competitive inhibitor or substrate.

1.3. Optical Cholesterol Biosensors

The cholesterol biosensors reported till date, are mostly electrochemical. However, various cholesterol biosensors which are based on optical detection methods have also been reported. Marazuela and group have reported an optical cholesterol biosensor where change in luminescence of ruthenium(II) complex as a function of cholesterol concentration was used as the response signal (Marazuela et al. 1997). During cholesterol catalysis by ChOx, oxygen is simultaneously consumed. Wu and Choi have exploited this phenomenon to develop an optical cholesterol biosensor which relied on

fluorescence quenching of ruthenium(II) complex by oxygen molecules. The increase in cholesterol concentration resulted in increased consumption of oxygen which further caused decreased quenching of ruthenium(II) complex. The change in fluorescence intensity was used as the direct measure of the cholesterol concentration (Wu and Choi 2003). Wang and coworker have utilized the similar phenomenon to develop a fiber-optic fluorescent based cholesterol biosensor based on oxygen dependent fluorescence properties of $Ru(Phen)_3Br_2$ (Wang et al. 2004). A number of optical cholesterol biosensors have also been reported which relied on an indicator dye. The enzymatic reaction of cholesterol oxidase is coupled with the conversion of an indicator dye into a chromogen. The increase in the color intensity of the chromogen with increasing concentration of analyte was measured spectrophotometrically and used for cholesterol sensing. Various indicator dyes such as 4-aminoantipyrine (4-AAP), *o*-dianisidine (ODA), 4- aminophenazone (APZ) etc have been used for the fabrication of optical cholesterol biosensors (Arya et al. 2007c; Law et al. 1997; Malik and Pundir 2002). Kouassi and group have reported the determination of cholesterol via detection of increase in the absorption intensity for 4-cholesten-3-one produced during enzymatic reaction (Kouassi et al. 2005). Besides this, the SPR technique has also been used as optical transducers for developing cholesterol biosensors (Arya et al. 2006; Arya et al. 2007d; Solanki et al. 2007).

CHAPTER 2

Cholesterol Oxidase from *Pseudomonas fluorescens*

2.1. Overview

Cholesterol oxidase (ChOx) catalyzes the first step in the degradation of cholesterol and thus enables the microorganism to utilize cholesterol as a carbon source in primary metabolism (Vrielink and Ghisla 2009). ChOx has been proven to have great industrial importance for application in bioconversions or detection or disruption of cholesterol-containing membranes etc. Mainly, the substrate specificity of ChOx has led to its implementation as a useful tool in clinical determination of serum cholesterol levels as part of human disease monitoring and treatment (Kreit and Sampson 2009; Pollegioni et al. 2009). For the clinical determination of cholesterol, the ChOx reaction is generally coupled to the peroxidation of aromatic dyes, catalyzed by peroxidase, to form an easily detectable and quantifiable colored product (Richmond 1973). This coupled assay has been in clinical use for more than 20 years, and is also one way in which the activity of the enzyme is followed in *in vitro* experiments. In the fabrication of a cholesterol biosensor, ChOx is most commonly used as the biosensing element (Arya et al. 2008).

ChOx is a flavin-adenine-dinucleotide (FAD)-containing flavoenzyme that catalyzes the oxidation of 3β-hydroxysteroids having trans double bond Δ^5– Δ^6 of the steroid ring and yields the corresponding Δ^4-3-ketosteroid and hydrogen peroxide (H_2O_2). The oxidized FAD is a primary acceptor of hydride from alcohol. Upon oxidation of substrate, the FAD is reduced to $FADH_2$. The reduced FAD then transfers the redox equivalents to dioxygen as the final acceptor (MacLachlan et al. 2000; Sampson 2001). Although the enzyme exhibits a broad range of steroid specificities, the presence of a 3β-hydroxyl group is an essential requirement for substrate activity in all cases (Smith and Brooks 1975) .

ChOx is produced by a number of microorganisms that are found in quite differing environments. ChOx was first isolated from *Nocardia erythropolis* by Turfitt (Turfitt 1944a; Turfitt 1944b) who has shown its effect as an oxidant of cholesterol. Since then, the enzyme has been isolated and purified from various microorganisms like *Arthrobacter*, *Corynebacterium*, *Nocardia*, *Rhodococcus*, *Mycobacterium*, *Pseudomonas*, *Streptomyces*, *Brevibacterium etc*. (MacLachlan et al. 2000). Although there is not a mammalian homolog of cholesterol oxidase, there are mammalian enzymes that catalyze the same chemistry as part of steroid biosynthesis. Here, ChOx from *Pseudomonas fluorescens*, commercially procured from Sigma, would be used throughout the study. In this chapter, some biochemical and kinetic characteristics of ChOx from *Pseudomonas fluorescens* has been studied.

2.2. Experimental Approaches

2.2.1. Reagents and stock solutions

Cholesterol oxidase (EC 1.1.3.6 from *Pseudomonas fluorescens*), peroxidase from horseradish (HRP), bovine serum albumin (BSA), cholesterol and standard protein markers for gel electrophoresis were purchased from Sigma-Aldrich (USA). Cholesterol was purchased from Tokyo Chemical Industries (Tokyo, Japan). Triton X-100 was procured from Sisco Research Laboratory Pvt. Ltd. (Mumbai, India). 4-Aminoantipyrine (4-AAP) was procured from HiMedia Laboratories Pvt. Ltd. (Mumbai, India). All other chemicals were of analytical grade and used without further purification. Deionized water from the Millipore water purification system was used throughout the experiments.

The stock solutions of ChOx (8 μM) and HRP (23 μM) were freshly prepared in phosphate buffer solution (PBS) (50 mM, pH 7.0) prior to being used. Cholesterol stock (10 mM) was prepared in 5 % Triton X-100 solution and stored at 4ºC. The stock solutions of 4-AAP (0.1 M) and phenol (0.1 M) were freshly in deionized water just before the experiments.

2.2.2. Enzyme and protein assays

The cholesterol oxidase activity was assayed using a continuous spectrophotometric rate determination method involving the measurement of H_2O_2 generation accompanying the oxidation of cholesterol (Allain et al. 1974). The reaction mixture consists of ChOx (8 nM), cholesterol (50 μM), HRP (114 nM), 4-AAP (1 mM) and phenol (6 mM) in total 1 mL PBS (50 mM, pH 7.0). For analysis, all the components except cholesterol were added to a quartz cuvette. Cholesterol was added finally to the cuvette, the solution was

mixed thoroughly and increase in absorbance at 500 nm wavelength (corresponding to the production of quinoneimine dye) was monitored for 10 min at 37°C with CARY 300 BIO double beam spectrophotometer (Varian, USA). The enzyme activity was determined according to the following formula:

$$\text{Units ml}^{-1}\text{ enzyme} = \frac{(\Delta A_{500\text{ nm}}/\text{min Test} - \Delta A_{500\text{ nm}}/\text{min Blank})(df)}{(0.5)(13.78)V_E} \qquad (2.1)$$

where, df = dilution factor, 13.78 = millimolar extinction coefficient of quinoneimine dye at 500 nm under the assay conditions, 0.5 = conversion factor based on one mole of H_2O_2 produces half a mole of quinoneimine dye, V_E = volume (in mL) of enzyme used. One unit will convert 1.0 µmole of cholesterol to 4-cholesten-3-one per minute at pH 7.0 at 37°C.

Protein contents were determined at 595 nm using Coomassie Brilliant Blue (CBB) G-250 with BSA as a standard by the method of Bradford (Bradford 1976).

2.2.3. Sodium dodecyl sulfate polyacrylamide gel electrophoresis (SDS-PAGE) of protein

Protein sample was denatured by dissolving in sample buffer containing SDS and 2-mercaptoethanol, and boiling at 90°C for around 5 min. The denatured protein sample along with standard SDS-PAGE protein markers were subjected to SDS-PAGE following the method of Laemmli (Laemmli 1970). The electrophoresis was carried out using 5 % stacking and 10 % separating gels of thickness 0.75 mm at constant 20 mA and 30 mA current for stacking and separating gel, respectively, for 1 h in a Protean II Mini-gel apparatus (Biorad, Richmond, California). After the completion of electrophoresis, the

gels were stained with the silver staining method. The standard protein markers used were carbonic anhydrase (Bovine erythrocyte) (29 kDa), fumarase (Porcine heart) (48.5 kDa), serum albumin (bovine) (66 kDa), phosphorylase B (Rabbit muscle) (97.4 kDa) and β-galactosidase (*E. coli*) (116 kDa).

2.2.4. Product analysis

Cholesterol oxidase (1 U) was incubated in 50 mL of the reaction mixture (50 mM PBS, pH 7.0, containing 64 mM sodium cholate, 0.34 % (vol/vol) Triton X-100, and 1 mM cholesterol) at 30°C for 8 h. A control without cholesterol was also run and analyzed to avoid any interference in the product analysis caused by the Triton X-100 and sodium cholate or their degraded products. Additional enzyme (0.5 U) was added in the reaction mixture intermittently after every 2 h during the reaction period. After completion of reaction, the incubation mixture was extracted with two volumes of chloroform/methanol (2:1, vol/vol) in a separating funnel. The chloroform phase was recovered, and the aqueous layer was re-extracted three times with one volume of chloroform. The chloroform extracts were combined, concentrated in a rotary evaporator (Equitron, India) at room temperature (RT) and then purified by silica gel column using solvent mixture of hexane/ diethyl ether (2:3 vol/vol). The purified products were further analyzed by thin layer chromatography (TLC) using a solvent mixture of n-hexane and diethyl ether (3:1, vol/vol) as the mobile phase. Spots were developed in iodine chamber. Each spot was recovered with chloroform, the products were dried, mixed with KBr and analyzed by fourier transform infrared spectroscopy (FTIR) (Perkin-Elmer).

2.2.5. N-terminal sequencing of cholesterol oxidase

N-terminal sequencing of the ChOx from *Pseudomonas fluorescens* was carried out by Intas Biopharmaceuticals Ltd. (Ahmedabad, India). The sequencing was done on Procise 492 (ABI) instrument using the Modi_Pulsed liquid 50B method. The sequencing employed Edman degradation, phenylthiohydantoin (PTH) derivatization of amino acids and HPLC separation followed by UV detection.

2.3. Results and Discussion

2.3.1. Molecular weight determination of ChOx

ChOx protein from *Pseudomonas fluorescens* was analyzed using SDS-PAGE. The homogeneity of the protein was demonstrated by single protein band (Figure 2.1, lane 1). The approximate molecular mass of the ChOx protein was determined to be ~57 kDa when compared with the retention factor (R_f) value of the standard protein markers ran parallel in the same gel (Figure 2.1, lane 2). The approximate molecular weight of ~57 kDa measured by us is closer to reported ChOx proteins from other sources (Fukuyama and Miyake 1979; Ishizaki et al. 1989; Kamei et al. 1978; Ohta et al. 1991; Purcell et al. 1993; Sojo et al. 1997).

2.3.2. Determination of kinetic parameters of ChOx

ChOx activity studies were carried out with different concentrations of cholesterol (0.01 to 0.6 mM). The catalysis of ChOx with increasing cholesterol concentrations followed Michaelis-Menten kinetics with apparent K_m of 33 μM as calculated from the Lineweaver-Burk plot with a linear equation of y = 1.9162x + 57.825 and correlation coefficient (R^2) of 0.9857 (Figure 2.2). The calculated K_m of *Psuedomonas fluorescens*

ChOx was found to be practically identical to the K_m of ChOx from *Rhodococcus erythropolis* (~31 μM) (Sojo et al. 1997). The catalytic efficiency of *P. fluorescens* ChOx (K_{cat}/K_m) was found to be of 1.6 × 10^5 M^{-1} s^{-1} which was deduced from its catalytic turnover number (K_{cat}) of 5.2 s^{-1} and apparent K_m.

2.3.3. Effect of pH and temperature on ChOx activity

The effect of pH on the activity of ChOx was investigated after incubating the enzyme sample in buffers of different pH from 3.5 to 11 and determining the ChOx activity in the test buffer of same pH following the similar spectrophotometric assay method stated earlier. The optimum pH for ChOx activity was found to be in the range of pH 6.0 to 7.0 (Figure 2.3A). The ChOx activity vanished completely below 4.0 and above 10.0. The optimum pH found in case of *P. fluorescens* ChOx is similar to ChOxs from other microbial sources like *Pseudomonas sp.*, *Nocardia rhodochrous* and *Streptomyces fradiae* (Cheetham et al. 1982; Doukyu and Aono 1998; Yazdi et al. 2001).

In order to determine the temperature optima of ChOx activity, the enzymatic reaction of ChOx was carried out as mentioned above at different reaction temperatures from 25 to 50ºC. From Figure 2.3B it can be noted that optimum temperature for ChOx activity was observed at 45°C. The enzymatic activity sharply decreased as the temperature was increased to 50ºC. The optimum temperature of *P. fluorescens* ChOx is near the optimum temperature of *Streptomyces sp.* ChOx (50 ºC) but lower than few other ChOxs from *Chromobacterium sp.*, *Pseudomonas sp.* etc. (Doukyu and Aono 1998; Doukyu et al. 2008; MacLachlan et al. 2000).

2.3.4. N-terminal sequence analysis of ChOx

To date, there is no sequence or structure information available in literature for cholesterol oxidase from *Pseudomonas fluorescens*. To realize some sequence information of the ChOx protein and to understand its molecular characteristics to the possible extent, its N-terminal sequencing was carried out. The N-terminal amino acid sequence of ChOx was found to be "DATPPGFPAD". The obtained N-terminal protein sequence of ChOx was subjected to NCBI BLAST. It was found that, the N-terminal sequence of *P. fluorescens* ChOx showed significant similarity with the protein sequences of ChOx from *Burkholderia cepacia* (100 %), *Burkholderia ambifaria* (90 %), *Brevibacterium sterolicum* (80 %), etc (Table 2.1). Multiple sequence alignment was carried out with the 10 amino acid long N-terminal sequence of ChOx with the protein sequences of the ChOxs obtained with BLAST results (Figure 2.4). The results of multiple sequence alignment showed that the sequences of ChOxs which are having similarity with the N-terminal sequence of *P. fluorescens* ChOx, also lie in the N-terminal region of these proteins.

Table 2.1 Result of NCBI BLAST of *P. fluorescens* ChOx with the proteins of protein data bank

Protein	Query coverage
Cholesterol oxidase from *Burkholderia cepacia*	100 %
Cholesterol oxidase substrate-binding *Burkholderia ambifaria* MEX-5	90 %
Cholesterol oxidase substrate-binding *Burkholderia ambifaria* IOP40-10	90 %
FAD linked oxidase domain protein *Burkholderia ambifaria* AMMD	90 %
FAD linked oxidase domain protein *Burkholderia ubonensis* Bu	90 %
Chain A, Cholesterol Oxidase from *Brevibacterium sterolicum*- His121ala Mutant	80 %
Chain A, Crystal Structure Of Cholesterol Oxidase from *Brevibacterium sterolicum*	80 %

2.3.5. Identification of the cholesterol oxidation product

ChOx in general catalyzes the oxidation of cholesterol (cholest-5-en-3β-ol) to form cholest-4-en-3-one (CEO) (Smith and Brooks 1974). However, Molnar and group first reported a bacterial enzyme that oxidizes cholesterol to 6β-hydroperoxycholest-4-en-3-ne (HCEO) but not the CEO produced by most ChOxs. This HCEO is formed by the oxygenation of the 6 position on the cholesterol nucleus by the ChOx (Molnar et al. 1993). Since then, two distinctive types of bacterial ChOxs have been found. One forms CEO and the other forms HCEO as the major product (Doukyu 2009). Formation of HCEO implicates dioxygenase action of the ChOx enzyme. ChOx from *Pseudomonas fluorescens* has also been shown to produce HCEO but not the usual CEO (Teng and Smith 1996). To confirm this further, the product of *Pseudomonas fluorescens* ChOx catalyzed reaction using cholesterol as substrate was analyzed with the help of FTIR spectroscopy. The spectral data shows significant peaks at 3433.05, 2945.39, 2868.24, 1678.12, 1612.54 and 867.99 cm^{-1} (Figure 2.5). The peaks at 3433.05 and 867.99 cm^{-1} correspond to peroxide group. It is reported that most of the hydroperoxide groups give IR peak near 2.8 microns (Shreve 1951). The obtained IR data show consensus results. The other peak at 2945.39 represents the ring structure in cholesterol nucleus. The peaks at 2868.24, 1678.12 and 1612.54 cm^{-1} correspond to C-H, C=O and C=C strechings respectively. These results validate HCEO as the sole product of *Pseudomonas fluorescens* ChOx catalysis of cholesterol. It has also been reported that the ChOxs from *Burkholderia cepacia* and *Pseudomonas sp.* (Doukyu 2009; Doukyu and Aono 1999; Doukyu and Aono 2001) also produce the HCEO product. From the analysis of the N-terminal sequence of *P. fluorescens* ChOx and its catalytic product, it is likely that the

ChOx from *Pseudomonas fluorescens* may have similar molecular characteristics as the ChOxs from *Burkholderia cepacia.*

2.4. Conclusions

The molecular weight of *Pseudomonas fluorescens* ChOx protein was determined with the help of SDS-PAGE and was found to be ~57 kDa. ChOx is most active in the pH range of 6.0 to 7.0 and at 45ºC temperature. The Michaelis-Menten constant (K_m) of ChOx was calculated to be 0.033 mM. The N-terminal sequence of the ChOx was determined and its analysis with NCBI BLAST and multiple sequence alignment showed its highest similarity with the N-terminal region of cholesterol oxidase from *Burkholderia cepacia*. ChOxs *from Pseudomonas fluorescens* and *Burkholderia cepacia* were also found to produce HCEO as the final product of cholesterol catalysis. Therefore, ChOx from *Pseudomonas fluorescens* may have molecular similarities with the ChOx of *Burkholderia cepacia*.

Figures

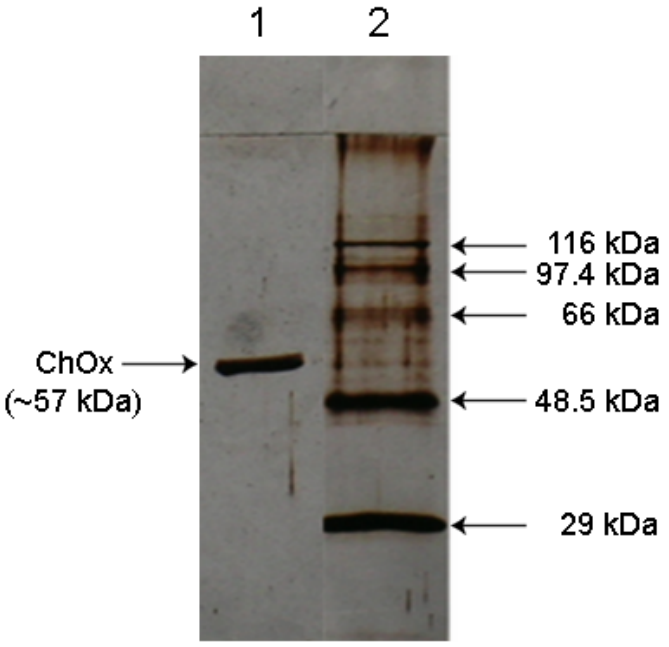

Figure 2.1 SDS-PAGE analysis of ChOx:
Lane 1: ChOx protein, lane 2: standard protein markers

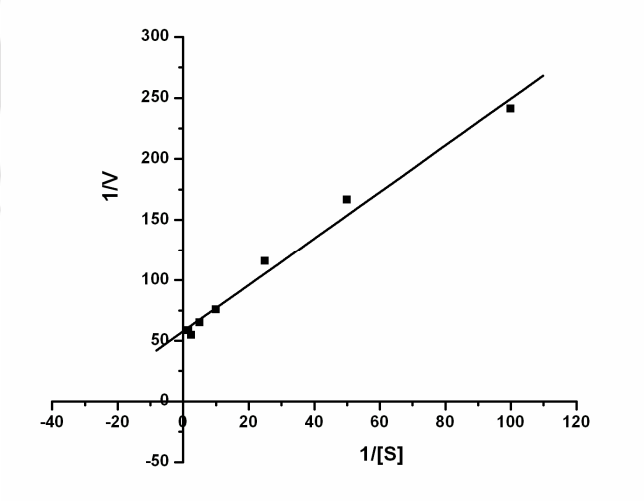

Figure 2.2 Lineweaver-Burk plot for determination of apparent *Km* of ChOx

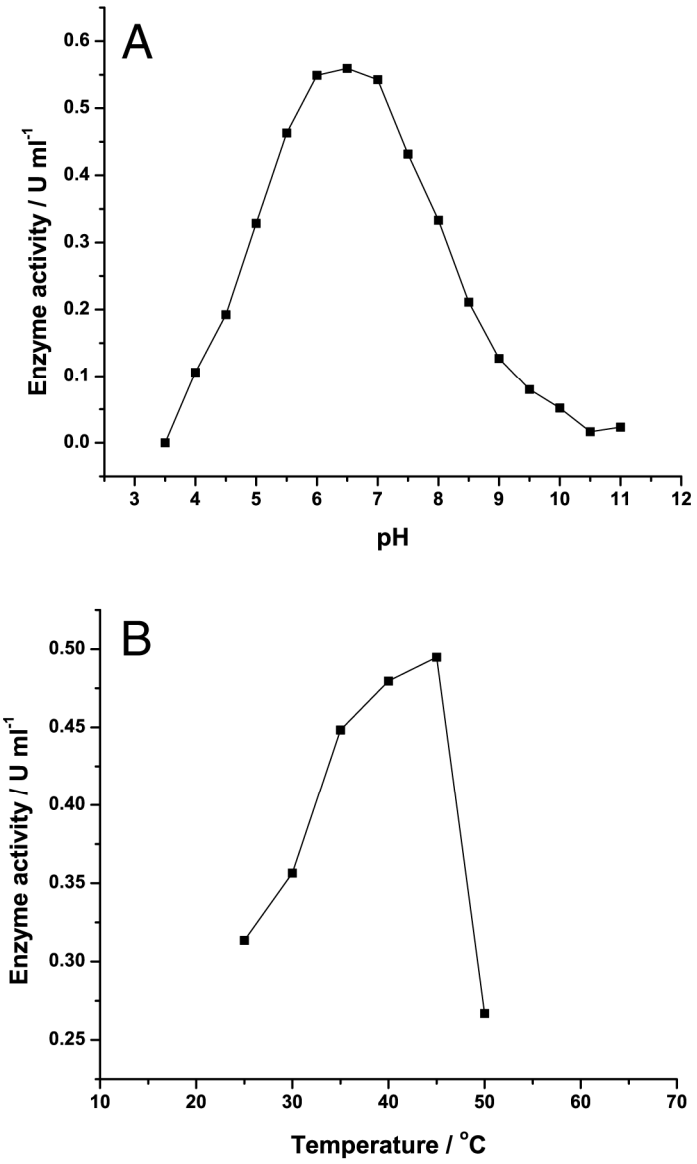

Figure 2.3 ChOx activities as a function of pH and temperature:
A: Effect of pH, **B**: Effect of temperature. The different pH buffers (each at a concentration of 50 mM) were sodium acetate (pH 3.5 to 5.5), potassium phosphate (pH 6.0 to 7.5), tris-HCl (pH 8.0 to 9.0), glycine-NaOH (pH 9.5 to 11)

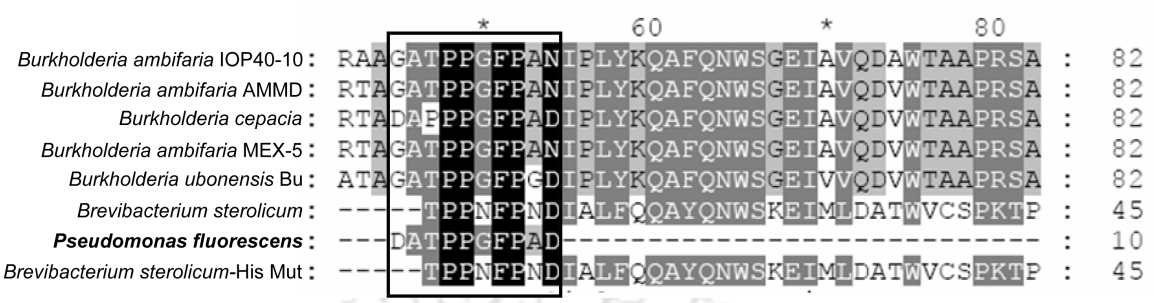

Figure 2.4 Multiple sequence alignment of the N-terminal sequence of *P. fluorescens* ChOx with the protein sequences of ChOxs from other sources

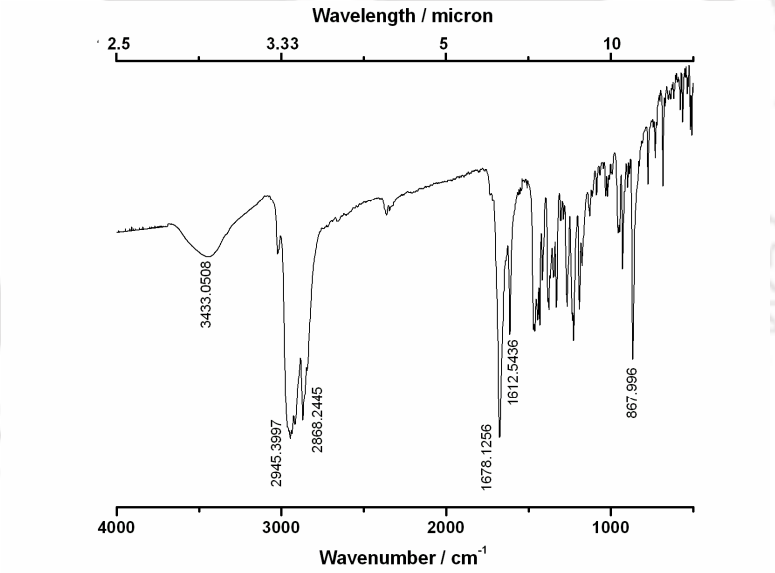

Figure 2.5 FTIR spectra of isolated product of cholesterol oxidation

CHAPTER 3

Silk-Mat based Cholesterol Biosensor

3.1. Overview

The matrix and method for immobilization of enzymes on the electronic unit are considered as the critical factors that govern the efficiency of the any fabricated biosensor (Khan et al. 2008; Sarma et al. 2009). Various matrices and methods for immobilization of cholesterol oxidase (ChOx) on different electrode systems for the construction of amperometric cholesterol biosensor have been reported (Arya et al. 2008). However, frequent loss of enzyme activity and stability resulting from the immobilization of the enzymes on the matrix is posing challenge in developing commercially viable and stable cholesterol biosensor. Hence, the biosensor research is currently focusing upon developing new materials that offer promise to solve the problem of impairment of enzyme activity and stability on immobilization (Holtz and Asher 1997; Sarma et al. 2009). One possible and effective way of improving the stability and activity of the immobilized enzyme is to incorporate the enzyme into suitable biomaterial matrix that is more biocompatible. Apart from the biocompatibility, the analysis where biosensor relies

upon the detection of the dissolved oxygen (O_2) or hydrogen peroxide (H_2O_2) by electrodes selective to them, the selection of the matrix material needs special attention to avoid any possible diffusion limitation for such electrochemically active gaseous and small redox species to their respective electrodes. In these perspectives, silk protein matrix may be chosen as an ideal bio-platform for enzyme immobilization. The backbone of silk is mainly protein fiber (Altman et al. 2003; Kaplan 1998), so it is expected to be biocompatible with enzymes. The intricate lattice network of stable and water-insoluble protein fibers of silk has high surface area which is useful for various applications. Enzymes can be physically or chemically entrapped in the three-dimensional interpenetrating network of the silk fiber that may provide a biocompatible microenvironment around the enzyme. Moreover, silk is inexpensive, inert, non-toxic, readily available, and can be obtained in a number of forms. There are some reports where silk protein-based materials (mainly silk fibroin) have found application as solid supports for potentially expensive and commercially important enzymes and organometallic catalysts including glucose oxidase, L-asparaginase, lipase, peroxidase, etc. (Chatterjee et al. 2009; Grasset et al. 1977; Lu et al. 2009). Demura and coworker first reported using a glucose oxidase-immobilized silk fibroin membrane sensor in a steady-state analysis system (Demura and Asakura 1989). Here, we aim to exploit woven silk-fiber (silk-mat) as the support matrix for the immobilization of ChOx. This ChOx-immobilized silk-mat was further assembled on the surface of a commercial oxygen probe for fabricating a highly sensitive, reproducible, and oxygen diffusion-limitation free cholesterol biosensor.

3.2. Experimental Approaches

3.2.1. Reagents and stock solutions

Cholesteol oxidase (EC 1.1.3.6 from *Pseudomonas fluorescens*), N-ethyl-N'-(3-dimethylaminopropyl) carbodiimide (EDC) and N-hydroxysuccinimide (NHS) were purchased from Sigma-Aldrich (USA). Cholesterol was purchased from Tokyo Chemical Industries (Tokyo, Japan). Triton X-100, urea and uric acid were procured from Sisco Research Laboratory Pvt. Ltd. (Mumbai, India). All other chemicals were of analytical grade and used without further purification. Deionized water from the Millipore water purification system was used throughout the experiments. Woven Muga silk fiber (silk-mat) produced by *Antheraea assamensis* was purchased from Sualkuchi (Silk village of Assam, India).

The stock solution of ChOx (8 μM) was freshly prepared in phosphate buffer solution (PBS) (50 mM, pH 7.0). Cholesterol stock (20 mM) was prepared in 10% Triton X-100 solution and stored at 4ºC. This stock solution was further diluted with PBS (50 mM, pH 7.0) to make different concentrations of the cholesterol. The final concentration of the Triton X-100 in the reaction mixture was not more than 0.05 % so that it does not have any effect on enzyme activity.

3.2.2. Apparatus

A biological oxygen monitor (BOM) (5300A, YSI, USA) with Clark-type polarographic oxygen probes (5331A, YSI, USA) and a thermostat water bath with magnetic stirrer (5301B, YSI, USA) were employed to construct the cholesterol biosensor. It was attached to a chart recorder (Kipp & Zonen, USA) used for real-time display and recording of the

experimental results. Scanning electron microscopy (SEM) of silk-mat was carried out with a scanning electron microscope (Leo 1430vp, Germany).

3.2.3. Enzyme immobilization on silk-mat

A silk-mat was washed thoroughly with deionized water and then dried at room temperature (RT) under laminar hood. A circular piece of diameter 15 mm was cut from this dried silk-mat and dipped for 2 h in a solution of EDC (0.4 M) and NHS (0.1 M) prepared freshly in PBS (50 mM, pH 6.5). The silk-mat was then washed thoroughly with PBS (50 mM, pH 7.0). After placing it on a clean glass slide, 5 µL of ChOx solution (8 µM) was dropped on its surface and then dried at ambient conditions for 24 h. For removing any loosely bound enzyme from the ChOx-immobilized silk-mat, it was immersed in 1 mL of PBS (50 mM, pH 7.0) containing 0.2 % Triton X-100 and gently vortexed for 15 min. The mat was then taken out and stored at 4ºC until use.

3.2.4. Determination of enzyme loading efficiency of the silk-mat

The amount of protein that is leached out in the wash solution was estimated following Bradford method using BSA as standard (Bradford 1976). The amount of protein retained in the ChOx-immobilized silk-mat was calculated from the protein mass balance among the amount that is initially added to the mat during immobilization and the amount that is leached out. The enzyme loading on the silk-mat was determined in terms of number of enzyme units retained per unit surface area of the silk-mat and the enzyme loading efficiency of the silk-mat was determined in terms of percent protein immobilized.

3.2.5. Scanning electron microscopy of the silk-mat

The unmodified and ChOx-immobilized silk-mats were placed onto round copper grids of about 10 mm diameter, coated with a thin layer of gold using a spray gun, and then examined under scanning electron microscope using the following setting conditions: 15 KeV EHT, 50 µm aperture, 1000 × magnification.

3.2.6. Fabrication of silk-mat based bioelectrode and measurement procedure

ChOx from *Pseudomonas fluorescens* catalyzes the conversion of cholesterol into 6β-hydroperoxycholest-4-en-3-ne and H_2O_2 according to Eq. 3.1:

$$\text{Cholesterol} + O_2 \xrightarrow{\text{ChOx}} 6\beta\text{-hydroperoxycholest-4-en-3-one} + H_2O_2 \qquad (3.1)$$

The ChOx activity can be measured by monitoring the rate of O_2 depletion in the presence of a specific amount of cholesterol. A commercial polarographic oxygen probe employed to measure the O_2 consumption in solution was assembled with ChOx-immobilized silk-mat to fabricate the ChOx electrode. Scheme 3.1 is showing the detailed scheme of the fabrication of the ChOx electrode and the measurement system of the biosensor. The ChOx electrode was assembled by mounting the ChOx-immobilized silk-mat on the top of the oxygen probe with the help of an O-ring. Air-saturated PBS (50 mM, pH 7.5) (3 mL) was taken in the reaction chamber and kept under stirring condition. The enzyme electrode was dipped into it and after it got stabilized, assay was started by injecting standard cholesterol stock solution into the reaction chamber. The biosensor response was determined by observing the O_2 depletion rate processed and recorded by

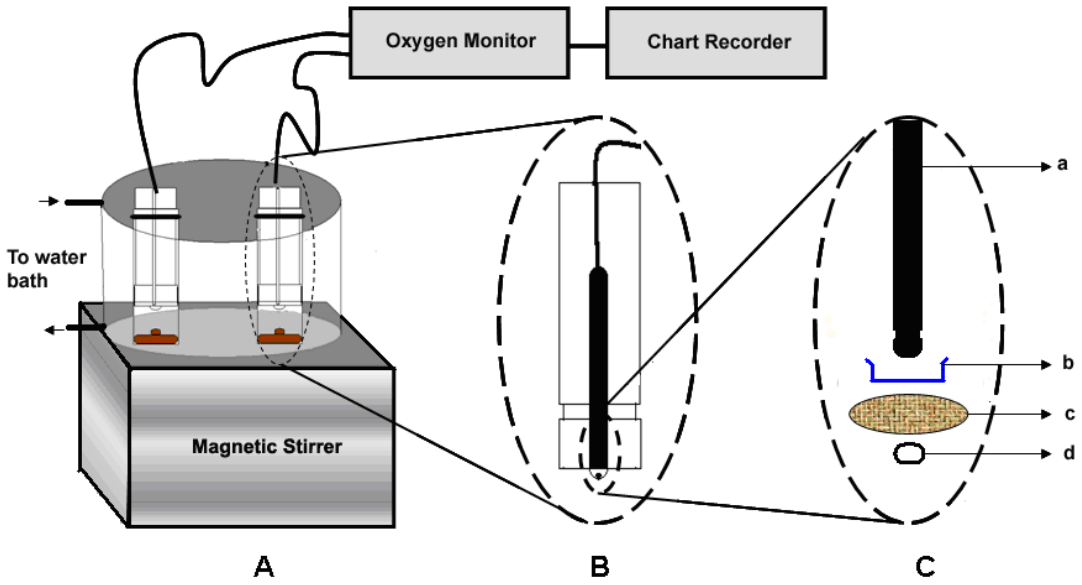

Scheme 3.1 Schematic diagram for the measurement system of silk-mat based biosensor: **A**: Thermostat standard bath and magnetic stirrer with the fabricated ChOx electrode, **B:** oxygen probe with adapter, **C**: exploded diagram of the assembly of ChOx electrode with (**a**) electrode body, (**b**) teflon membrane, (**c**) ChOx-immobilized silk-mat and **(d)** O-ring

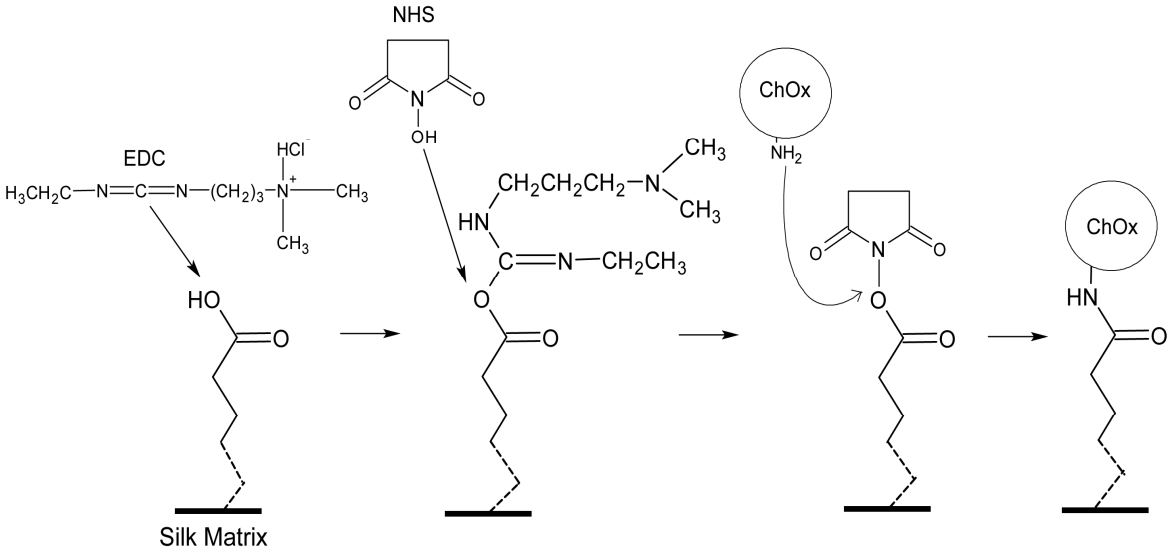

Scheme 3.2 Mechanism of covalent immobilization of ChOx to the surface of silk-mat

the oxygen monitor and chart recorder. Once the assay is complete, the ChOx-immobilized silk-mat was removed from the oxygen probe, washed several times with PBS (50 mM, pH 7.0) and stored at 4ºC.

3.3. Results and Discussion

3.3.1. Immobilization of cholesterol oxidase on silk-mat

ChOx was covalently immobilized onto the silk-mat via formation of amide bond between –COOH group of silk-mat protein and $–NH_2$ group of ChOx using EDC as the coupling agent and NHS as activator (Grabarek and Gergely 1990; Staros et al. 1986). Scheme 3.2 is showing the chemistry of covalent coupling of ChOx to the surface of silk-mat. EDC activates the –COOH functional groups present in the silk protein to form an unstable O-acyl intermediate. NHS converts this unstable derivative to a stable amine-reactive ester. The $–NH_2$ groups of the ChOx acts as nucleophile and attack the amine-reactive ester to form an amide link between silk protein and ChOx. The attachment of ChOx to the silk-mat was demonstrated by SEM. Figure 3.1A and B shows the SEM images of silk-mat before and after immobilization of the enzyme, respectively. Silk-mat shows a network-like fibrous morphology (Figure 3.1A) which provides large effective surface area to load large amount of enzyme. Short irregular globules or aggregates of enzyme are distributed randomly on the protein fibers of the ChOx–immobilized silk-mat (Figure 3.1B), whereas such attachments are void on the unmodified silk-mat (Figure 3.1A). The highly hydrophobic nature of silk (Altman et al. 2003) and rapid cross-linking reaction adapted for this immobilization approach are attributed to the observed aggregation of the enzyme molecules on the silk surface. The enzyme loading on the silk-mat was found to be 0.046 U cm^{-2} of silk-mat and the enzyme loading efficiency was

determined to be 70 %. The optimum enzyme loading resulted from the cross-linking reaction could effectively facilitated the reaction between the substrate and the enzyme that resulted good response of the biosensor as shown later.

3.3.2. Response characteristics of the cholesterol biosensor

The typical response curve of the biosensor was made by plotting biosensor response (μmol O_2 consumed min^{-1}) vs. cholesterol concentration (μM) as shown in Figure 3.2. A linear relationship was noticed over a concentration range of 20 to 90 μM cholesterol. The detection limit (DL) of 8.5 μM was determined from the expression $DL = (3 \times SD) / Sensitivity$ (where SD is the estimated standard deviation for the points used to construct the calibration curve and the $Sensitivity$, its slope). The DL found in our case is well comparable with the reported DL of 12.4 μM for ChOx entrapped in ferrocene monocarboxylic acid-PPy/Pt/Ptpoly matrix (Situmorang et al. 1999; Vidal et al. 2002) and 6.2 μM when ChOx and HRP were coimmobilized in potassium ferrocyanide-graphite-teflon matrix (Pena et al. 2001). Using the Lineweaver-Burk plot, the apparent Mchaelis-Menten constant (K_m^{app}) was determined to be 0.259 mM. The K_m^{app} was found to be higher as compared to the K_m of free ChOx (0.033 mM). The specificity constant (K_{cat} / K_m^{app}) which is the measure of how efficiently an enzyme converts a substrate into product was determined to be 1.3×10^6 M^{-1} s^{-1}. Even with the increase of K_m, the specificity constant of the immobilized ChOx was found to be higher than the free enzyme (1.6×10^5 M^{-1} s^{-1}).

The response time that is the time needed by the biosensor to reach 95% of the steady-state response when a biosensor was exposed to a known concentration of standard

solution was 20s. This response time is parallel to several other reported cholesterol biosensors which has response times of 20-30s (Bongiovanni et al. 2001; Brahim et al. 2002; Yang et al. 2006c). The proposed biosensor is also faster than some other reported cholesterol biosensors having response times between 1-20 min (Law et al. 1997; Salinas et al. 2006; Shumyantseva et al. 2004). The fast response is attributed to the large catalytic surface area over the silk-mat and highly porous (average pore size of 2 x 10^3 μm^2) and thin membrane structure (0.3 mm), which were conducive to fast diffusion of O_2 from bulk solution to the electrode surface. The silk-mat did not pose obstacle on the diffusion of O_2 from the sample compartment to the electrode surface as evident from the similar biosensor response independently obtained by placing the ChOx-immobilized silk-mat on the surface of the oxygen electrode and suspending to the bulk reaction mixture. This result is in consensus with some reports on the oxygen-permeability of silk-mat (Minoura et al. 1990). The reproducibility of the fabricated ChOx electrode was studied by exposing five different enzyme electrodes prepared nominally in the same way to a 50 µM cholesterol standard under optimum conditions (50 mM PBS, pH 7.5 and temp 30ºC). The results revealed a high reproducibility of the fabrication procedure with a relative standard deviation (RSD) of 4.5 ± 0.43 % (n=5).

3.3.3. Effects of pH and temperature on the response of the cholesterol biosensor

The effect of pH on the biosensor response was investigated by subjecting it to 50 µM cholesterol standards in various pH (4.0 -10.0) buffer solutions. The results (Figure 3.3A) showed that the response increased with increasing pH value from 4 to 7.5 and then declined as pH increases further. The optimum biosensor response was achieved at pH 7.5. Consequently, 50 mM PBS with pH 7.5 was chosen for all the remaining studies.

The other most critical parameter affecting biosensor response is the working temperature as it affects both the kinetics of the enzymatic reactions as well as the performance of the oxygen electrode. The effect of temperature on the biosensor response was studied by exposing the biosensor to a 50 µM cholesterol solution over the temperature range of 25 to 45ºC. From Figure 3.3B it can be noted that the oxygen depletion rate was increased with increasing temperature from 25 to 40ºC. But the response decreases sharply as the temperature increases further to 45ºC. This decrease in biosensor response may be attributed to the partial denaturation of the ChOx and low solubility of O_2 in water at higher temperatures. The temperature above 45ºC couldn't be studied because of limitations of the commercial oxygen sensor. Although the response of the biosensor was highest at 40ºC, further experiments were carried out at 30ºC to prevent enzyme denaturation after repeated use and thus prolong the lifetime of the biosensor.

3.3.4. Interference study

To study the selectivity of the cholesterol biosensor to cholesterol, the effect of some potential interferents present in real samples for example, ascorbic acid (AA), lactic acid (LA), glucose (Glu), urea (U) and uric acid (UA), on biosensor response was studied. Biosensor response was examined when it is separately exposed to these interferents, each present with 50 µM cholesterol solutions in 1:1 ratio. Selectivity coefficient (SC) of the biosensor for each interferent was estimated with respect to the response of the biosensor obtained when it is subjected to only cholesterol using the formula, $SC = I_{c+i}/I_c$ where I_{c+i} and I_c are biosensor response for cholesterol (50 µM) in the presence and absence of each interferents respectively. In most of the cases, it was found that the contribution of these compounds to the biosensor response is ≤ 5 % implying no

significant interference (Figure 3.4). This study implies that the biosensor could be used in the physiological conditions without any significant interference from the substances present in the body fluids.

3.3.5. Operational and storage stability

The operational stability of the ChOx electrode was examined by subjecting a freshly prepared electrode at optimal working conditions to a 50 µM cholesterol standard and assessing its response successively for 27 times for a period of 6 h. After each measurement the bioelectrode was washed with PBS (50 mM, pH 7.0). Our results (Figure 3.5A) demonstrated that the ChOx electrode maintained its initial activity till the fourth successive measurement and retained ~50 % of its initial activity at the end of the 25 measurements.

In order to determine the operational stability of the ChOx electrode with intermittent storage, response of two different electrodes prepared in the similar manner to 50 µM cholesterol was assessed periodically at 3 days and 7 days intervals for 45 and 60 days respectively. When the biosensor was not used, the ChOx-immobilized silk-mat was removed from the tip of the oxygen electrode, washed with 50 mM phosphate buffer (pH 7) and stored at 4ºC under dry conditions. It was observed that when the measurements were made at 3 days interval, the ChOx electrode could retain ~50 % of its original activity after 45 days of storage and when the same carried out with 7 days interval, ~70% of its original activity was retained till 60 days (Figure 3.5B). This indicates that the stability of the constructed ChOx electrode for repeated use is governed by both the number of measurements made and the storage time. The half life ($t_{1/2}$ of initial activities)

of the constructed enzyme electrode when stored in a closed container at 4ºC without being used was nearly 13 months.

3.4. Conclusions

The present study demonstrates the silk-mat as a suitable immobilizing matrix for construction of oxygen electrode-based cholesterol biosensor. The fibrous and porous morphology of the silk-mat provide an ideal microenvironment to the immobilized ChOx that resulted good analytical performance with high stability, sensitivity, reproducibility and good selectivity for cholesterol of the fabricated biosensor. The other promising feature of our device is that the ChOx-immobilized silk-mat did not stand as diffusion barrier for the dissolved oxygen, which is the sole electrochemical species considered for biosensing of cholesterol in the investigation. The silk-mat used as the immobilizing matrix is a commercially available low cost material. The overall performance of the constructed biosensor shows great promise for a simple and economic analysis of cholesterol in real samples.

Figures

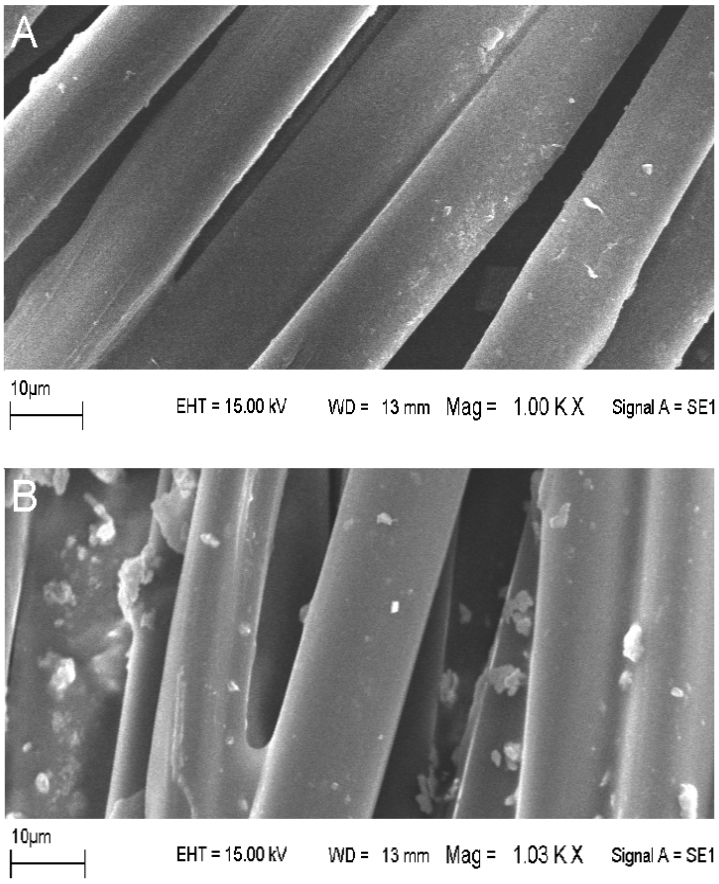

Figure 3.1 Scanning electron microscopy of silk mat:
A: fresh silk-mat treated with EDC and NHS, **B:** silk-mat after immobilization of ChOx

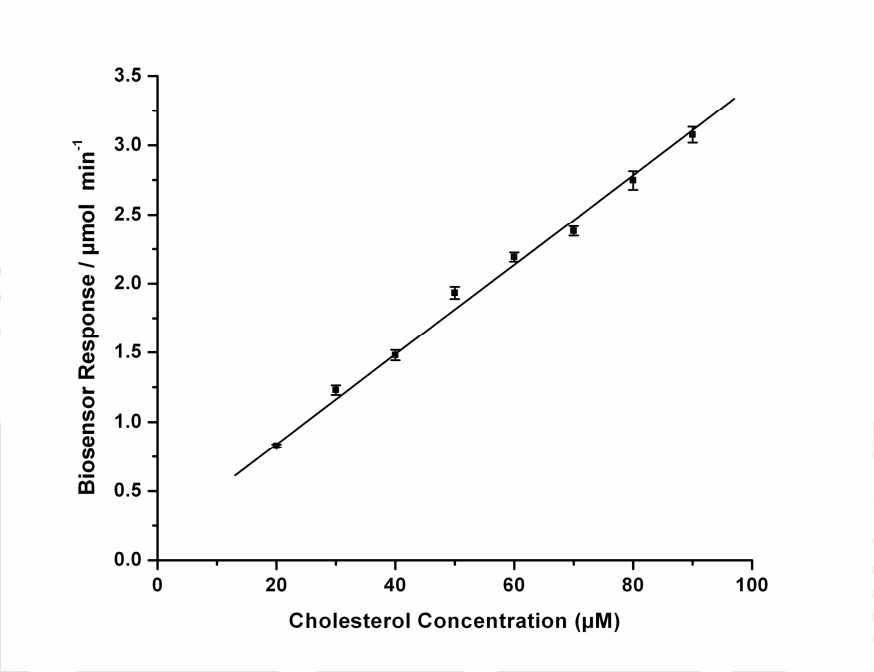

Figure 3.2 Response of silk-mat based biosensor towards cholesterol: Each value represents the mean of five experiments ± standard error (P <0.05)

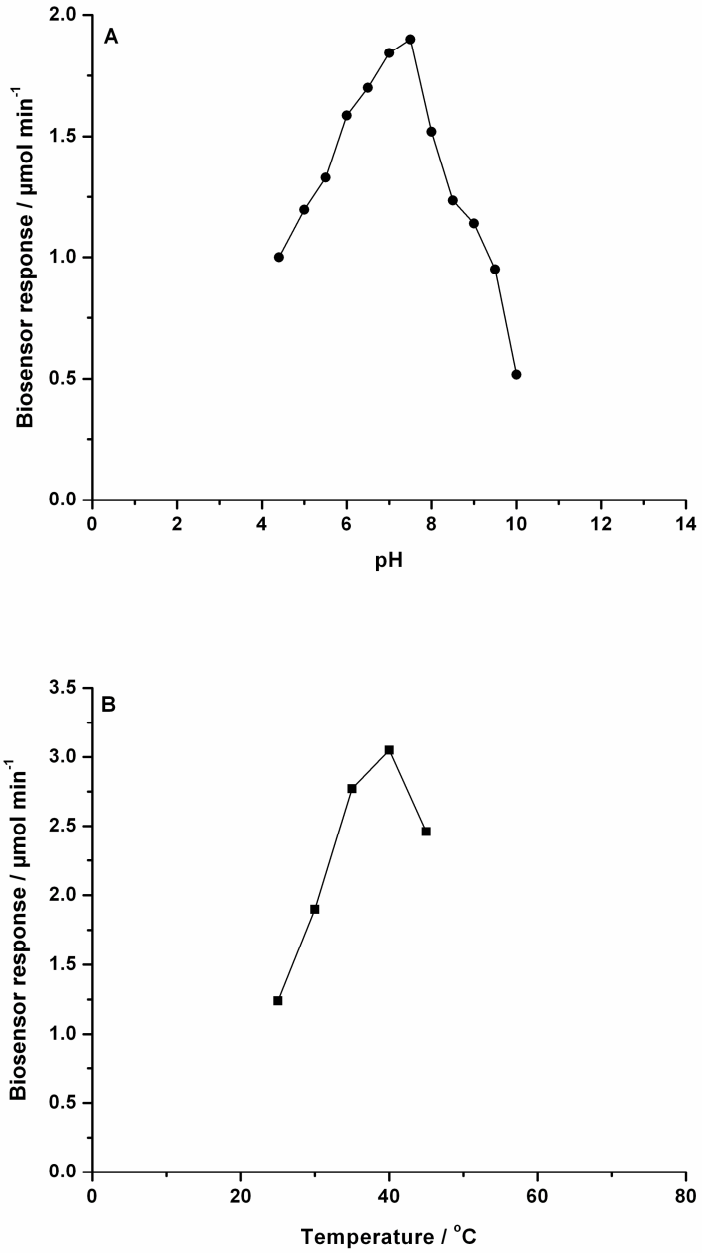

Figure 3.3 Effect of pH and temperature on the response of silk-mat based biosensor: **A:** Effect of pH, **B**: effect of temperature. The different pH buffers (each at a concentration of 50 mM) were sodium acetate (pH 4 to 5), potassium phosphate (pH 6 to 7), tris-HCl (pH 8 to 9), glycine-NaOH (pH 10)

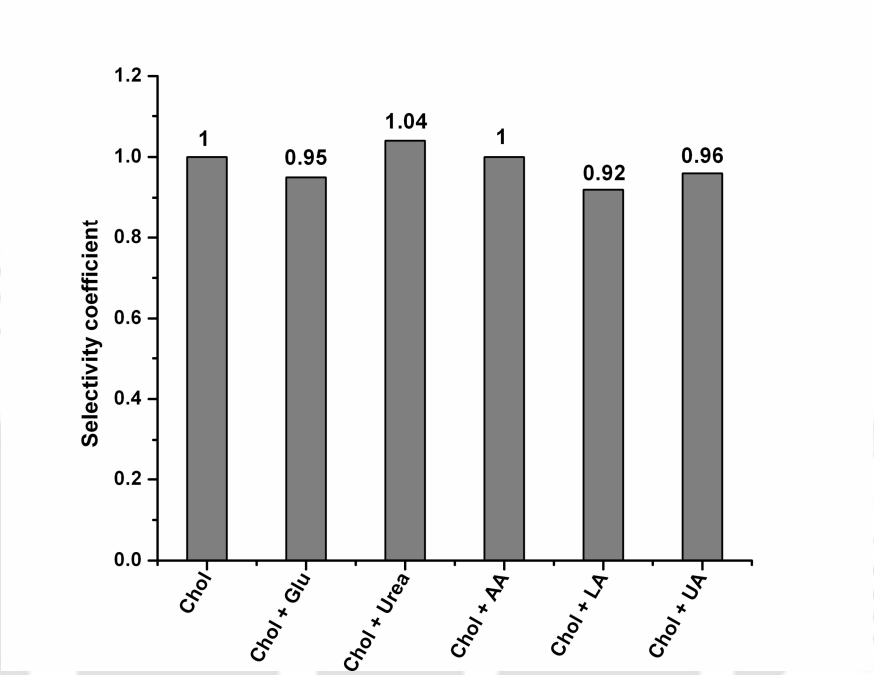

Figure 3.4 Effect of potential interferents on the silk-mat based biosensor response: (Chol: cholesterol, Glu: Glucose, AA: ascorbic acid, LA: lactic acid, UA: uric acid)

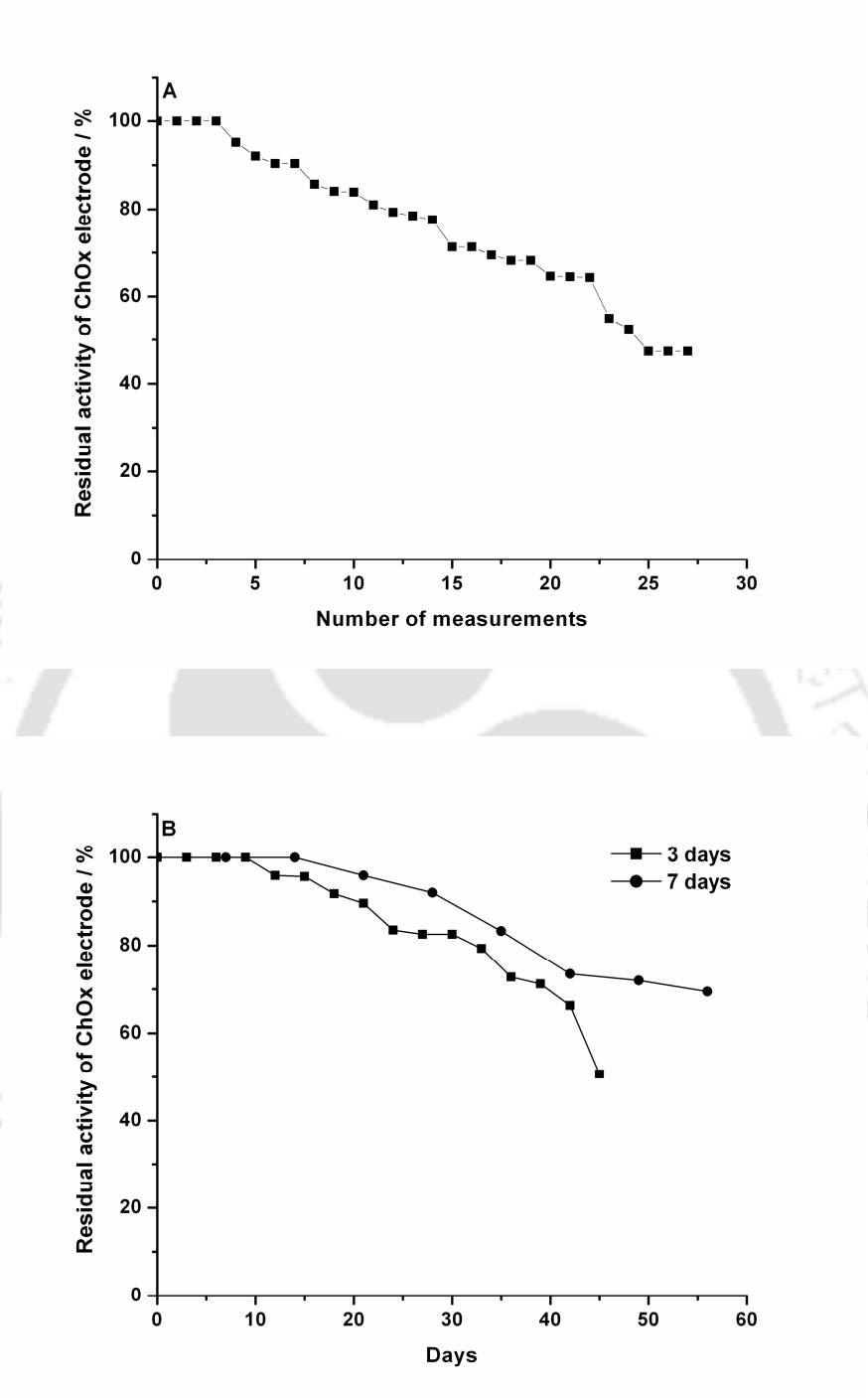

Figure 3.5 Stability of silk-mat based biosensor:
A: Operational stability, **B:** Operational stability with different intermittent storage time

CHAPTER 4

Carbon Nanotubes based Cholesterol Biosensor

4.1. Overview

The majority of the cholesterol biosensors reported till date are based on the detection of electro-oxidation of hydrogen peroxide (H_2O_2) produced during the catalysis of cholesterol by ChOx (Ram et al. 2001; Vidal et al. 2004b). This requires a high anodic potential (Iannello and Iacynych 1981) that can induce simultaneous oxidation of other electrochemically active species present in the samples leading to false positive signals. Therefore, in recent years, cholesterol biosensor research is focused on the direct electron transfer between redox active site of ChOx and electrode surfaces (Willner et al. 2002). But deep embedment of redox active site containing flavin adenine dinucleotide (FAD) in the protein core prevents direct electrical communication between FAD and electrode (Willner and Katz 2000; Willner and Willner 2001). In such cases, an electron transfer mediator is often used either in solution or co-immobilized with enzyme on electrode, to shuttle electrons between the redox centres of enzymes and the electrode. There are several reports on different types of electron transfer mediators immobilized with ChOx

to fabricate cholesterol biosensors (Kumar et al. 2001; Nakaminami et al. 1997; Salinas et al. 2006).

Carbon nanotubes (CNTs) have been demonstrated as a promising material for applications in various amperometric biosensors due to their unique chemical and electronic properties (Baughman et al. 2002; Lin et al. 2005; Sarma et al. 2009; Wang et al. 2011). In such biosensing devices, they can be used for two purposes. Firstly, due to their high surface area, they can serve as immobilization platforms for biomolecules. Secondly, due to their dimensional similarity with proteins and high electrical conductivity, they exhibit good electronic communication with active site of redox proteins (Chen et al. 2004; Luong et al. 2007; Vashist et al. 2011), and therefore can mediate heterogeneous electron transfer between the active site of the redox enzymes and the electrode. They have been reported to decrease the overvoltage for the oxidation of substrate by enzyme and thereby prevent the interference caused by ascorbic acid, uric acid and H_2O_2 (Goran et al. 2011). There are many reports on CNTs along with different immobilizing supports having been used for the construction of cholesterol biosensors (Dhand et al. 2008; Gopalan et al. 2009; Roy et al. 2006; Tan et al. 2005; Yang et al. 2006c). The major problem faced for developing CNT-based devices is their poor solubility in most solvents. Nafion (Nf), a perfluorinated ionomer, is widely used to solubilize CNTs. Apart from solubilizing CNTs, Nf has other attractive features, such as good biocompatibility, optimum porosity and chemical inertness, which makes it an excellent support material to confine biomolecules at the electrode surface in the construction of various biosensors (Roberts et al. 2011; Xie et al. 2010). It is also known to exclude interference from different electroactive compounds present in physiological

samples (Cui et al. 2001; Wang et al. 2003). CNT/Nf nanocomposite electrodes were prepared and found to have excellent electrocatalytic activities and shown to minimize interference from non-target substances (Tsai et al. 2005). Here, the unique features of Nf as a biocompatible enzyme immobilization support and multiwalled carbon nanotubes (MWCNTs) as a mediator in electron transfer between the enzyme and the electrode have been combined and used to develop an amperometric cholesterol biosensor for serum total cholesterol estimation. This was carried out through immobilization of ChOx and ChEt in a Nf–MWCNTs matrix deposited on Au electrode.

4.2. Experimental Approaches

4.2.1. Reagents and stock solutions

ChOx (EC 1.1.3.6 from *Pseudomonas fluorescens*), ChEt (EC 3.1.1.13 from *Pseudomonas sp.*), Nf (5 wt %) and MWCNTs were bought from Sigma–Aldrich (USA). Cholesterol was purchased from Tokyo Chemical Industries (Tokyo, Japan). Cholesterol estimation kit was obtained from Merck. All other chemicals were of analytical grade and used as received without further purification. Human serum samples from normal individuals were collected from the institute hospital.

Stock solution of cholesterol (10mM) was prepared in deionised (DI) water having 5 % Triton X-100 and stored at 4ºC. Stock solutions of ChOx (8 μM) and ChEt (8 μM) were freshly prepared in 50 and 400 mM phosphate buffer solution (PBS) (pH 7.0), respectively, prior to being used. All solutions were prepared with deionized (DI) water from the Millipore water purification system (Millipore, Bedford, MA).

4.2.2. Fabrication of bioelectrodes

Scheme 4.1 shows the schematic diagram for the fabrication of the bioelectrode. A gold (Au) electrode (AuE) (diameter = 0.5 cm) was cleaned, first by polishing it with alumina powder, then washing it ultrasonically with 70% ethanol and water separately for 15 min each and finally drying in air. The cleaned AuE was dip coated three times with 1% Nf, with intermittent drying after each coating step. Nf dip coating is applied for the better attachment of the Nf-MWCNTs matrix onto the surface of the Au electrode. 1 mg MWCNTs were dispersed in 100 µl of 5% Nf and sonicated for 20 min to obtain a stable homogeneous suspension. 10 µl of this mixture was dropped on Nf-coated AuE and dried. For preparing Au–Nf–MWCNTs–ChOx–Nf bioelectrode, 12 µl of freshly prepared ChOx (8 µM) solution was dropped on Nf–MWCNTs-modified Au electrode, dried and covered with 8 µl Nf (5%) layer. Au–Nf–MWCNTs–ChOx–Nf–ChEt–Nf bioelectrode was prepared by applying an additional coating of 12 µl ChEt (8 µM) onto ChOx–Nf coating. Finally, 8 µl Nf (5%) was poured and dried. The fabricated bioelectrodes were immersed in 50 mM PBS (pH 7) for 15 min prior to being used. One electrode was prepared following the similar procedure of fabricating the Au–Nf–MWCNTs–ChOx–Nf–ChEt–Nf except the incorporation of MWCNTs (Au–Nf–ChOx–Nf–ChEt–Nf). When not in use, the bioelectrodes were stored in 50 mM PBS (pH 7) at 4ºC.

4.2.3. Apparatus and measurements

Cyclic voltammetry (CV) was performed in a three-electrode configuration with an Autolab PGSTAT 1212 (Eco Chemie, The Netherlands). The working electrodes were gold electrodes or modified gold electrodes. Ag/AgCl (3M KCl) and platinum (Pt)

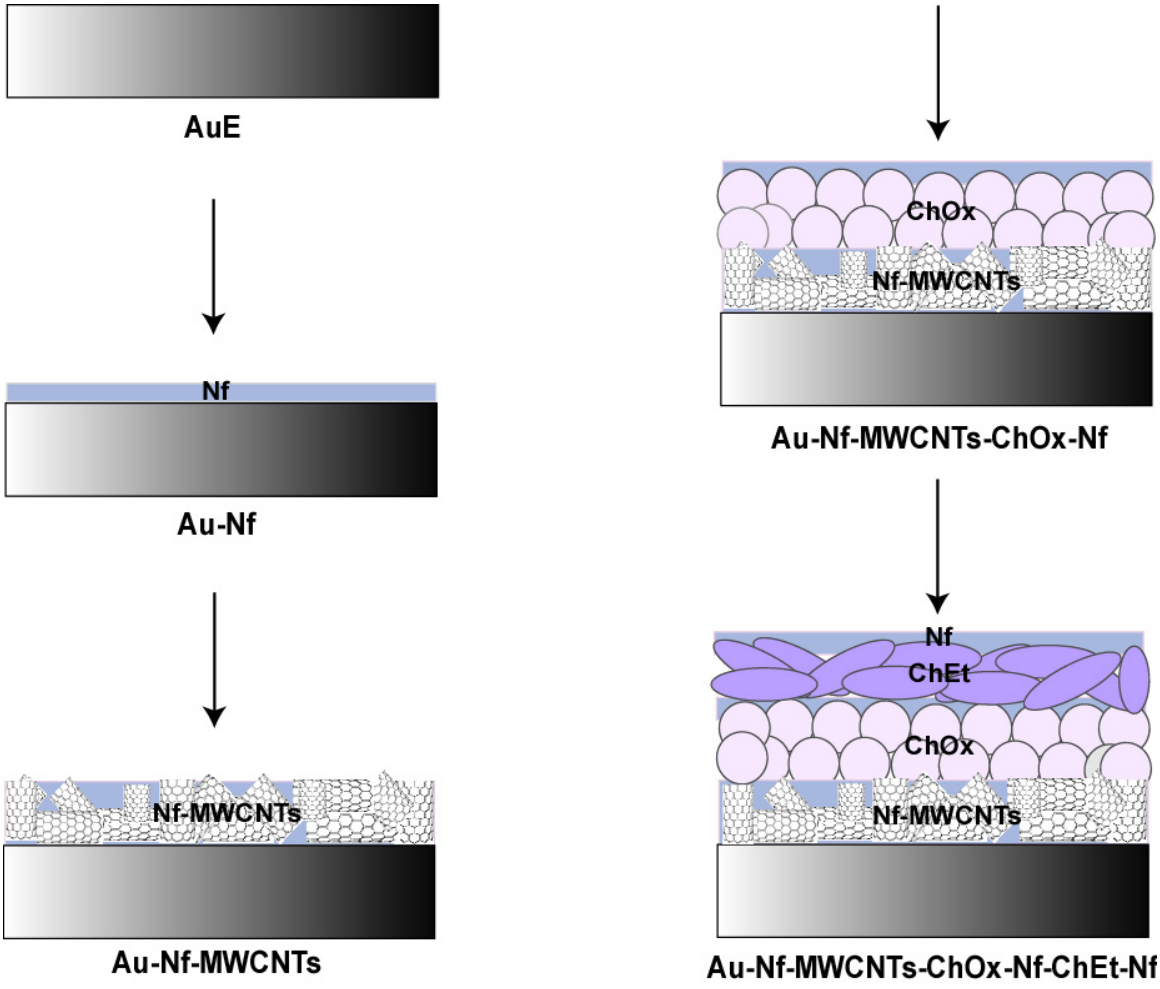

Scheme 4.1 Fabrication scheme of Au-Nf-MWCNTs-ChOx-Nf-ChEt-Nf bioelectrode: AuE: gold electrode, Nf: nafion, MWCNTs: multiwalled carbon nanotubes, ChOx: cholesterol oxidase, ChEt: cholesterol esterase

rod served as reference and counter electrodes, respectively. PBS (50mM, pH 7) was used as the supporting electrolyte. All potentials were measured and reported relative to the Ag/AgCl reference electrode. All experiments were performed at room temperature (RT). During the CV measurements, the electrolyte solution was constantly purged with argon gas. Electrochemical impedance spectroscopy (EIS) measurements were performed in a background solution of 5mM $K_3Fe(CN)_6/K_4Fe(CN)_6$ (1:1) and 0.1 M KCl in PBS (50 mM, pH 7) within the frequency range of 0.05 Hz to 10 kHz. The amplitude of the alternate voltage was 5 mV. All experiments were performed at room temperature (RT). Scanning electron microscopy (SEM) images were obtained on a scanning electron microscope (Leo 1430vp, Germany) using the following setting conditions: 15 KeV EHT, 50 mm aperture.

4.3. Results and Discussion

4.3.1. Morphological characterization of the bioelectrodes using SEM

Figure 4.1 shows the SEM images of Au–Nf, Au–Nf–MWCNTs and Au–Nf–MWCNTs–ChOx–Nf–ChEt–Nf electrodes revealing the stepwise changes in the electrode surface morphology at different stages of bioelectrode fabrication. As shown in figure, AuE modified with Nf shows the homogeneous surface (Figure 4.1A), whereas the SEM image of Au–Nf–MWCNTs electrode (Figure 4.1B) shows the granular porous morphology demonstrating the distribution of MWCNTs in Nf matrix on the electrode surface. When ChOx and ChEt were entrapped in this Nf–MWCNTs film to fabricate Au–Nf–MWCNTs–ChOx–Nf–ChEt–Nf bioelectrode, SEM image showed that the surface morphology changed into uniform globular and fibrillar structures (Figure 4.1C), attributed to the presence of ChOx and ChEt.

4.3.2. Electrochemical characterization of the bioelectrodes using EIS

Figure 4.2 represents the results of EIS studies carried out with electrodes in 5 mM $K_3Fe(CN)_6/K_4Fe(CN)_6$ (1:1) and 0.1 M KCl solution in PBS (50 mM, pH 7). Nature of the obtained impedance spectra, presented as Nyquist plots reveals that polarization at the electrode surface is due to a combination of kinetic and diffusion processes. The value of electron transfer resistance (R_{et}) at the electrode surface can be estimated directly from the diameters of Nyquist plots. It can be observed that R_{et} value dramatically increased when the gold electrode was coated with nafion (Au-Nf). Further, when MWCNTs were incorporated in the nafion film (Au-Nf-MWCNTs), the impedance got decreased that may be ascribed to the nanosize structure and high conductivity of MWCNTs. When ChOx and ChEt were immobilized in the Nf-MWCNTs film (Au-Nf-MWCNTs-ChOx-Nf and Au-Nf-MWCNTs-ChOx-Nf-ChEt-Nf), the R_{et} value further decreased upon each immobilization step. The result is intriguing as it is against the expectation that protein immobilization increases the R_{et} values by blocking the route for charge transfer from the electrolyte solution to the electrode surface. The incorporation of ChOx and ChEt may have altered the organization of Nf-MWCNTs matrix and thus facilitated electron exchange between bulk ferrocyanide solution and the electrode surface. Also, one bioelectrode was fabricated with both the ChOx and ChEt enzymes following similar procedure but no MWCNTs were incorporated (Au-Nf-ChOx-Nf-ChEt-Nf). As expected, in the absence of MWCNTs, again the R_{et} increased and became nearly equal to that of Au-Nf electrode. These results indicate that MWCNTs provide increased electroactive surface and favor enhanced electron transfer.

4.3.3. Response mechanism of the fabricated bioelectrodes

Figure 4.3 shows the results of CV studies carried out with Au, Au–Nf, Au–Nf–MWCNTs and Au–Nf–MWCNTs–ChOx–Nf electrodes in PBS (50mM, pH 7). No major difference was observed among the cyclic voltammograms of the bare Au (curve a) and Au–Nf electrodes (curve b). When the AuE is modified with Nf–MWCNTs matrix, an increase in the background current intensity was observed, which is attributed to the increased electroactive surface area provided by MWCNTs. Also, a pair of redox peaks were observed at 0.153 and 0.002V (curve c). These redox peaks are attributed to Nf–MWCNTs as these are absent in the CVs of Au and Au–Nf electrodes (curves a and b). Cyclic voltammogram for Au–Nf–MWCNTs–ChOx–Nf bioelectrode (curve d) shows a shift in the oxidation peak from 0.153 to 0.184 V. When the CV was done with Au-Nf–MWCNTs–ChOx–Nf bioelectrode in the presence of cholesterol, there is a further shift in the oxidation peak to 0.21V and an increase in the oxidation current intensity at 0.21V (curve f). Also, a CV was taken with Au–Nf–ChOx–Nf without the MWCNTs. In this case, the CV was similar to that of Au–Nf electrode without any additional peak showing the absence of electronic communication between ChOx and the electrode in the absence of MWCNTs. For the visual clarity, the CV is not included in the figure. From these CV results, it may be concluded that MWCNTs play a role in the electro-catalytic activity of the ChOx. It may be proposed that during ChOx catalysis, the Nf–MWCNTs matrix accepts electrons from the reduced ChOx and subsequently gets oxidized at the electrode surface. This suggests that the ChOx gets electrically contacted with Nf–MWCNTs matrix. Based on the CV studies, the working mechanism of the fabricated bioelectrodes in detecting total cholesterol can be proposed as shown in equations 4.1 to 4.4.

$$\text{Cholesterol ester} + H_2O \xrightarrow{\text{ChEt}} \text{Cholesterol} + \text{Fattyacids} \quad (4.1)$$

$$\text{ChOx-FAD}_{ox} + \text{Cholesterol} \longrightarrow \text{ChOx-FAD}_{red} + \text{HCEO} \quad (4.2)$$

$$\text{ChOx-FAD}_{red} + \text{MWCNTs}_{ox} \longrightarrow \text{ChOx-FAD}_{ox} + \text{MWCNTs}_{red} \quad (4.3)$$

$$\text{MWCNTs}_{red} \longrightarrow \text{MWCNTs}_{ox} + ne^- \quad (4.4)$$

where $ChOx–FAD_{ox}$ and $ChOx–FAD_{red}$ represent the ChOxs having oxidized and reduced forms of FAD, respectively.

4.3.4. Electron transfer properties of Au–Nf–MWCNTs–ChOx–Nf bioelectrode

Cyclic voltammetry was carried out with Au–Nf–MWCNTs–ChOx–Nf bioelectrode in PBS (50 mM, pH 7.0) at different potential scan rates (ν) (50 to 700 mV s^{-1}) to obtain its various electron transfer parameters. At ν =50 mVs^{-1}, the peak separation (ΔEp) was about 155 mV (Figure 4.4A), which is more than the peak separation of a reversible process (59 mV), indicating a quasi-reversible redox process (Scott and Lukehart 2007). Moreover, as the scan rate increases, the anodic (E_{pa}) and cathodic (E_{pc}) peak potentials shift to more positive and more negative values respectively increasing the ΔEp (Figure 4.4A) further suggesting a quasi-reversible process. Besides this, the magnitudes of anodic (I_{pa}) and cathodic (I_{pc}) peak currents increase linearly with increasing scan rate in the range of 50 to 700 mVs^{-1} (Figure 4.4B) as expected for a surface confined redox process and indicating a thin-layer electrochemical behavior (Scott and Lukehart 2007). Both I_{pa} and I_{pc} are also proportional to the square root of scan rate ($\nu^{1/2}$) over the range of 50-700 mV s^{-1} (Figure 4.4C), suggesting that the electrode reaction is a diffusion-controlled process (Yang et al. 2006c).

For a quasi-reversible wave, the relationship between peak potential and scan rate conforms the following equation (Laviron's equation) (Laviron 1974):

$$E_p = E^{o'} + \frac{RT}{\alpha nF} + \frac{RT}{\alpha nF} \ln \nu \qquad (4.5)$$

E_p is the peak potential (cathodic or anodic), $E^{o'}$ is the apparent standard potential. R is the thermodynamic gas constant (8.314 J K^{-1} mol^{-1}), F is the Faraday constant (96,500 C mol^{-1}) and T is the temperature (298 K). The symbols n and ν are the electron transfer number and scan rate, respectively. The product of charge transfer coefficient (α) and n, αn was found to be 0.53, calculated from the slope of the E_{pa} versus $\ln \nu$ plot (Figure 4.4D). Because of $0.5 < \alpha < 1.0$ in general, we valued that $n = 1$ and $\alpha = 0.53$. This result revealed that the redox reaction of ChOx in MWCNTs film was a single electron transfer process.

The surface concentration of the ionic species (Γ) (mol cm^{-2}) onto Au–Nf–MWCNTs–ChOx–Nf bioelectrode can be estimated from the plot of peak current versus scan rate (ν) using Brown-Anson model that is based on the following equation (Laviron 1979):

$$Ip = \frac{n^2 F^2 \Gamma A \nu}{4RT} \qquad (4.6)$$

where n is the number of electrons transferred which is 1 in the case of Au–Nf–MWCNTs-ChOx-Nf electrode, and A is the surface area of the electrode (0.196 cm^2). The symbols F, R and T have their usual meanings. When the scan rate (ν) was 100

mV/s, the anodic peak current (I_{pa}) was 5.942×10^{-5}A. The total surface concentration is found to be 3.22×10^{-9} mol cm^{-2}.

The heterogeneous electron transfer constant (k_s) of the Au–Nf–MWCNTs–ChOx–Nf bioelectrode could be obtained by the following equation (Laviron 1979):

$$\log k_s = \alpha \log(1-\alpha) + (1-\alpha)\log\alpha - \log\frac{RT}{nF\nu} - \frac{\alpha(1-\alpha)nF\Delta E_p}{2.3RT} \qquad (4.7)$$

Taking ΔEp =239 mV, at ν = 100 mVs^{-1}, n =1 and α = 0.53, the vale of k_s for Au–Nf–MWCNTs–ChOx–Nf bioelectrode was calculated to be 0.189 s^{-1} which signifies efficient electron transfer between ionic species in Nf–MWCNTs–ChOx–Nf film and the electrode.

4.3.5. Response characteristics of the fabricated bioelectrodes towards cholesterol

The response characteristics of both Au–Nf–MWCNTs–ChOx–Nf and Au–Nf–MWCNTs–ChOx–Nf–ChEt–Nf bioelectrodes were determined to examine whether the incorporation of ChEt in the bioelectrode has any interference in the detection of cholesterol by ChOx. Figure 4.5A and B displays the amperometric response of Au–Nf–MWCNTs–ChOx–Nf and Au–Nf–MWCNTs–ChOx–Nf–ChEt–Nf bioelectrodes, respectively, for successive step changes of cholesterol concentrations in PBS (50mM, pH 7) at an operating potential of 0.21 V. For both the bioelectrodes, the magnitude of the anodic peak current at 0.21V was found to increase linearly with increase in cholesterol concentration. The response characteristics for both the electrodes are summarized in Table 4.1.

Table 4.1 Response characteristics of bioelectrodes

Response Characteristics	Bioelectrode	
	Au-Nf-MWCNTs-ChOx-Nf	Au-Nf-MWCNTs-ChOx-Nf-ChEt-Nf
Linear Range	0.080 to 0.950 mM	0.080 to 0.645 mM
Detection limit	0.025 mM	0.010 mM
Sensitivity	308.90 µA mM^{-1}	690.13 µA mM^{-1}
SD* limit	2.676 µA	2.150 µA

*Standard deviation

It can be observed from Table 4.1 that the sensitivity of Au–Nf–MWCNTs–ChOx–Nf–ChEt–Nf is more than Au–Nf–MWCNTs–ChOx–Nf bioelectrode. This may be attributed to better substrate sequestration to the ChOx active site in the presence of ChEt. The increased sensitivity in turn led to smaller detection limit (DL) in case of Au–Nf–MWCNTs–ChOx–Nf–ChEt–Nf bioelectrode. The present system was observed to show a wider cholesterol response range when compared to some other reported range of 0.5–25 µM for ChOx and ChEt immobilized in laponite clay nanoparticle-poly(12-pyrrol-1-yldodecyl)triethylammonium tetrafluoroborate on Pt disc electrode (Arya et al. 2008) and 0.04–0.27mM obtained when ChOx and horseradish peroxidase (HRP) were co-immobilized in tributylmethyl phosphonium chloride polymer membrane on pyrolitic graphite electrode (Bongiovanni et al. 2001) etc. The DL for the constructed bioelectrodes was determined from the expression $DL = (3 \times SD) / Sensitivity$ (where SD is the estimated standard deviation for the points used to construct the calibration curve and the $Sensitivity$ its slope). The calculated DL for our constructed bioelectrodes compares favorably with values reported for ChOx entrapped in ferrocene monocarboxylicacid-PPy/Pt/Pt electrode (0.012mM) (Vidal et al. 2002) and when ChOx covered in Nf was

entrapped in PPy/PB/1-propanethiol (SAM)/Pt electrode (0.012mM) (Vidal et al. 2004b). The fabrication reproducibility of both the bioelectrodes was estimated from the response to 0.33 mM cholesterol at three bioelectrodes prepared by the same procedure. The results showed an acceptable reproducibility with a RSD of 2.6% for Au–Nf–MWCNTs–ChOx–Nf and 2.1% for Au–Nf–MWCNTs–ChOx–Nf–ChEt–Nf bioelectrodes.

4.3.6. Interference study

For exploring the efficient use of the fabricated Au–Nf–MWCNTs–ChOx–Nf–ChEt–Nf bioelectrode in the specific determination of total cholesterol in real samples, effects of some common interferents in cholesterol determination, such as glucose (Glu), ascorbic acid (AA), uric acid (UA), lactic acid (LA) and urea (U) on the bioelectrode response have been studied. The current response at 0.21V of the Au–Nf–MWCNTs–ChOx–Nf–ChEt–Nf bioelectrode in solutions containing equal concentration of cholesterol (0.33mM) and each interferent (0.33mM) has been determined. Selectivity coefficient (SC) of the fabricated bioelectrode for each interferent was calculated using the formula, $SC = I_{c+i}/I_c$ where I_{c+i} and I_c are bioelectrode response at 0.21 V for cholesterol (0.33 mM) in the presence and absence of each interferents respectively. The bioelectrode response did not get significantly affected in the presence of either of these interferents (Figure 4.6). Moreover, the actual level of these interferents in serum is usually very low as compared to the concentration used for this study, so interference from these compounds is negligible when the biosensor is used for analyzing real serum samples. The optimum selectivity of the bioelectrode towards cholesterol may be attributed to two factors. Firstly, the working potential chosen is 0.21 V. At such a lower potential, the contribution of many interferents towards current response may get substantially

minimized. Secondly, Nf polymer acts as a selective barrier for the restricted access of many interferents to the electrode surface by electrostatic repulsion (Cui et al. 2001; Wang et al. 2003). The use of Nf polymer has been reported earlier also to decrease the interferences caused by compounds present in biological samples (Lim et al. 2005; Manesh et al. 2008; Shobha Jeykumari and Sriman Narayanan 2008). Based on these results, the fabricated bioelectrode can be proposed for use in physiological conditions.

4.3.7. Determination of cholesterol in serum samples

For practical applications, the analysis of total cholesterol in serum samples is important. The practical usability of the fabricated Au–Nf–MWCNTs–ChOx–Nf–ChEt–Nf bioelectrode was judged by the determination of total cholesterol content in human serum samples. Five serum samples were first analyzed using enzymatic cholesterol estimation kit (CHOD-PAP method) using three enzymes, ChEt, ChOx and peroxidase, and the chromogenic reagents p-hydroxybenzenesulphonate and 4-aminoantipyrine. In the CHOD-PAP method, ChEt first hydrolyzes the esterified cholesterol fraction into cholesterol and ChOx subsequently oxidizes the cholesterol liberating H_2O_2. Peroxidase utilizes H_2O_2 to convert 4-aminoantipyrine into quinoneimine (Trinder's reaction) (Trinder and Webster 1984) detected spectrophotometrically at 500 nm. Then, the same five serum samples were analyzed using the Au–Nf–MWCNTs–ChOx–Nf–ChEt–Nf bioelectrode by diluting the samples with a dilution factor of 30 to make the concentrations fall in the linear range of the bioelectrode. The current response against each serum sample at 0.21V was measured. The cholesterol concentration was then determined by interpolation on the linear region of the calibration curve (Figure 4.6B inset). The cholesterol amount in all the serum samples, determined with the bioelectrode

and the cholesterol kit, were compared using paired t-test (Sigma 11) and the results show that there is no significant difference (P = 0.395) between the values obtained with both the methods. These results imply a reasonable agreement between both the methods of analysis for serum cholesterol, and verify the reliability of the responses obtained using the Au–Nf– MWCNTs–ChOx–Nf–ChEt–Nf bioelectrode.

4.3.8. Operational and storage stability

The repeatability or operational stability of both the fabricated bioelectrodes was investigated from 16 successive measurements with 0.33 mM cholesterol during a period of 4 h. No change in the current response was observed till the last measurement. This high operational stability indicates that there was no enzyme leakage from the bioelectrodes. The storage stability of both the bioelectrodes was checked by carrying out voltammetric measurements at the regular intervals of three days and it has been found that these electrodes retain about 90% of the original response even after three weeks when stored in PBS (pH 7) at 4ºC (Figure 4.7). The half life ($t_{1/2}$ of initial activities) of the constructed enzyme electrode was found to be nearly 6 months. The high stability of the bioelectrode can be ascribed to the Nf–MWCNTs matrix which provides a suitable microenvironment for enzyme entrapment and also prevent enzyme from leaching.

4.4. Conclusions

In this study, a bioelectrode was fabricated for total cholesterol estimation in serum by entrapping ChOx and ChEt onto Nf–MWCNTs hybrid matrix deposited on an Au electrode. MWCNTs in combination with Nf are used for the first time as the matrix for the immobilization of ChOx and ChEt for total cholesterol estimation in human serum. It

is found that the granular morphology of Nf–MWCNTs provides a better biocompatible environment for the enzyme and the MWCNTs provide an enhanced electronic communication between the ChOx and Au electrode for a highly sensitive and selective estimation of cholesterol. The bioelectrode exhibited good response characteristics with a proper linearity, good sensitivity, high selectivity and high operational and storage stability.

Figures

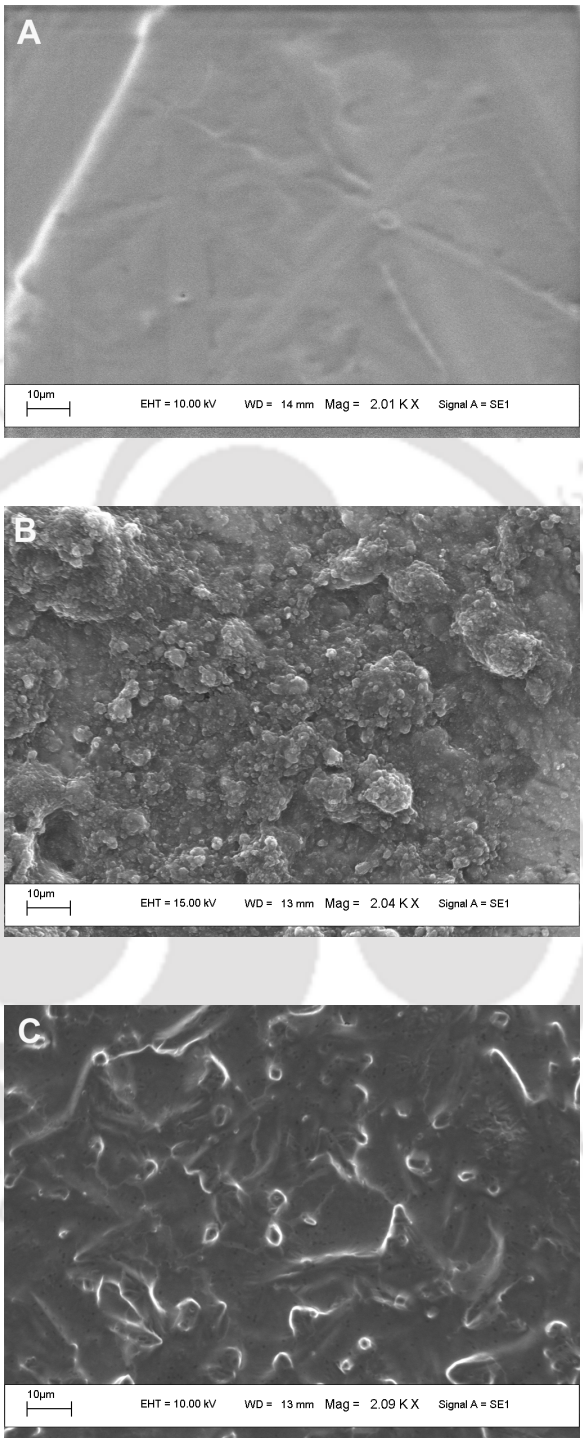

Figure 4.1 Scanning electron microscopy at major steps of Au-Nf-MWCNTs-ChOx-Nf-ChEt-Nf bioelectrode fabrication:
A: Au-Nf, **B**: Au-Nf-MWCNTs and **C**: Au-Nf-MWCNTs-ChOx-Nf-ChEt-Nf electrodes

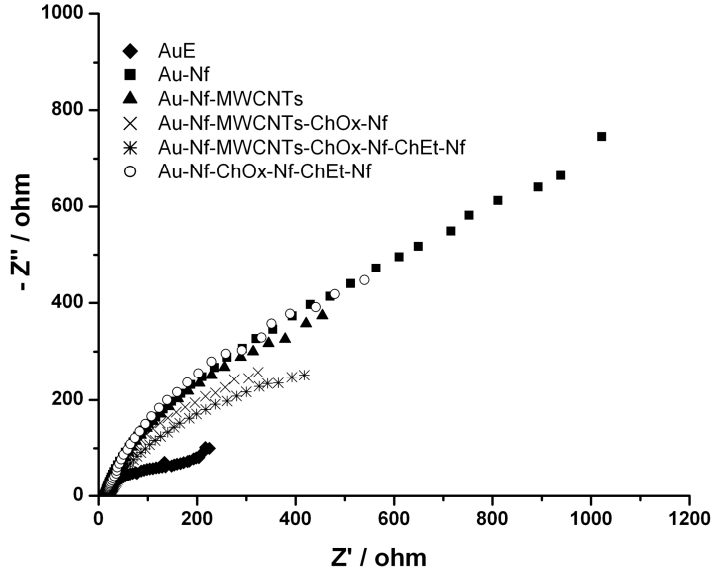

Figure 4.2 Electrochemical impedance spectroscopy at major steps of Au-Nf-MWCNTs-ChOx-Nf-ChEt-Nf bioelectrode fabrication:
Spectra were obtained at AuE, Au-Nf, Au-Nf-MWCNTs, Au-Nf-MWCNTs-ChOx-Nf, Au-Nf-MWCNTs-ChOx-Nf-ChEt-Nf and Au-Nf-ChOx-Nf-ChEt-Nf electrodes in 5 mM $K_3Fe(CN)_6/K_4Fe(CN)_6$ (1:1) and 0.1 M KCl in PBS

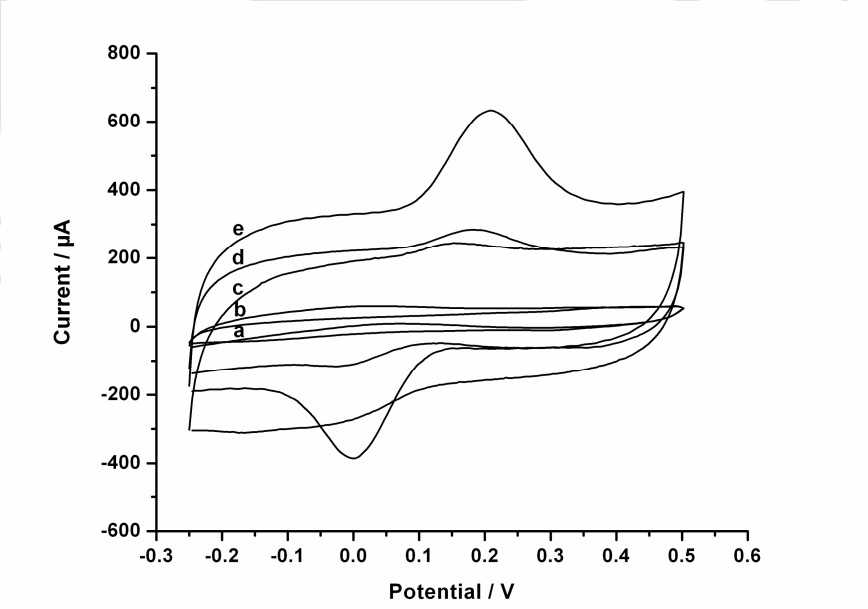

Figure 4.3 Response characteristics of the bioelectrodes:
CVs were recorded with (a) Au, (b) Au-Nf, (c) Au-Nf-MWCNTs and (d) Au-Nf-MWCNTs-ChOx-Nf in PBS (50 mM, pH 7). CVs was also recorded with (e) Au-Nf-MWCNTs-ChOx-Nf in presence of 0.33 mM cholesterol in PBS (50 mM, pH 7). In all cases a potential scan rate of 0.1V/s was used

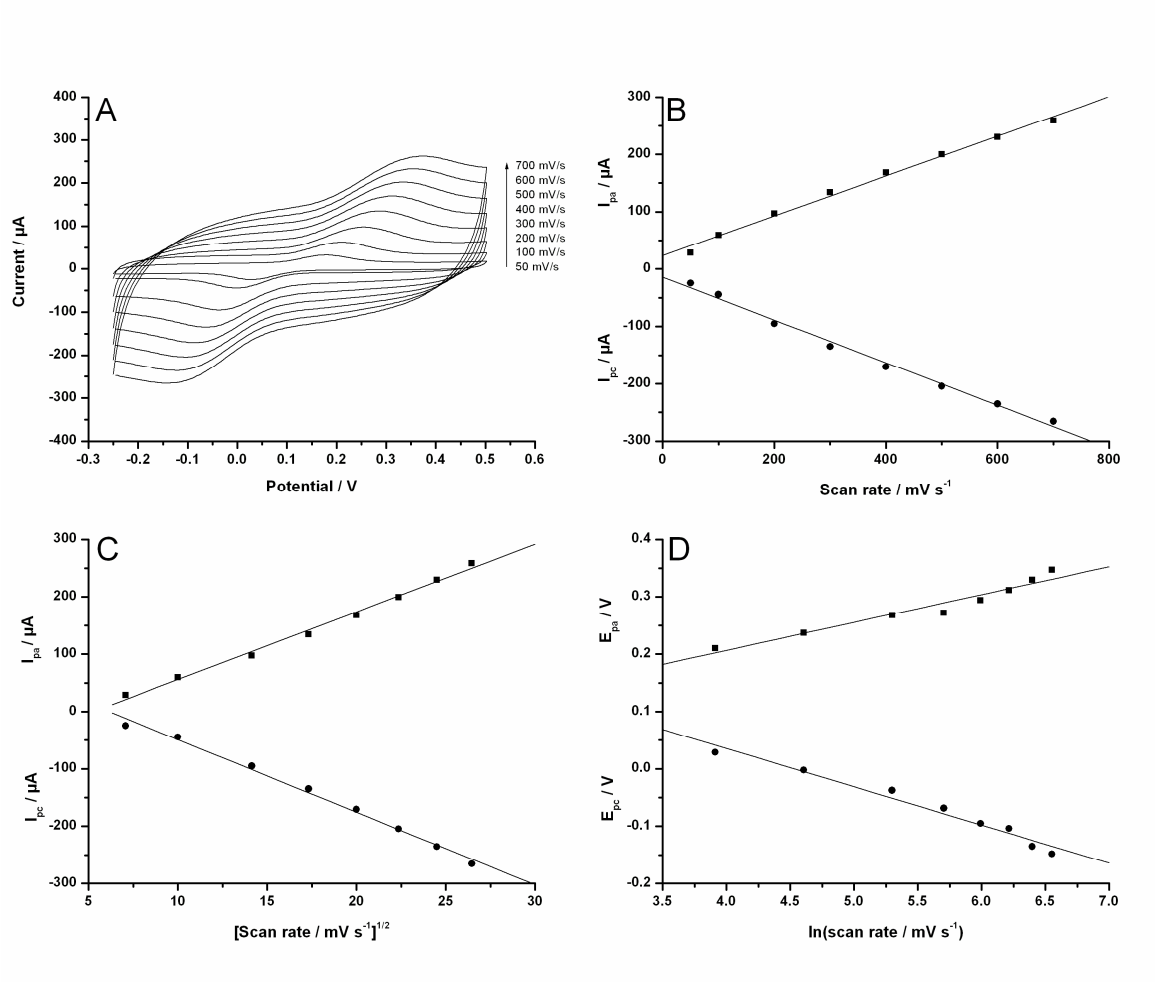

Figure 4.4 Scan rate dependent electrochemical studies of the Au–Nf–MWCNTs–ChOx–Nf bioelectrode:
A: CVs recorded with Au–Nf–MWCNTs–ChOx–Nf bioelectrode in PBS (50 mM, pH 7.0). Scan rate: from 50 to 700 mV s^{-1}. **B:** Plot of anodic (I_{pa}) and cathodic (I_{pc}) peak currents vs. scan rate. **C:** Plot of anodic (I_{pa}) and cathodic (I_{pc}) peak currents vs. square root of scan rate. **D:** Plot of anodic (E_{pa}) and cathodic (E_{pc}) peak potentials vs. ln(scan rate)

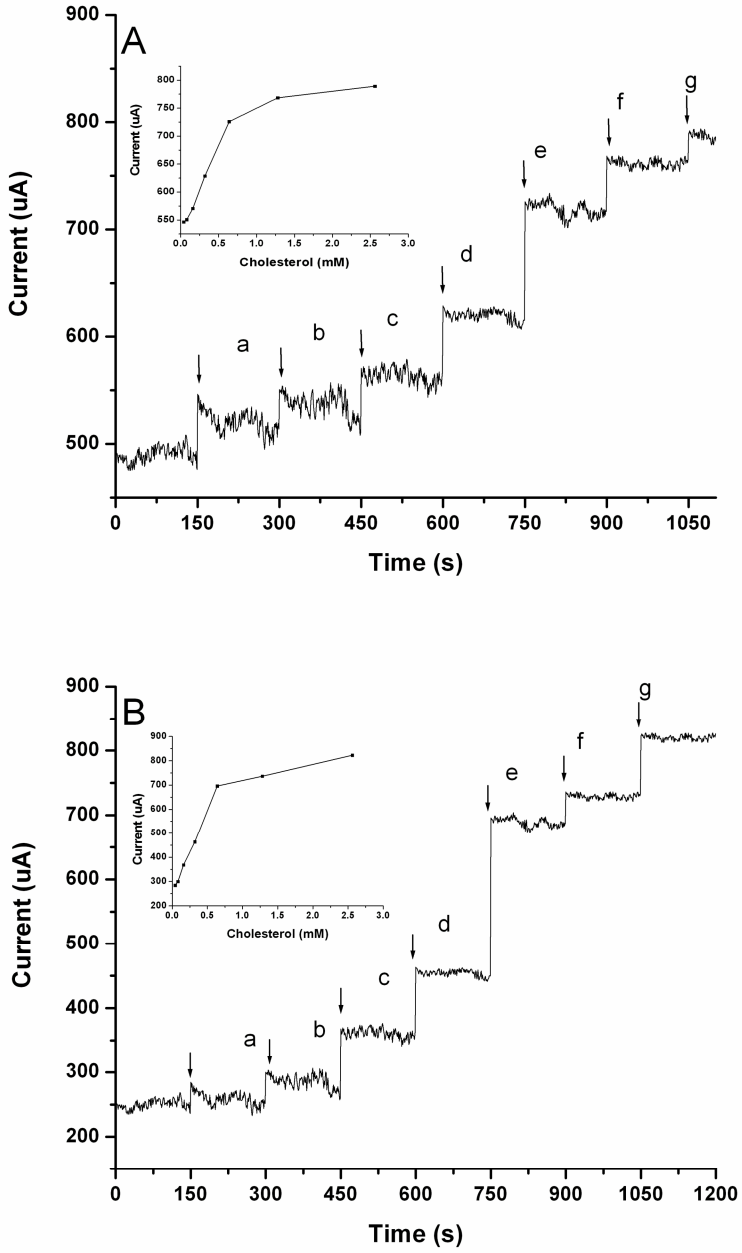

Figure 4.5 Chronoamperometric current responses of the Au-Nf-MWCNTs-ChOx-Nf and Au-Nf-MWCNTs-ChOx-Nf-ChEt-Nf bioelectrodes with cholesterol:
A: Au-Nf-MWCNTs-ChOx-Nf and **B**: Au-Nf-MWCNTs-ChOx-Nf-ChEt-Nf bioelectrodes with successive addition of (a) 0.04 mM, (b) 0.08 mM, (c) 0.16 mM, (d) 0.32 mM, (e) 0.64 mM, (f) 1.28 mM and (g) 2.56 mM cholesterol. Inset of both (A) and (B) shows calibration plots for the respective bioelectrodes

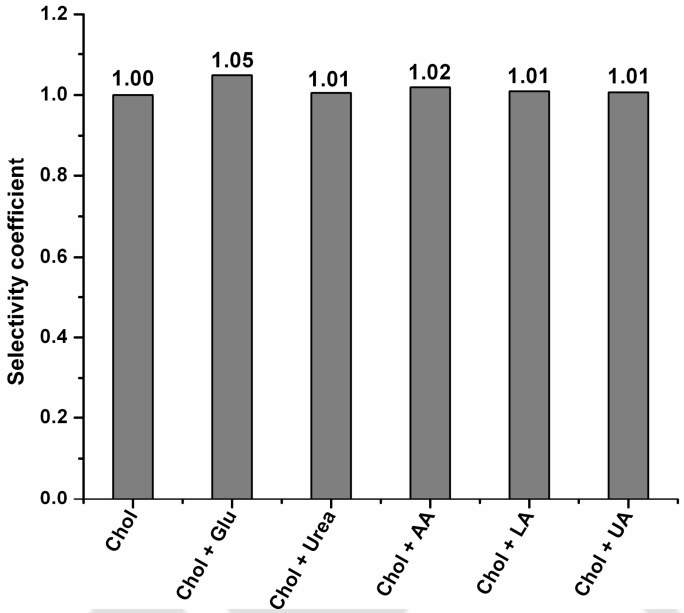

Figure 4.6 Effect of potential interfering agents on the Au-Nf-MWCNTs-ChOx-Nf-ChEt-Nf bioelectrode response:
(Chol: cholesterol, Glu: Glucose, AA: ascorbic acid, LA: lactic acid, UA: uric acid)

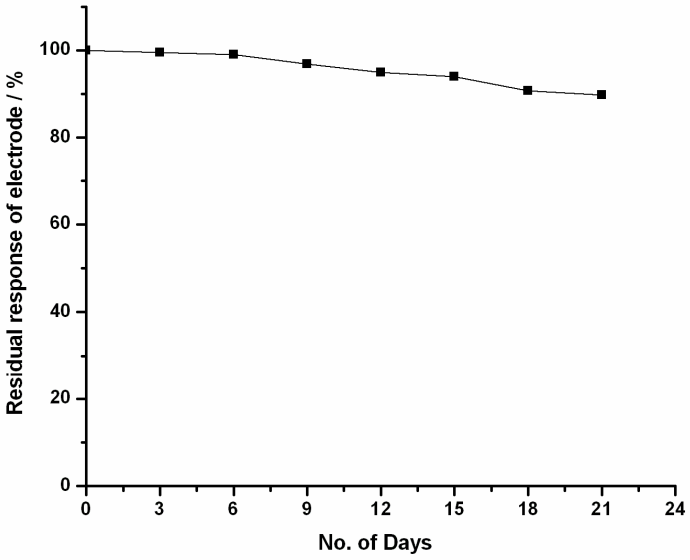

Figure 4.7 Stability of the Au-Nf-MWCNTs-ChOx-Nf-ChEt-Nf bioelectrode

CHAPTER 5

Gold Nanoparticles based Cholesterol Biosensor

5.1. Overview

The major challenge to develop amperometric cholesterol biosensors is the establishment of suitable electrical communication between the redox center of ChOx i.e. FAD and the electrode surface which is prevented by the deep embedment of FAD in the protein core (Willner and Katz 2000; Willner et al. 2002). Another common problem is that the total number of catalytically active immobilized enzyme units is usually small due to the random orientation and partial denaturation of the immobilized enzyme molecules on the electrode surface. As a result, cholesterol biosensors based on ChOx do not exhibit high signals leading to low sensitivity. Also, the poor compatibility of the support matrix may restrict the analytical efficiency of the developed biosensor (Sarma et al. 2009). Many efforts have been made for developing suitable support matrix that provides better environment for the efficient enzyme loading and maintenance of the enzymatic bioactivity so as to increase the sensitivity of the biosensor.

Varieties of nanoparticles, including metal nanoparticles and oxide nanoparticles have been widely used in constructing electrochemical biosensors (Li et al. 2006; Yang et al. 2006a). Especially, gold nanoparticles (AuNPs) have been extensively used as enhancing interfacial platform for developing electrochemical sensors (Guo and Wang 2007). The high surface area and a biocompatible microenvironment provided by the AuNPs based matrices facilitate higher enzyme loading and help enzyme to retain its bioactivity, respectively (Crumbliss et al. 1992; Jena et al. 2010). The excellent conductivity of the AuNPs makes them suitable for acting as "electronic wires" to enhance the transfer of electrons generated from the enzyme catalytic redox reaction to the electrode surfaces (Sun et al. 2010; Willner et al. 2006a) which in turn can decrease the overpotentials of many analytically important electrochemical reactions. These properties of AuNPs make them excellent candidate for replacing potentially harmful mediators in the construction of biosensors (Willner et al. 2007b).

Although AuNPs have been widely used for other biosensors, they are not adequately studied in case of cholesterol biosensors. The objective of this study is to develop a suitable scheme for fabricating AuNPs based cholesterol bioelectrode with improved stability and sensitivity. Among various enzyme immobilization approaches for the construction of AuNPs based biosensors, technique based on electrostatic interaction has attracted much attention because of its simplicity in procedure (Yi et al. 2000). Although, AuNPs could efficiently adsorb proteins, the physical adsorption technique has a fatal drawback of reduced stability. Also, the random and non-optimized positioning of the proteins reduces the overall bioactivity of the adsorbed enzymes. In the present study,

ChOx molecules were covalently immobilized on the surface of AuNPs which were previously deposited on gold electrode (AuE) using dithiol via Au–S bond.

5.2. Experimental Approaches

5.2.1. Reagents and stock solutions

Cholesterol oxidase (EC 1.1.3.6 from *Pseudomonas fluorescens*), cholesterol esterase (ChEt) (EC 3.1.1.13 from *Pseudomonas sp*.), peroxidase from horseradish (HRP), cholesterol, gold (III) chloride solution (~30 wt.% in dilute HCl), N-ethyl-N'-(3-dimethylaminopropyl) carbodimide (EDC), N-hydroxysuccinimide (NHS), 1,6-hexanedithiol, and 11-mercaptoundecanoic acid (MUA) were bought from Sigma–Aldrich (USA). Cholesterol estimation kit was obtained from Merck. All other chemicals were of analytical grade. Human serum samples were collected from normal healthy volunteers.

Cholesterol stock (10mM) was prepared in 5% Triton X-100 solution and stored at 4ºC. Stock solutions of ChOx (8 μM) and HRP (23 μM) were freshly prepared in phosphate buffer solution (PBS) (50 mM, pH 7.0) and that of ChEt (1 mg mL^{-1}) in 400 mM PBS (pH 7) prior to being used. The stock solutions of 4-aminoantipyrine (4-AAP) (0.1 M) and phenol (0.1 M) were freshly prepared in de-ionized water just before the experiments. AuNPs were prepared by the method of citrate reduction of gold (III) chloride solution in water at boiling temperature according to the literature (Frens 1973; Turkevich et al. 1953). All solutions were prepared with deionized water (Millipore, Bedford, MA).

5.2.2. Fabrication of the bioelectrode

Scheme 5.1 shows the schematic diagram for the fabrication of the bioelectrode. An AuE (diameter = 0.5 cm) was cleaned by polishing it with alumina powder, washing it ultrasonically with 70% ethanol and water separately for 15 min each and finally drying in air. The cleaned AuE was dipped in 10 mM freshly prepared ethanolic solution of 1,6-hexanedithiol for 24 h. The dithiol modified electrode (AuE/dithiol) was rinsed with water and then dipped in freshly prepared AuNPs solution for 6 h under mild shaking condition. The AuNPs modified electrode (AuE/dithiol/AuNPs) was rinsed with water and then dipped in 0.5 mM freshly prepared ethanolic solution of MUA for 5 h to obtain a layer of carboxylic group functionalized AuNPs. This AuE/dithiol/AuNPs/MUA electrode was dipped for 10 min in a freshly prepared solution of EDC (200mM) and NHS (50mM) to activate the carboxylic group on the AuNPs surface. Then it was dipped in freshly prepared ChOx solution (8 μM) for 12 h to obtain AuE/dithiol/AuNPs/MUA/ChOx bioelectrode. For preparing AuE/MUA/ChOx electrode, a cleaned AuE was first functionalized with MUA as above, treated with a solution of EDC (200mM) and NHS (50mM) for 10 min and then dipped in freshly prepared ChOx solution (8 μM) for 12 h. The fabricated bioelectrodes were immersed in PBS (50 mM, pH 7) for 15 min prior to being used. The fabricated bioelectrodes were stored at 4ºC when not in use.

5.2.3. Apparatus and measurements

Cyclic voltammetry (CV) and electrochemical impedance spectroscopy (EIS) were performed with an Autolab PGSTAT 1212 (Eco Chemie, Netherlands). A three-electrode

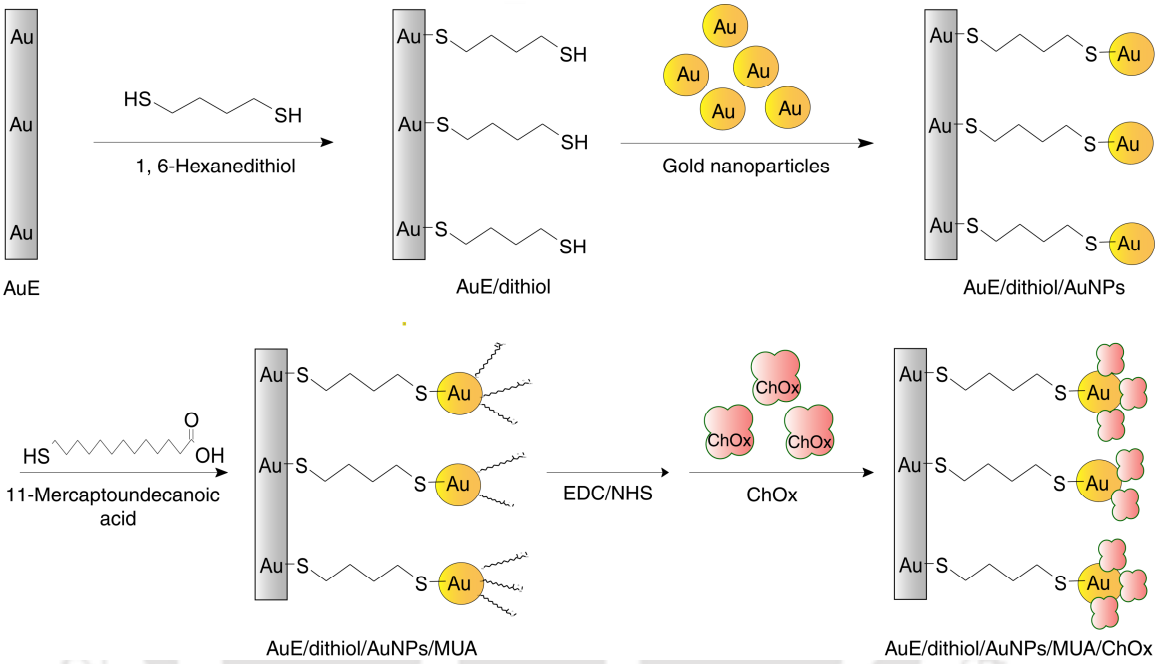

Scheme 5.1 Fabrication scheme of AuE/dithiol/AuNPs/MUA/ChOx bioelectrode

system was employed with platinum rod as counter electrode, Ag/AgCl (saturated KCl) as reference electrode, and AuE or modified AuE the working electrode. All potentials were measured and reported relative to the Ag/AgCl reference electrode. During the CV measurements, the electrolyte solution was constantly purged with argon gas. EIS measurements were performed in a background solution of 5mM $K_3Fe(CN)_6/K_4Fe(CN)_6$ (1:1) and 0.1 M KCl in PBS (50 mM, pH 7) within the frequency range of 0.05 Hz to 10 kHz. The amplitude of the alternate voltage was 5 mV. All experiments were performed at room temperature (RT). Atomic force microscopy (AFM) was performed using an ambient air scanning probe microscope (Agilent Technologies 5500, USA). Images were recorded with typical contact mode using Picoscan 5 software. Transmission electron microscopy (TEM) images are acquired with a 200 KV electron microscope (JEOL JEM, 2100) (CIF, IIT Guwahati). UV-Vis experiments were carried out with a CARY 300 BIO double beam spectrophotometer (Varian, USA).

The enzyme loading of the electrode was determined in terms of number of enzyme units retained per unit surface area (U cm^{-2}) of the electrode. The enzyme units were calculated using a spectrophotometric rate determination method involving the measurement of H_2O_2 generation accompanying the oxidation of cholesterol (Allain et al. 1974). The ChOx immobilized electrode was immersed and incubated for 10 min at RT in a reaction mixture containing cholesterol (0.5 mM), HRP (114 nM), 4-AAP) (1 mM) and phenol (6 mM) in total 1 mL PBS (50 mM, pH 7.0). The electrode was removed and the appearance of quinoneimine dye formed during the reaction was measured at 500 nm. The enzyme loading (U cm^{-2}) was calculated using the following formula:

$$U\ cm^{-2} = \frac{\Delta A}{0.5\varepsilon_{500} at} \qquad (5.1)$$

where, ΔA is the change in absorbance in time t of incubation of the ChOx immobilized electrode and a is the area of the electrode. The molar extinction coefficient of quinoneimine dye at 500 nm (ε_{500}) is taken as 13.78 $mM^{-1}\ cm^{-1}$.

5.3. Results and Discussion

5.3.1. Characterization of the gold nanoparticles

The synthesized AuNPs were characterized using UV-Vis spectroscopy and TEM. The synthesized AuNPs showed an absorption maximum at 527 nm. TEM pictures were analyzed with ImageJ software. The average AuNPs size (diameter, D) was calculated by considering ~100 particles from multiple TEM pictures of the same sample acquired from different locations of TEM grid. One representative TEM picture of the synthesized AuNPs is presented in Figure 5.1. The average diameter of the synthesized AuNPs was found to be 21 nm.

5.3.2. Morphological characterization of the fabricated bioelectrode with atomic force microscopy

AFM measurements were carried out to characterize the morphological changes of the electrode surface obtained after major steps of bioelectrode fabrication. Figure 5.2A shows the representative 2D and 3D AFM images of the bare gold disc. Figure 5.2B shows the AFM images of AuNPs attached to the dithiol-modified gold disc with the formation of numerous clusters the diameter of which varied from 20 to 100 nm distributed homogenously over the gold surface. Also, the surface of the gold

nanoparticles modified disc is rougher than that of bare gold disc. This provided a significant increase of effective electrode surface area relevant for greater immobilization of biomolecules. When ChOx was assembled on the AuNPs modified gold disc, the AFM images further changed (Figure 5.2C). The AuE/dithiol/AuNPs/MUA/ChOx disc surface shows aligned structures which are formed by the assembling of globular ChOx molecules on the AuNP cluster surfaces. The AFM images indicate that the enzyme was successfully incorporated on the immobilized AuNPs over the electrode surface. AFM image was also taken for an AuE/MUA/ChOx disc in which ChOx molecules were immobilized directly on the bare Au disc without an interfacial layer of AuNPs. For preparing such disc, the Au disc was first functionalized with MUA and then ChOx molecules were covalently immobilized on the modified surface using EDC and NHS. It can be observed that ChOx were immobilized on the functionalized bare disc as evident from Figure 5.2D.

5.3.3. Electrochemical characterization of the fabricated bioelectrodes

5.3.3.1. Cyclic voltammetry

CV of bare AuE and modified AuEs was done in a solution of 5mM $K_3Fe(CN)_6/K_4Fe(CN)_6$ (1:1) and 0.1 M KCl in PBS (50 mM, pH 7.0) to monitor changes in their electrochemical behavior introduced at different steps of electrode modification (Figure 5.3A). The CV at bare AuE shows a well defined electrochemical response for $Fe(CN)_6^{4-/3-}$ with a couple of redox peaks. After the electrode was modified with dithiol (AuE/dithiol), the CV curve changed drastically and the peak currents at the AuE/dithiol decreased dramatically in comparison with those of AuE. This may be due to the slow electron transfer kinetics through the negatively charged dithiol film. However, when

AuNPs were self-assembled on the dithiol film (AuE/dithiol/AuNPs), a quasi-reversible CV was obtained with increased peak currents. This shows that AuNPs have a marked influence on improving the conductivity of the modified electrode. Since the citrate stabilized AuNPs are negatively charged species, they repulse the negatively charged $Fe(CN)_6^{4-/3-}$ and interfere with the diffusion of ferricyanide towards the electrode surface and therefore, the observed peak current of AuE/dithiol/AuNPs is less than that of AuE. CV of AuE/dithiol/AuNPs/MUA electrode is almost similar with that obtained from AuE/dithiol/AuNPs electrode except a little decrease in the peak current. This indicates that the MUA does not have much effect on the electron transfer process of AuNPs because only the surface citrate ions are replaced by the MUA molecules and the overall surface charge density has not changed. CV of AuE/dithiol/AuNPs/MUA/ChOx electrode shows a greatly diminished ferricyanide response and enlarged peak to peak separation which indicates that an insulating layer of ChOx is introduced.

5.3.3.2. Electrochemical impedance spectroscopy

EIS was employed to further monitor the interfacial properties on the electrode surface during the stepwise assembly of the bioelectrode. Figure 5.3B shows the impedance spectra presented as Nyquist plots (−Z' vs Z') obtained on different modified electrodes in a solution of 5mM $K_3Fe(CN)_6/K_4Fe(CN)_6$ (1:1) and 0.1 M KCl in PBS (50 mM, pH 7.0). The value of the electron-transfer resistance (R_{et}) at the electrode surface can be estimated directly from the diameters of the high frequency semicircle. The impedance spectra of the bare AuE (curve a) consist of a small semicircle (R_{et}: 71 Ω) with an almost straight tail line, which is characteristic of a diffusional limiting step of the electrochemical process. The diameter of the high frequency semicircle was significantly

increased (R_{et}: 26,000 Ω) by the surface deposition of the 1,6-hexanedithiol layer (curve b). This implies that the assembled dithiol film generated an obstruction to the electron transfer of the electrochemical probe at electrode surface. After the AuNPs were assembled on the dithiol film, the diameter of the high frequency semicircle was significantly reduced with a R_{et} value of 474 Ω (curve c), implying that AuNPs may play an important role in accelerating the electron transfer process. Since, the surface of the AuNPs is covered with a shell of citrate ions, therefore the R_{et} value of AuE/dithiol/AuNPs (curve c) is larger than that of AuE (curve a). The impedance spectrum of AuE/dithiol/AuNPs/MUA (curve d) was almost coincided with that of AuE/dithiol/AuNPs (curve c) with a R_{et} value of 586 Ω. This indicates that chemosorption of MUA molecules on AuNPs surface did not have much effect on the electron transfer process. As shown in curve e, great increase in semicircular diameter of the impedance spectrum was found again when incubating the AuE/dithiol/AuNPs/MUA electrode in a ChOx solution for 12 h indicating the formation of a ferrocyanide transport-blocking layer on the electrode. These results are consistent with that of CV experiments (Figure 5.3A) implying that ChOx is successfully immobilized on a layer of AuNPs and AuE/dithiol/AuNPs/MUA/ChOx bioelectrode is developed.

5.3.4. Response mechanism of the AuE/dithiol/AuNPs/MUA/ChOx bioelectrode

CV was done in PBS (50 mM, pH 7.0) for AuE and different modified AuEs at major steps of bioelectrode fabrication. No redox peaks were observed for bare AuE (Figure 5.4A; curve a) and AuE/dithiol/AuNP electrode (Figure 5.4A; curve b) whereas CV of AuE/dithiol/AuNPs/MUA/ChOx electrode shows a pair of redox peaks with a broad oxidation peak at around 0.46 V (Figure 5.4A; curve c). After the addition of cholesterol

on AuE/dithiol/AuNPs/MUA/ChOx electrode, the anodic peak current at 0.46V increased sharply (Figure 5.4B; curve b) as compared to that in the absence of cholesterol (Figure 5.4B; curve a). Thus, the oxidation peak at 0.46 V can be attributed to the electro-catalytic activity of ChOx. These results exhibit that ChOx gets electrically contacted with the AuNPs modified electrode. The electron transfer rates are highly sensitive to the type of self assembled monolayer (SAM) and the linking distance between the enzyme and the electrode surface (Benitez et al. 2004; Gooding et al. 2001). Thus, the overpotential (0.46 V) of ChOx may originate from the tunnelling barrier between the mixed SAM that is dithiol/AuNPs/MUA and the AuE surface. Addition of cholesterol also leads to an increase in current at around 0.7 V which is mainly because of H_2O_2 produced due to leaching of small amount of atmospheric O_2 inside the reaction chamber. In order to ascertain the influence of AuNPs, ChOx was immobilized on AuE via self-assembled monolayer of MUA without AuNPs (AuE/MUA/ChOx electrode). No clear oxidation peak was observed on AuE/MUA/ChOx electrode in absence (Figure 5.4C; curve a) or presence of cholesterol (Figure 5.4C; curve b). Different aspects may account for this phenomenon. It is suggested that in absence of AuNPs, the total number of catalytically active ChOx units may be small due to comparatively lesser surface area and poor biocompatible environment provided by the bare AuE than the AuNPs modified surface. To confirm this, enzyme loading was calculated on both AuE/dithiol/AuNPs/MUA/ChOx and AuE/MUA/ChOx electrodes and found to be 0.0037 U cm^{-2} and 0.00098 U cm^{-2}, respectively. There may be partial denaturation of the immobilized enzymes on the naked Au surface. The amount of immobilized electroactive enzyme was enhanced on incorporation of AuNPs. AuNPs can also provide

conduction pathways to accelerate electron transfer and thus may act as the relayer of electrons to the electrode surface (Chen et al. 1998). Moreover, greater spatial freedom in the orientation of immobilized ChOx resulted in closer proximity of its redox center to electrode surface facilitating greater electron transfer. Thus, interfacial layer of AuNPs plays key role in enhancing the current response of the developed bioelectrode.

5.3.5. Electron transfer properties of AuE/dithiol/AuNPs/MUA/ChOx bioelectrode

Cyclic volatammetry was carried out with AuE/dithiol/AuNPs/MUA/ChOx bioelectrode in PBS (50 mM, pH 7.0) with cholesterol (0.2 mM) at different potential scan rates (ν) (50 to 700 mV s^{-1}) to obtain its various electron transfer parameters. At ν =50 mVs^{-1}, the peak separation (ΔEp) was about 66 mV (Figure 5.5A), which is more than the peak separation of a reversible process (59 mV), indicating a quasi-reversible redox process (Scott and Lukehart 2007). Moreover, as the scan rate increases, the anodic (E_{pa}) and cathodic (E_{pc}) peak potentials shift to more positive and more negative values respectively increasing the ΔEp (Figure 5.5A) further suggesting a quasi-reversible process. Besides this, the magnitudes of anodic (I_{pa}) and cathodic (I_{pc}) peak currents increase linearly with increasing scan rate in the range of 50 to 700 mVs^{-1} (Figure 5.5B) as expected for a surface confined redox process and indicating a thin-layer electrochemical behavior (Scott and Lukehart 2007). Both I_{pa} and I_{pc} are also proportional to the square root of scan rate ($\nu^{1/2}$) over the range of 50-700 mV s^{-1} (Figure 5.5C), suggesting that the electrode reaction is a diffusion-controlled process (Yang et al. 2006c).

For a quasi-reversible wave, the relationship between peak potential and scan rate conforms the following equation (Laviron's equation) (Laviron 1974):

$$E_p = E^{o'} + \frac{RT}{\alpha nF} + \frac{RT}{\alpha nF} \ln \nu \qquad (5.2)$$

where E_p is the peak potential (cathodic or anodic), $E^{o'}$ is the apparent standard potential. R is the thermodynamic gas constant (8.314 J K^{-1} mol^{-1}), F is the Faraday constant (96,500 C mol^{-1}) and T is the temperature (298 K). The symbols n and ν are the electron transfer number and scan rate, respectively. The product of charge transfer coefficient (α) and $n, \alpha n$ was found to be 0.78, calculated from the slope of the E_{pa} versus $\ln \nu$ plot (Figure 5.5D). Because of $0.5 < \alpha < 1.0$ in general, we valued that $n = 1$ and $\alpha = 0.78$. This result revealed that the redox reaction occurring at the AuE/dithiol/AuNPs/MUA/ChOx bioelectrode surface involves a single electron transfer process.

The surface concentration of the ionic species (Γ) (mol cm^{-2}) onto AuE/dithiol/AuNPs/MUA/ChOx bioelectrode can be estimated from the plot of peak current versus scan rate (ν) using Brown-Anson model that is based on the following equation (Laviron 1979):

$$Ip = \frac{n^2 F^2 \Gamma A \nu}{4RT} \qquad (5.3)$$

where n is the number of electrons transferred which is 1 in the case of AuE/dithiol/AuNPs/MUA/ChOx bioelectrode, and A is the surface area of the electrode (0.196 cm^2). The symbols F, R and T have their usual meanings. When the scan rate

(v) was 100 mV/s, the anodic peak current (I_{pa}) was 5.8 × 10^{-6}A. The total surface concentration is found to be 3.144 ×10^{-10} mol cm^{-2}.

The heterogeneous electron transfer constant (k_s) of the AuE/dithiol/AuNPs/MUA/ChOx bioelectrode was obtained by the following equation (Laviron 1979):

$$\log k_s = \alpha\log(1-\alpha) + (1-\alpha)\log\alpha\text{-}\log\frac{RT}{nF\nu} - \frac{\alpha(1-\alpha)nF\Delta E_p}{2.3RT} \quad (5.4)$$

Taking ΔEp =97.4 mV, at v = 100 mVs^{-1}, n =1 and α = 0.78, the vale of k_s for AuE/dithiol/AuNPs/MUA/ChOx bioelectrode was calculated to be 0.35 s^{-1} which suggests significant electron transfer between the ChOx and the electrode.

5.3.6. Response characteristics of AuE/dithiol/AuNPs/MUA/ChOx bioelectrode towards cholesterol

Figure 5.6 shows the CVs of AuE/dithiol/AuNPs/MUA/ChOx bioelectrode in PBS (50 mM, pH 7.0) with increasing concentrations of cholesterol. The calibration curve in Figure 5.6 inset shows the peak current at 0.46V increased linearly (R^2 = 0.997) with increase in cholesterol concentrations in the range of 0.04–0.22 mM. The sensitivity, calculated from the slope of the plot, was found to be 9.02 µA mM^{-1} (45.96 µAmM^{-1} cm^{-2}). The detection limit (DL) for the constructed bioelectrode calculated from the expression $DL = (3\times SD)/Sensitivity$ (where SD is the estimated standard deviation for the points used to construct the calibration curve and the $Sensitivity$, its slope) was found to be 34.6 µM. The relative standard deviation (RSD) reflecting the accuracy of the measurement was determined by subjecting the same AuE/dithiol/AuNPs/MUA/ChOx

bioelectrode to three different 0.2 mM cholesterol solutions and found to be 2.6 %. The apparent Michaelis–Menten constant (K_m^{app}) (based on Lineweaver–Burk plot) was calculated to be 0.062 mM. The K_m^{app} found in our case is better than those reported for other nanoparticle based cholesterol biosensors (Ansari et al. 2009; Khan et al. 2008). This can be attributed to favorable conformation of ChOx provided by the AuNPs film. The detection range of the fabricated bioelectrode is wider as compared to cytochrome P450scc immobilized on AuNPs (Shumyantseva et al. 2005) but narrower than some methods based on other nanomaterials (Matharu et al. 2009; Yang et al. 2006b). The detection limit in our case is lower than ZnO NPs-CHIT composite (Khan et al. 2008) and SnO_2 NPs-CHIT (Ansari et al. 2009).

5.3.7. Interference study

Effect of some common interferents in cholesterol determination such as ascorbic acid (AA), glucose (Glu), uric acid (UA), lactic acid (LA) and urea (U) on the AuE/dithiol/AuNPs/MUA/ChOx bioelectrode response has been studied. For this, CVs were taken in PBS (50 mM, pH 7.0) containing cholesterol (Chol) (0.2 mM) and each interferent (AA: 0.01mM; Glu: 0.2mM; UA: 0.01mM; LA: 0.2mM; U: 0.2mM) individually (Figure 5.7). Selectivity coefficient (SC) of the fabricated bioelectrode for each interferent was calculated using the formula, $SC = I_{c+i}/I_c$ where I_{c+i} and I_c are bioelectrode response at 0.46 V for cholesterol (0.2mM) in the presence and absence of each interferents, respectively. The results indicate that response of bioelectrode did not get significantly affected due to presence of these interferents (Figure 5.7). The concentration of AA and UA above 0.01 mM, significantly increased the oxidation current at 0.46 V. This may be due to the fact that both of them may be easily oxidized at

electrodes. But the interference from these compounds become insignificant while analyzing real samples because of the dilution step involved during the amperometric measurements. These results show that AuE/dithiol/AuNPs/MUA/ChOx biosensor exhibited high selectivity towards the determination of cholesterol.

5.3.8. Determination of cholesterol in serum samples

The fabricated bioelectrode was used as a biosensor for determining total cholesterol content of human serum samples collected from five healthy volunteers. Serum samples were first analyzed using commercial cholesterol estimation kit (CHOD-PAP method) employing three enzymes, ChEt, ChOx and peroxidase, and 4-aminoantipyrine. In the CHOD-PAP method, ChEt first hydrolyzes the esterified cholesterol fraction into cholesterol and ChOx subsequently oxidizes the cholesterol liberating H_2O_2. Peroxidase utilizes H_2O_2 to convert 4-aminoantipyrine into quinoneimine (Trinder's reaction) (Trinder and Webster 1984) detected spectrophotometrically at 500 nm. The same serum samples were analyzed using the AuE/dithiol/AuNPs/MUA/ChOx bioelectrode. Before the measurement, the serum samples were pretreated by mixing it with ChEt (1 mg mL^{-1}) in the presence of sodium cholate (0.75%) and Triton X-100 (0.1%) and incubating it at 37ºC for 30 min to hydrolyze the esterified cholesterol fraction followed by dilution with PBS (1:50) to make the cholesterol concentrations fall in the linear range of the bioelectrode. The dilution procedure can also reduce the interference effects. Current response for each sample was recorded at the working potential of 0.46V and the cholesterol concentration was determined using the calibration curve (Fig. 5.7 inset). The cholesterol amount in all the serum samples determined with the bioelectrode and the cholesterol kit was compared using paired t-test (Sigma 11) and the results show that

there is no significant difference (P = 0.920) between the values obtained with both the methods. The results demonstrate that the fabricated bioelectrode can be used as a biosensor for precise determination of cholesterol in real samples.

5.3.9. Operational and storage stability

A freshly prepared AuE/dithiol/AuNPs/MUA/ChOx bioelectrode was taken and the variation in its current response towards cholesterol was monitored as a function of time and the number of measurements. For a period of 6 h, 30 measurements of a 0.2 mM cholesterol solution were performed by the bioelectrode. After each measurement, the bioelectrode was washed with PBS. Our results demonstrated that the bioelectrode still maintained 80% of its initial activity at the end of 30 measurements (Figure 5.8A). The storage stability of AuE/dithiol/AuNPs/MUA/ChOx bioelectrode has been determined by measuring change in its current response for a 0.2 mM cholesterol solution at regular interval of 1 week for about 1 month. This AuE/dithiol/AuNPs/MUA/ChOx bioelectrode is stored at 4^{o}C in PBS (50 mM, pH 7.0) when not in use. It has been found that the bioelectrode retained ~ 95% of its initial response after 1 month (Figure 5.8B). The half life ($t_{1/2}$ of initial activities) of the fabricated bioelectrode was found to be nearly 14 months. Good operational and storage stability is attributed to the covalent attachment of the ChOx molecules with the AuNPs which prevents the leakage of the enzyme from the electrode surface.

5.4. Conclusions

A novel scheme for the fabrication of ChOx and AuNPs based bioelectrode has been developed. The self-assembled AuNPs on the gold electrode was found to enhance the

current response of the fabricated bioelectrode by increasing the electroactive surface area for higher enzyme loading, providing a biocompatible environment for the ChOx and improving the conductivity of the electrode surface. The fabricated bioelectrode shows a favorable effect on the electrochemical oxidation of cholesterol and at the same time maintaining the good bioactivity of the immobilized ChOx. The covalent attachment of the ChOx to the AuNPs provided high stability of the bioelectrode. The bioelectrode was also demonstrated to be effectively used as an amperometric biosensor for the determination of cholesterol in real samples. Therefore, taking into account the good performance of the fabricated bioelectrode, the proposed fabrication method is of great interest for the development of highly sensitive and stable nanostructured biosensors. The electrochemical studies on the fabricated electrode demonstrated that incorporated AuNPs have a marked influence on the interface property of the modified electrode and played an important role in improving its current response.

Figures

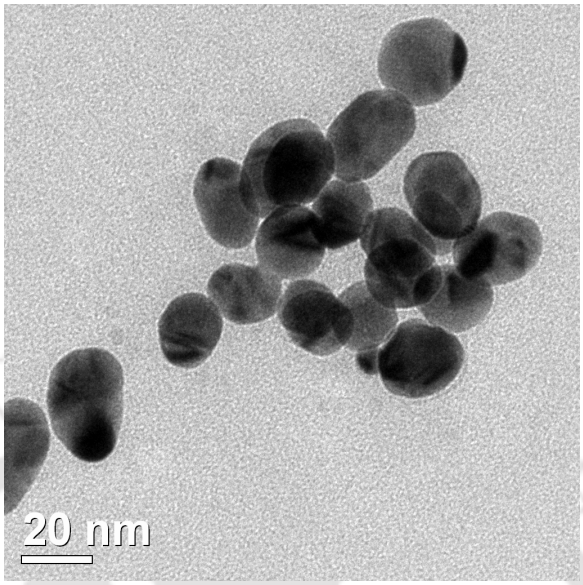

Figure 5.1 Transmission electron microscopy of gold nanoparticles

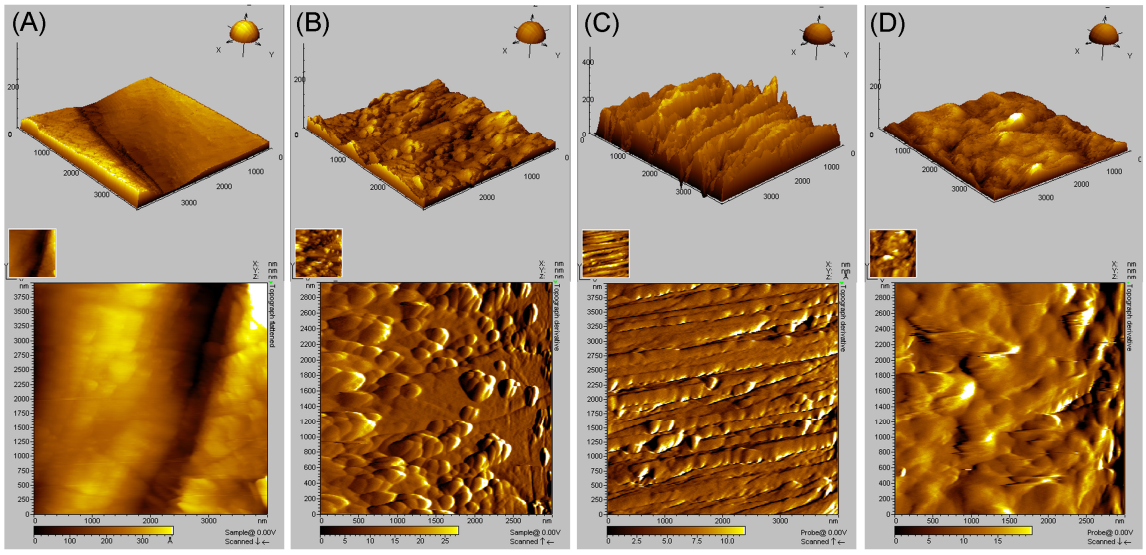

Figure 5.2 Atomic force microscopy at major stages of AuE/dithiol/AuNPs/MUA/ChOx bioelectrode fabrication:
A: AuE, **B:** AuE/dithiol/AuNPs, **C:** AuE/dithiol/AuNPs/MUA/ChOx and **D:** AuE/MUA/ChOx

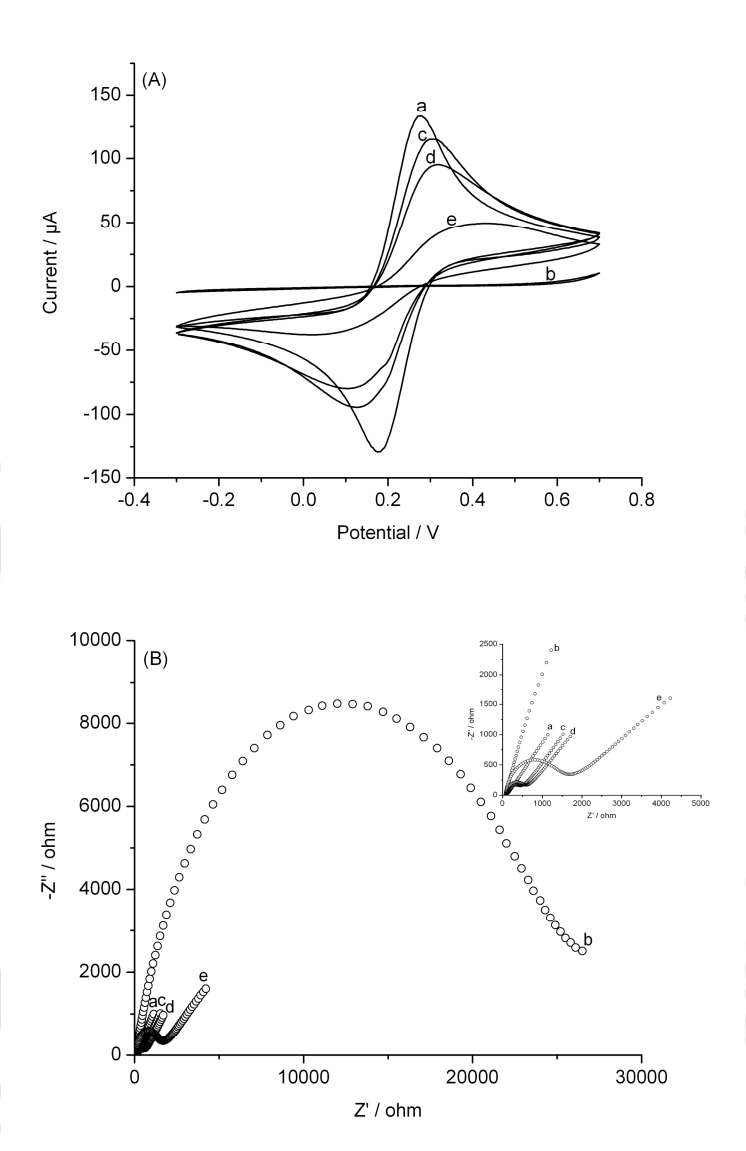

Figure 5.3 Cyclic voltammetry and electrochemical impedance spectroscopy studies at major steps of AuE/dithiol/AuNPs/MUA/ChOx bioelectrode fabrication:
A: Cyclic voltamograms of AuE (a), AuE/dithiol (b), AuE/dithiol/AuNPs (c), AuE/dithiol/AuNPs/MUA (d) and AuE/dithiol/AuNPs/MUA/ChOx (e) electrodes in 5 mM $K_3Fe(CN)_6/K_4Fe(CN)_6$ (1:1) and 0.1 M KCl in PBS. Scan rate: 50 mVs^{-1}, **B:** Electrochemical impedance spectra of AuE (a), AuE/dithiol (b), AuE/dithiol/AuNPs (c), AuE/dithiol/AuNPs/MUA (d) and AuE/dithiol/AuNPs/MUA/ChOx (e) electrodes in 5 mM $K_3Fe(CN)_6/K_4Fe(CN)_6$ (1:1) and 0.1 M KCl in PBS. Figure inset: Enlarged impedance spectra corresponding to curves (a), (b), (c), (d) and (e)

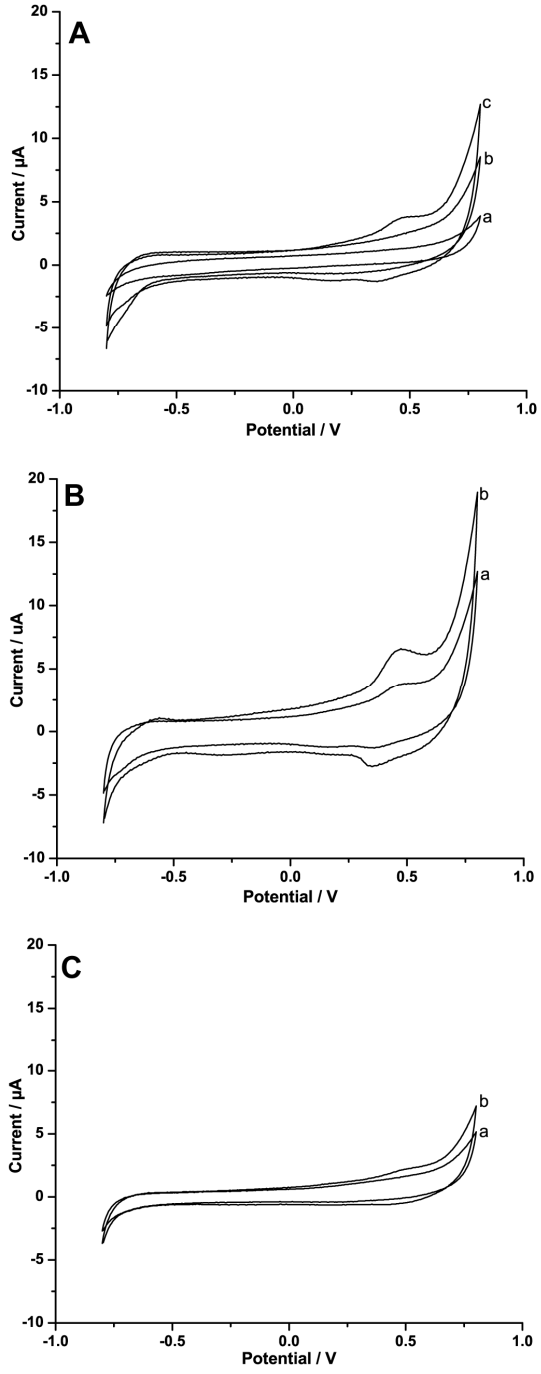

Figure 5.4 Response characteristics of the AuE/dithiol/AuNPs/MUA/ChOx bioelectrode: **A**: CV of AuE (a), AuE/dithiol/AuNPs (b) and AuE/dithiol/AuNPs/MUA/ChOx (c) electrodes in PBS, **B**: CV of Au/dithiol/AuNPs/MUA/ChOx electrode in PBS in the absence (a) and in presence of 0.3 mM cholesterol (b), **C**: CV of Au/MUA/ChOx electrode in PBS in the absence (a) and in the presence of 0.3 mM cholesterol (b)

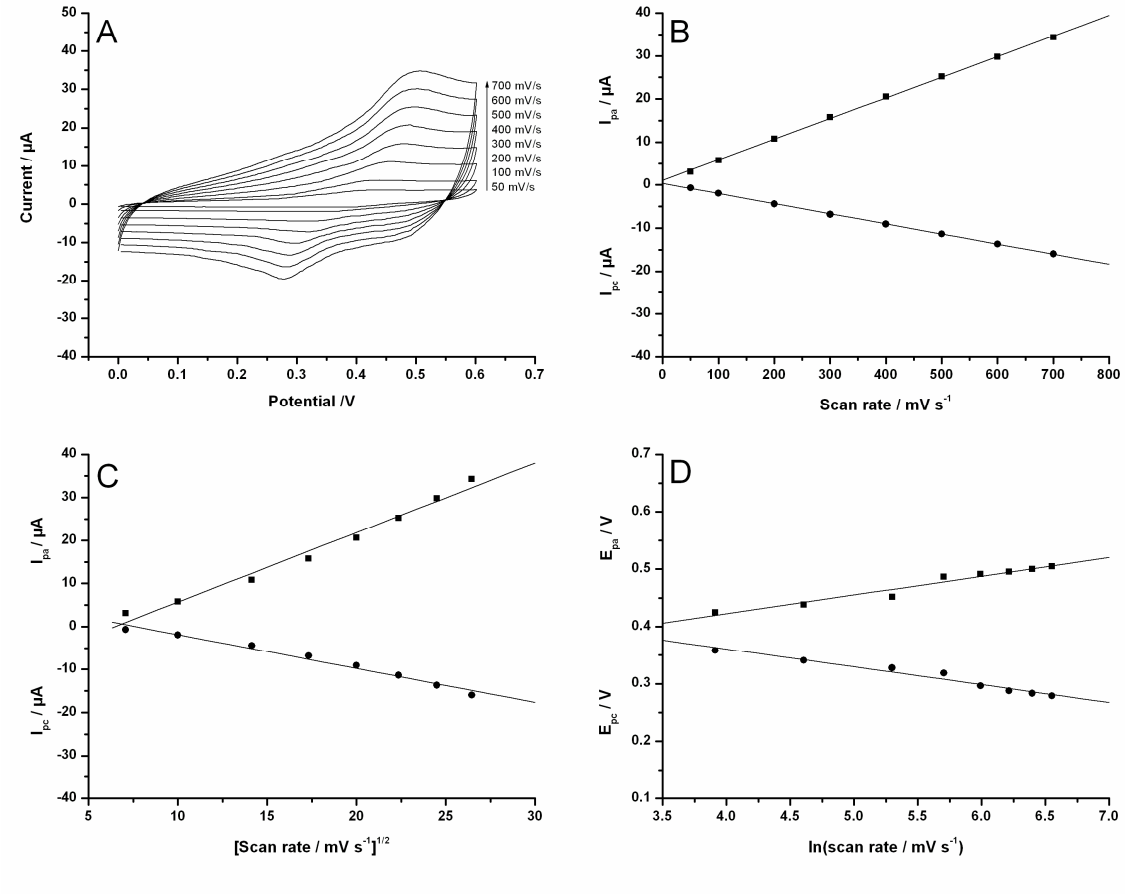

Figure 5.5 Scan rate dependent electrochemical studies of the Au/dithiol/AuNPs/MUA/ChOx bioelectrode:
A: CVs recorded with Au/dithiol/AuNPs/MUA/ChOx bioelectrode in PBS (50 mM, pH 7.0) with 0.2 mM cholesterol. Scan rate: from 50 to 700 mV s^{-1}. **B:** Plot of anodic (I_{pa}) and cathodic (I_{pc}) peak currents vs. scan rate. **C:** Plot of anodic (I_{pa}) and cathodic (I_{pc}) peak currents vs. square root of scan rate. **D:** Plot of anodic (E_{pa}) and cathodic (E_{pc}) peak potentials vs. ln(scan rate)

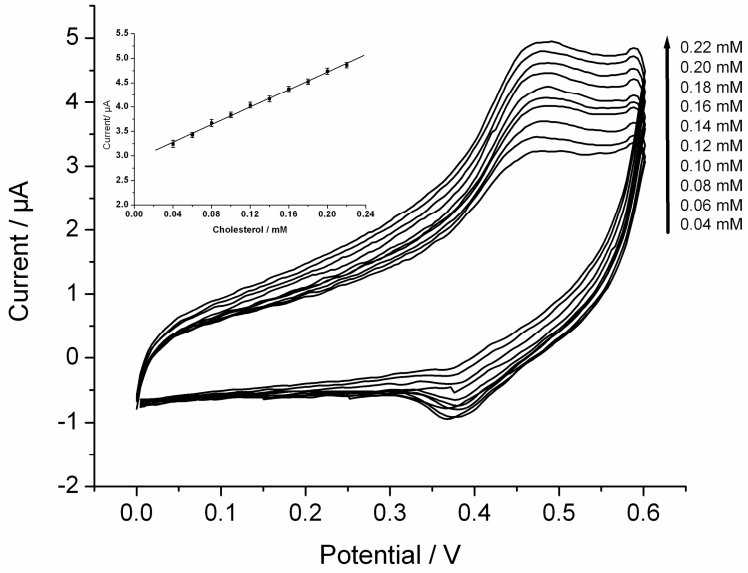

Figure 5.6 Cyclic voltammetric response of the AuE/dithiol/AuNPs/MUA/ChOx bioelectrode with various concentrations of cholesterol:
Cyclic voltammograms taken with AuE/dithiol/AuNPs/MUA/ChOx electrode in PBS (50 mM, pH 7.0) with increasing concentrations of cholesterol. Figure inset: Calibration plot for Au/dithiol/AuNPs/MUA/ChOx electrode. Each datum point represents the average of the analysis of triplicate values (n =3), with the range indicated with error bars. In all cases a potential scan rate of 0.1 Vs^{-1}

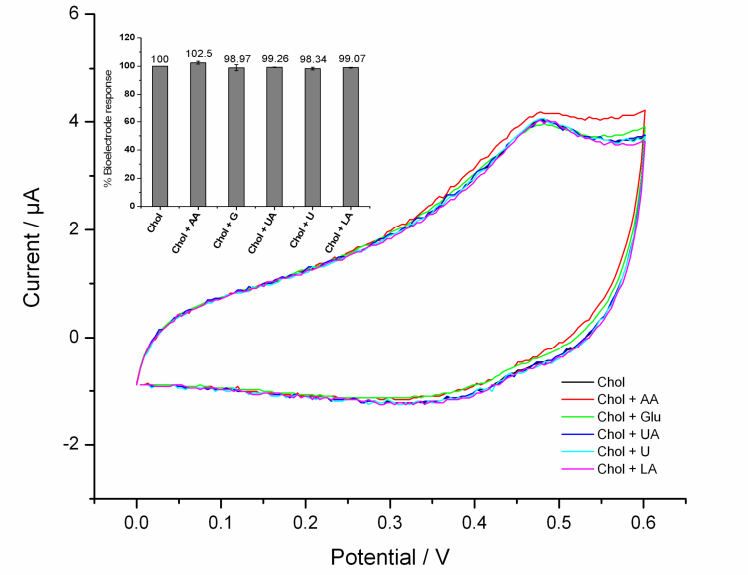

Figure 5.7 Interference studies with AuE/dithiol/AuNPs/MUA/ChOx bioelectrode:
(Chol: cholesterol, AA: ascorbic acid, Glu: glucose, UA: uric acid, U: Urea, LA: lactic acid). Each datum point represents the average of the analysis of triplicate values (n =3), with the range indicated with error bars

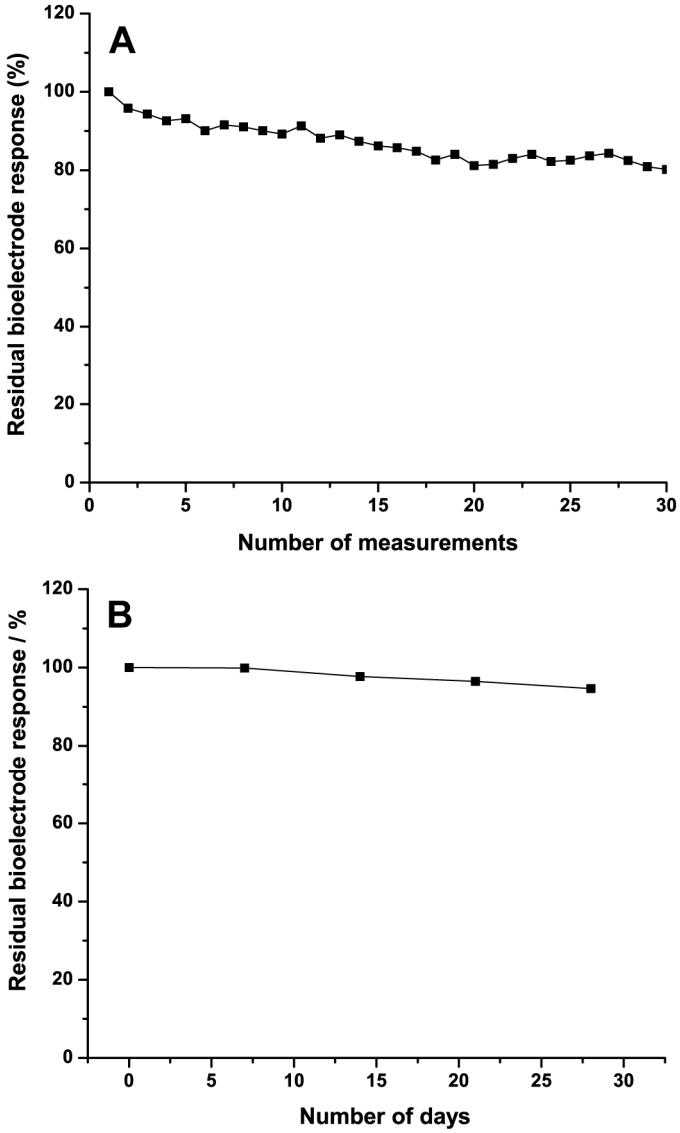

Figure 5.8 Stability of the AuE/dithiol/AuNPs/MUA/ChOx bioelectrode
A: Operational stability (**A**) and storage stability (**B**) of the fabricated AuE/dithiol/AuNPs/MUA/ChOx electrode

CHAPTER 6

Biochemical and Biophysical Studies of Cholesterol Oxidase and Gold Nanoparticles Interactions

6.1. Overview

From the past decade, nanoparticles (NPs) have attracted extensive interest in the area of analytical biotechnology (Willner and Willner 2010; Willner et al. 2007c). Their dimensional similarities with biomolecules made it possible to amalgamate the unique electronic and optical properties of NPs with the selective and catalytic functions of biomolecules and develop different NPs-biomolecules hybrid systems that reveal novel functional properties (Katz and Willner 2004; Niemeyer 2003). Gold nanoparticles (AuNPs) are the most extensively studied NPs and are the center of fascination among scientific community because of their excellent biocompatibility, large effective surface area and distinctive size-dependent optical and electronic properties (Cao et al. 2011; Crumbliss et al. 1992; Jena et al. 2010). Owing to their excellent conductivity, AuNPs are a great success in the area of electrochemical biosensors where AuNPs amplify biorecognition signals and improve the analytical performance of biosensor (Ozsoz et al. 2005; Willner et al. 2007b). They have been used to promote electron transfer between

the active centers of various redox proteins and electrodes (Feng et al. 2005; Yi et al. 2000; Zhao et al. 2006).

AuNPs also exhibit unique and interesting optical properties. Mainly the property of surface plasmon resonance (SPR) has led AuNPs to find promising potentials in optical biosensing, where a shift in SPR resulting from the aggregation of AuNPs upon analyte addition serves as the optical signal (Nath and Chilkoti 2002; Thanh and Rosenzweig 2002). Recently, a novel kind of AuNPs-biomolecule hybrid system has been developed where biocatalytic growth of AuNPs is employed to develop optical enzyme assays (Shang et al. 2008; Willner et al. 2006b). Various oxidases produce hydrogen peroxide (H_2O_2) during their catalytic reactions. This H_2O_2 can reduce Au^{3+}(aq) from chloroauric acid ($HAuCl_4$) to Au^0(s), which deposits on the surface of AuNPs "seeds" in solution. As a result, the AuNP seeds are enlarged which is reflected in the visible spectrum by a color shift and an increase in the optical extinction (scattering and absorption) of the solution. As the concentration of H_2O_2 is controlled by the analyte concentration, the increase in the optical extinction can be used as an optical read-out signal. The potential of this approach has been successfully demonstrated for various enzymes (Baron et al. 2005; Willner et al. 2007a).

We have used AuNPs in conjunction with ChOx to develop amperometric cholesterol biosensor where they have shown to provide an environment for increased electrocatalytic activity of ChOx and hence resulted in improved analytical performance of the biosensor. ChOx also produces H_2O_2 during its catalysis, with which it can be successfully used in the method of seed mediated growth of AuNPs to produce an optical cholesterol biosensor. Here, we have studied the electrocatalytic and optocatalytic

properties of AuNPs in conjunction with ChOx which can be exploited in the AuNPs-ChOx hybrid systems designed for cholesterol estimation. We have also investigated the relationship between the catalytic activities of AuNPs with their size.

6.2. Experimental Approaches

6.2.1. Reagents and stock solutions

Cholesterol oxidase from *Pseudomonas fluorescens*, bovine serum albumin (BSA), cholesterol, Gold (III) chloride solution (~30 wt. % in dilute HCl), N-ethyl-N'-(3-dimethylaminopropyl) carbodimide (EDC), N-hydroxysuccinimide (NHS), 1,6-hexanedithiol, 11-mercaptoundecanoic acid (MUA) and 2,6-dichloroindophenol sodium salt hydrate (DCPIP) were bought from Sigma-Aldrich (USA). All other reagents used were of analytical grade.

Stock solution of cholesterol (10 mM) was prepared in 5 % Triton X-100 aqueous solution and stored at 4°C. Stock solutions of ChOx (8 μM) and BSA (15 μM) were freshly prepared in phosphate buffer solution (PBS) (50 mM, pH 7.0) prior to use. Stock solutions of 8 mM H_2O_2 and 0.01 % $HAuCl_4$ were prepared in water just before the experiments. Citrate stabilized AuNPs were prepared following Turkevich method (Frens 1973; Turkevich et al. 1953). AuNPs of four different sizes were obtained by varying [Au(III)]/[citrate] ratio (Table 6.1) during the reduction step of the preparation method (Ghosh et al. 2004). All solutions and buffers are prepared in deionized water (Millipore, Bedford, MA).

6.2.2. Covalent attachment of ChOx on AuNPs in-solution

The covalent attachment of ChOx on AuNPs in-solution was performed with the slightly modified method described by Li and group (Li et al. 2007). This involves first, the functionalization of AuNPs surface with carboxyl groups using MUA and then covalent immobilization of ChOx on the functionalized AuNPs. The AuNPs-ChOx conjugates were synthesized with AuNPs of each size. In detail, separately each of the freshly synthesized AuNPs solution (I: 0.58, II: 0.34, III: 0.21 and IV: 0.12 nM) was purged with nitrogen gas, gently added to an equal volume of degassed PBS (10 mM, pH 6.8, with 0.002 % Tween-20 (v/v)) and the mixture was allowed to stand at room temperature (RT) for 30 min. Then equal volume of 0.5 mM freshly prepared ethanolic solution of MUA was added into the mixture and the final mixture was subjected to a gentle shake for 5 h at RT. The mixture was then centrifuged to remove excess alkanethiol and the MUA-modified AuNPs were resuspended in PBS (10 mM, pH 6.8, with 0.002 % Tween-20 (v/v)). These carboxyl-functionalized AuNPs were reacted for 10 min with a solution of EDC (200 mM) and NHS (50 mM), freshly prepared in PBS (10 mM, pH 6.8, with 0.002 % Tween-20). The NHS-terminated AuNPs were separated by centrifugation and washed and resuspended in PBS (10 mM, pH 6.8, with 0.002 % Tween-20) with ultrasonication. The supernatant was discarded, and the NHS-terminated AuNPs were incubated with a freshly prepared ChOx solution (100 nM) in PBS (10 mM, pH 6.8) for ~12 h under nitrogen atmosphere. The resultant AuNPs-ChOx conjugates were pelleted down by centrifugation to remove free ChOx, washed with PBS with Tween-20 and finally dispersed in PBS (50 mM, pH 7) and stored at 4^{o}C until use.

6.2.3. Spectrophotometric studies using DCPIP

The efficiency of AuNPs as electron transfer mediator was studied spectrophotometrically using a redox dye DCPIP. DCPIP has been reported to act as electron acceptor and show rate enhancement with other oxidase enzyme. The large extinction coefficient of DCPIP (ε = 20.6 mM^{-1} cm^{-1} at pH 7.0) and significant rate enhancement allow accurate measurement of the activity of small amounts of enzyme (Laskey et al. 2003). For a control experiment, reaction mixture consisting of ChOx (100 nM) and DCPIP (10 µM) in PBS (10 mM, pH 6.8) was taken in a quartz cuvette. Cholesterol (final concentration: 100 µM) was added to start the enzymatic reaction, the solution was quickly mixed and change in absorbance at λ = 600 nm was monitored for 5 min. The experiment was also conducted with ChOx either adsorbed or covalently attached to AuNPs. For studying the adsorption based system, the above experiment was performed in the presence of either of the AuNPs stock solution (I: 0.58, II: 0.34, III: 0.21 and IV: 0.12 nM). For covalent based system, AuNPs-ChOx conjugates (as prepared before) were used in the reaction mixture instead of adding AuNPs and ChOx separately. Equivalent protein and gold nanoparticle concentration was maintained in both the systems. The rate of enzymatic reaction in each case was calculated using the following equation:

$$\text{Activity (U } \mu l^{-1}) = \frac{\Delta A \times 10^3}{t \times V_i \times \varepsilon \times l} \qquad (6.1)$$

Where, ΔA: change in absorbance during time t (5 min), V_i: volume of initial ChOx solution added into spectrophotometer cell (mL) from the stock of 8 µM; ε: molar

extinction coefficient of DCPIP at λ = 600 nm (9600 L mol^{-1} cm^{-1}), *l* : optical path length (1 cm).

6.2.4. Fabrication of the AuNPs based ChOx bioelectrode

A gold electrode (AuE) (diameter = 0.5 cm) was cleaned, first by polishing it with alumina powder, then washing it ultrasonically with 70% ethanol and water separately for 15 min each and finally drying in air. The cleaned AuE was dipped in 10 mM freshly prepared ethanolic solution of 1, 6- hexanedithiol for 24 h. The dithiol modified electrode (AuE/dithiol) was rinsed with water, dipped in freshly prepared AuNPs solution (either of the stock I, II, III or IV) and kept for incubation for 6 h under mild shaking conditions. After rinsing with water, the AuNPs modified electrode (AuE/dithiol/AuNPs) was dipped in 0.5 mM freshly prepared ethanolic solution of MUA for 5 h to obtain a layer of carboxylic group functionalized AuNPs. This AuE/dithiol/AuNPs/MUA electrode was dipped for 10 min in a freshly prepared solution of EDC (200 mM) and NHS (50 mM). This was done to activate the carboxylic group on the surface of AuNPs assembled on the electrode. Finally, it was dipped in freshly prepared ChOx solution (8 μM) for 12 h to obtain AuE/dithiol/AuNPs/MUA/ChOx bioelectrode which was immersed in PBS (50 mM, pH 7) for 15 min prior to use and stored at 4ºC when not in use.

6.2.5. Catalytic growth of AuNPs

The growth of AuNPs with H_2O_2 was monitored with the help of UV-Vis spectroscopy. The reaction mixture for AuNPs growth consists of either of the gold colloid stock as seeds (I: 0.58, II: 0.34, III: 0.21 and IV: 0.12 nM), $HAuCl_4$ (0.0005 %), H_2O_2 (0 to 0.1 mM) and ChOx (20 to 100 nM) in deionized water. For a control experiment, AuNPs growth was monitored in the presence of all the above components except ChOx. For

comparison, the ChOx used in the above reaction is replaced with BSA (40 to 320 nM). For analysis, all the components except H_2O_2 were added to a quartz cuvette. H_2O_2 was added finally to the cuvette, the solution is mixed thoroughly, allowed to stand for exactly 10 minutes at RT and scanned with UV-Vis spectrophotometer from 400 to 700 nm. The sensitivity of the growth reaction will be equal to the slope of change in the particles solutions' absorbance (at λ_{max} for original AuNPs seed solution used) with increasing H_2O_2 concentration.

6.2.6. Instruments and measurements

The UV-Vis spectra were recorded in a CARY 300 BIO double beam spectrophotometer (Varian, USA). Trasmission electron microscopy (TEM) images are acquired with a 200 KV electron microscope (JEOL JEM, 2100) (CIF, IIT Guwahati). Electrochemical experiments were performed with an Autolab PGSTAT 1212 potentiostat (Eco Chemie, Netherlands) in a three-electrode system with platinum rod as counter electrode, Ag/AgCl (saturated KCl) as reference electrode, and AuE/dithiol/AuNPs/MUA/ChOx electrodes as the working electrodes. During all the electrochemical experiments, the electrolyte solution was deareated by constant purging with argon gas. All experiments were performed at RT.

6.3. Results and Discussion

6.3.1. Characterization of the gold nanoparticles

The synthesized AuNPs were characterized using UV-visible spectroscopy and TEM. TEM pictures were analyzed with ImageJ software. For each AuNPs sample, the average NP size (diameter, D) was calculated by considering ~100 particles from multiple TEM

pictures of the same sample acquired from different locations of TEM grid. One representative TEM picture for each sample was presented in Figure 6.1. The molar extinction coefficients (ε) of the AuNPs solutions were determined from their average diameter according to the equation $\ln \varepsilon = 3.32 \ln D + 10.80$ as reported by Liu and group (Liu et al. 2007). The characteristic parameters for different sets of AuNPs are summarized in Table 6.1.

Table 6.1 Synthesis and characterization parameters of AuNPs solution

Stock	Amount of $HAuCl_4$ solution (10 mM, mL)	Amount of trisodium citrate solution (1 %, mL)	λ_{max}	Average diameter (nm)	ε (M^{-1} cm^{-1})
I	1.25	1.3	520	13	2.31×10^8
II	1.25	1.15	521	15	3.98×10^8
III	1.25	1.0	523	18	6.26×10^8
IV	1.25	0.85	527	21	1.14×10^9

6.3.2. Electrocatalytic activity of AuNPs as a redox mediator for ChOx

AuNPs have found application in various enzymatic electrochemical biosensors where they are shown to enhance the analytical response of the biosensor (Ozsoz et al. 2005; Willner et al. 2007b). We have exploited AuNPs in combination with ChOx for the fabrication of a cholesterol biosensor. Here AuNPs were found to promote heterogenous electron transfer between ChOx and the electrode surface and played an important role in improving the current response of the biosensor. The possible mechanism of electron transfer from ChOx to electrode through AuNPs is represented in Scheme 6.1A.

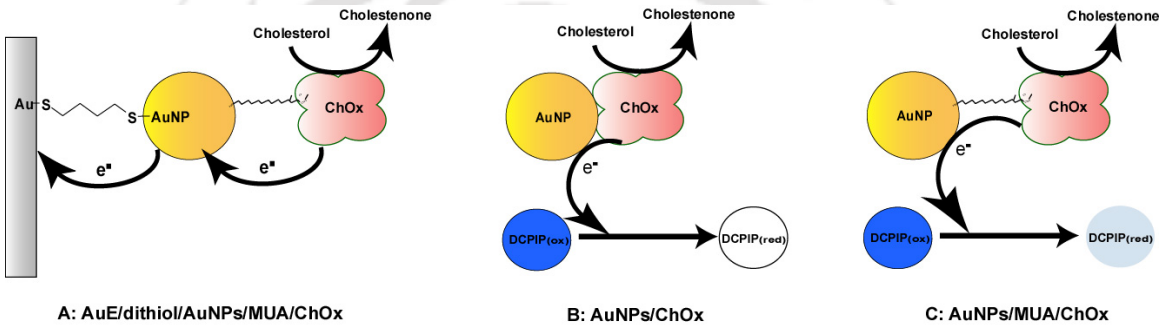

Scheme 6.1 Mechanism of electron transfer between cholesterol oxidase and gold nanoparticles:
A: AuE/dithiol/AuNPs/MUA/ChOx electrode, **B**: ChOx adsorbed on AuNPs (AuNPs/ChOx), and **C**: ChOx covalently attached to AuNPs (AuNPs/MUA/ChOx)

In the present study, the electrocatalytic activity of AuNPs as a redox mediator for ChOx was further studied with a spectrophotometric method using a redox dye DCPIP. In a general reaction cycle, *P. fluorescens* ChOx catalyzes the oxidation of cholesterol to 6β-hydroperoxycholest-4-en-3-ne (HCHO), concomitant with the reduction of O_2 to H_2O_2. During the catalysis of cholesterol by ChOx in the presence of DCPIP, DCPIP accepts electron from reduced FAD of ChOx and gets reduced. The oxidized form of DCPIP is blue and it has λ_{max}= 600 nm. When DCPIP becomes reduced, it loses its specific color which can be monitored spectrophotometrically at 600 nm. The enzyme activities calculated from this indicator reaction gives a measure of the rate of electron transfer between ChOx and DCPIP. To evaluate the influence of AuNPs on electron transfer from ChOx towards DCPIP, we have performed ChOx catalysis with DCPIP in the absence and presence of AuNPs and checked whether AuNPs accelerate the rate of enzymatic reaction or the electron transfer rate between ChOx and DCPIP. The related reactions of this study are:

$$\mathrm{ChOx_{(ox)} + cholesterol \rightarrow ChOx_{(red)} + \ Cholestenone} \qquad (6.2)$$

$$\mathrm{ChOx_{(red)} + DCPIP_{(ox)} \rightarrow ChOx_{(ox)} + DCPIP_{(red)}} \qquad (6.3)$$

$$\mathrm{ChOx_{(red)} + AuNPs_{(ox)} \rightarrow ChOx_{(ox)} + AuNPs_{(red)}} \qquad (6.4)$$

$$\mathrm{AuNPs_{(red)} + DCPIP_{(ox)} \rightarrow AuNPs_{(ox)} + DCPIP_{(red)}} \qquad (6.5)$$

Among various enzyme immobilization approaches for the construction of AuNPs based biosensors, adsorption and covalent attachment techniques are most widely used. To study the influence of the mode of attachment of ChOx with AuNPs on the electrocatalytic activity of the gold nanoparticles, the above study was conducted with

ChOx either adsorbed or covalently attached to AuNPs (21 nm). The enzyme activities of ChOx calculated in different systems is shown in Table 6.2.

Table 6.2 Average rate of enzymatic reaction

Sample	Average ChOx activity (A) in solution (U / µL)[a]
ChOx + DCPIP	0.756 ± 0.010
ChOx + AuNPs+ DCPIP	1.267 ± 0.020
AuNPs-ChOx+ DCPIP	0.934 ± 0.023

[a]The values are expressed as mean ± S.E.M. (n = 3)

The results illustrates that when AuNPs are added into the system (where ChOx molecules gets adsorbed on AuNPs surface), there is ~1.68 fold increase in reaction rate explicating that ChOx are re-oxidized more efficiently with DCPIP in presence of AuNPs. Interestingly, when similar studies were conducted with ChOx covalently immobilized on AuNPs, reaction rates are found to be increased upto ~1.24 fold, which is bit less than the case where ChOx molecules are physically immobilized on the AuNPs surface. The linkers used for the covalent attachment of ChOx with AuNPs may create the tunneling barrier between the AuNPs and the ChOx and thus may slow down the electron transfer process. The schematic diagram for the electron transfer mechanism from ChOx to DCPIP through AuNPs with different modes of ChOx attachment to AuNPs is represented in Scheme 6.1B and C. These results confirm that AuNPs played as an efficient electron mediator for ChOx and the electron transfer process to some extent is affected by the mode of AuNPs-ChOx attachment with a slightly higher electrocatalytic activity with ChOx adsorbed on the AuNPs surface. The adsorption based immobilization is mostly used because of its simplicity in procedure (Yi et al. 2000;

Zhang et al. 2005a). However, biosensors based on this technique, usually experience reduced stability. Therefore, in many cases, covalent immobilization method has also been used for improving the stability of the biosensor (Zhang et al. 2005b). In brief, both the methods of immobilization may be effectively used for the fabrication of gold nanoparticles based electrochemical biosensors depending upon the precedence upon stability or sensitivity.

6.3.3. Optocatalytic activity of AuNPs towards the estimation of cholesterol

Apart from the electrocatalytic properties of AuNPs, one may also utilize the unique optical property of AuNPs to follow biocatalytic processes. Metal nanoparticles have an intrinsic property to catalyze the reduction of metal ions on the surface of NPs and thereby to enlarge the metallic nanoparticles. This phenomenon is employed in different biosensing paths (Willner et al. 2006b). Various oxidases generate H_2O_2 during their catalysis. In the presence of H_2O_2, chloroauric acid ($HAuCl_4$) and seed AuNPs, the seed AuNPs catalyzes the reduction of Au^{3+}(aq) from chloroauric acid ($HAuCl_4$) to Au^0(s) by in-situ generated H_2O_2 . This Au^0(s) gets deposited on the AuNPs seed surface leading to the growth of AuNPs. This nanoparticle enlargement can be monitored with spectrophotometry with a shift in the absorption maxima and increase in optical extinction (Zayats et al. 2005). Figure 6.2A demonstrates the evolution of absorbance spectra in the reaction system containing seed AuNPs (21 nm) and chloroauric acid ($HAuCl_4$) with variable concentrations of H_2O_2. The increase in H_2O_2 concentration enhanced the overall particle extinction due to the AuNPs enlargement as reduced chloroauric acid gets deposited onto the surface of AuNPs seeds. The red shift in the

absorbance maximum observed with increasing H_2O_2 concentrations also supports the concept of particle enlargement (Shang et al. 2008; Zayats et al. 2005).

Like other oxidases, ChOx also generates H_2O_2 during its catalysis and therefore, the AuNPs seed mediated biocatalytic enlargement of AuNPs can be used to develop an optical detection path for cholesterol by ChOx. Since most of the proteins are known to bind strongly to gold surface (Brewer et al. 2005), the presence of ChOx in AuNPs growth system may affect the growth kinetics. The interaction of ChOx protein with AuNPs can be monitored by following the change in the sensitivity of the AuNPs growth process with increasing concentration of ChOx. For this, AuNPs growth was monitored with different ChOx concentrations (20 to 100 nM).

From the Figure 6.2(B to F), we can observe that the presence of ChOx in the growth mixture decreased the sensitivity of the AuNPs growth reaction and the sensitivity progressively decreased with increasing ChOx concentration (Figure 6.2G). For comparison, BSA (40 to 320 nM) was used in place of ChOx and from Figure 6.2H, we can see that sensitivity of the AuNPs growth decreased with BSA in an analogous fashion to ChOx. A recent study conducted by Chen and group (Chen et al. 2010) on the effect of BSA on the AuNPs growth process also reported similar results. They have suggested that BSA binding to the AuNPs surface blocks the biocatalytic growth sites, forcing additional deposition onto any uncovered sites and thereby non-uniform growth of the NP seeds. It can be hypothesized that, ChOx works in the similar manner. The only difference between the two proteins is the concentration of these proteins at which the inhibition of the response begins. ChOx starts inhibiting the AuNPs growth process at a

comparatively lower concentration (40 nM) then BSA (150 nM). This elucidates that ChOx interacts strongly with AuNPs.

The seed mediated growth of AuNPs can be used for the optical detection of cholesterol by replacing H_2O_2 in the growth medium with cholesterol and carrying out the reaction in the similar way with 21 nm AuNPs seeds (Stock D) (0.12 nM) and ChOx (40 nM). Figure 6.3 shows the spectral changes of the AuNPs seed solution upon the addition of different concentrations of cholesterol. The total extinction of the AuNPs increased as the concentration of cholesterol is elevated from 0 to 0.1 mM. This is because as the concentration of cholesterol increases, the concentration of the in-situ generated H_2O_2 is increased and the growth of the AuNPs is enhanced. This is the same effect observed using NPs as seeds in other enzymatic reactions (Willner et al. 2007a). The calibration curve was derived and the sensitivity of the optical biosensor thus produced was calculated from the slope of the calibration curve and found to be 0.34 au mM^{-1} (au = absorbance unit). The sensitivity was found to be decreased as compared to the system in which H_2O_2 is used with the same amount of ChOx (40 nM), in which case it was 0.60 au mM^{-1}. This may be due to the time lag between the H_2O_2 generation by ChOx and then growth of AuNPs by the in-situ generated H_2O_2. Also, presence of Triton X-100 (although minimal amount) may have some inhibitory effect on the AuNPs growth kinetics. This was confirmed by comparing the sensitivity of AuNPs growth with H_2O_2 with and without Triton X-100. Triton X-100 was found to decrease the sensitivity of the AuNPs growth reaction. The detection limit (DL) for the biosensor was calculated from the expression $DL = (3 \times SD) / Sensitivity$ (where SD is the estimated standard deviation for the points used to construct the calibration curve and the $Sensitivity$, its slope) and is

found to be 30 µM. The lower detection limit calculated from the linear range of the bioelectrode was found to be 10 µM. The relative standard deviation (RSD) reflecting the accuracy or reproducibility of the measurement method was determined by three independent measurements with 0.05 mM cholesterol solution and it was found to be 1.9 %. These studies reveal that the optocatalytic property of gold nanoparticles in conjunction with ChOx can also be successfully used for the detection of cholesterol. These studies show that ChOx remain functional while interacting with AuNPs.

6.3.4. Effect of size on electrocatalytic and optocatalytic properties of AuNPs

It should also be noted that in nanometer range, the particle's size and surface characteristics has an increasingly important role in controlling the overall energy of the particles which ultimately affect the NP's optical and electronic properties (Eckenrode et al. 2005; Jain et al. 2006). This interesting fact has gained increased scientific interest to explore the size dependent catalytic properties of AuNPs (Cuenya et al. 2003; Tsunoyama et al. 2005; Zhang et al. 2006). In the present study, the relationship between the catalytic properties of AuNPs with respect to the size has been explored.

6.3.4.1. Effect of size on the electrocatalytic properties of AuNPs

To investigate the effect of AuNPs' size on their electrocatalytic property, we have investigated the in-solution electron transfer efficiency of AuNPs with respect to their size. For this, we have used AuNPs of different sizes (13 to 21 nm) in conjunction with DCPIP and calculated the rate of enzymatic reaction spectrophotometrically in each case by monitoring the change in absorbance at λ= 600 nm. The concentration of AuNPs of each size was chosen such that the total available surface area remains the same. These studies were conducted with ChOx either adsorbed (Figure 6.4A) or covalently attached

(Figure 6.4B) on AuNPs. The results obtained for both the cases show that the electron mediation efficiency of AuNPs is more with their lower sizes when compared to their larger sizes. The effect of size of AuNPs was further studied in case of the AuNPs based ChOx electrode. For this, four AuE/dithiol/AuNPs/MUA/ChOx bioelectrodes were fabricated as mentioned in experimental section, each with AuNPs of different sizes (13 nm (I), 15 nm (II), 18 nm (III) and 21 nm (IV)). The current response of each of these bioelectrodes was measured with increasing concentrations of cholesterol and the sensitivity of each bioelectrode was calculated from the slope of the response curve. It was found that with increase in size, the sensitivity of the biosensor decreased as shown in Figure 6.4C. The diminution of AuNPs size to fabricate the AuE/dithiol/AuNPs/MUA/ChOx bioelectrode may have resulted in increase in the surface area obtainable by AuNPs for the higher enzyme loading that lead to enhanced electrocatalytic activity towards cholesterol and thus to the increased sensitivity of the resulting bioelectrode. The results indicate that the improved response of AuNPs based electrochemical ChOx electrode is the outcome of, both the enhanced electron transfer efficiency with smaller AuNPs as demonstrated by using redox dye, and the increase in surface area caused by smaller AuNPs sizes.

6.3.4.2. Effect of size on the optocatalytic properties of AuNPs

Different sized AuNPs are also expected to show differences in their ability to catalyze the reaction between gold ions and H_2O_2 and their affinity to ChOx. To determine whether the size of the NPs have any effect on the sensitivity of the AuNPs growth kinetics, different sized AuNPs seeds were tested in the model biosensor. For the experiment, the concentration of nanoparticles seeds of each size was chosen such that

the total available surface with each type of the NP size remains constant. Figure 6.4D shows the change in the sensitivity of the AuNPs growth reaction with four different sized AuNPs after the addition of H_2O_2 in the presence of 40 nM ChOx. It can be observed that with the increase of particle seed size from 13 to 21nm, there is no significant change in sensitivity. Overall, these results indicate that if the available surface area of the AuNPs is kept constant, there is no significant effect of particle size on the sensitivity of the AuNPs growth reaction and thus the optocatalytic properties of AuNPs is independent of there size.

6.4. Conclusions

For exploring the interaction of ChOx with AuNPs, two different types of AuNPs-ChOx hybrid systems were studied. The electrocatalytic and optocatalytic activity of AuNPs of different sizes were examined. It was found that the electrocatalytic efficiency of AuNPs improved with decrease in the nanoparticle size. The spectrophotometric method showed that the electron transfer efficiency of the AuNPs with ChOx depends upon the size of the NPs and the method of immobilization. However, the size of the NPs does not have a significant impact upon the optocatalytic ability of the NPs. This study provides an insight into the design of biosensors based on AuNPs and the role that size of the NPs play in these studies. The findings have potential applications for the optimization of the AuNPs-protein complex for the analytical applications.

Figures

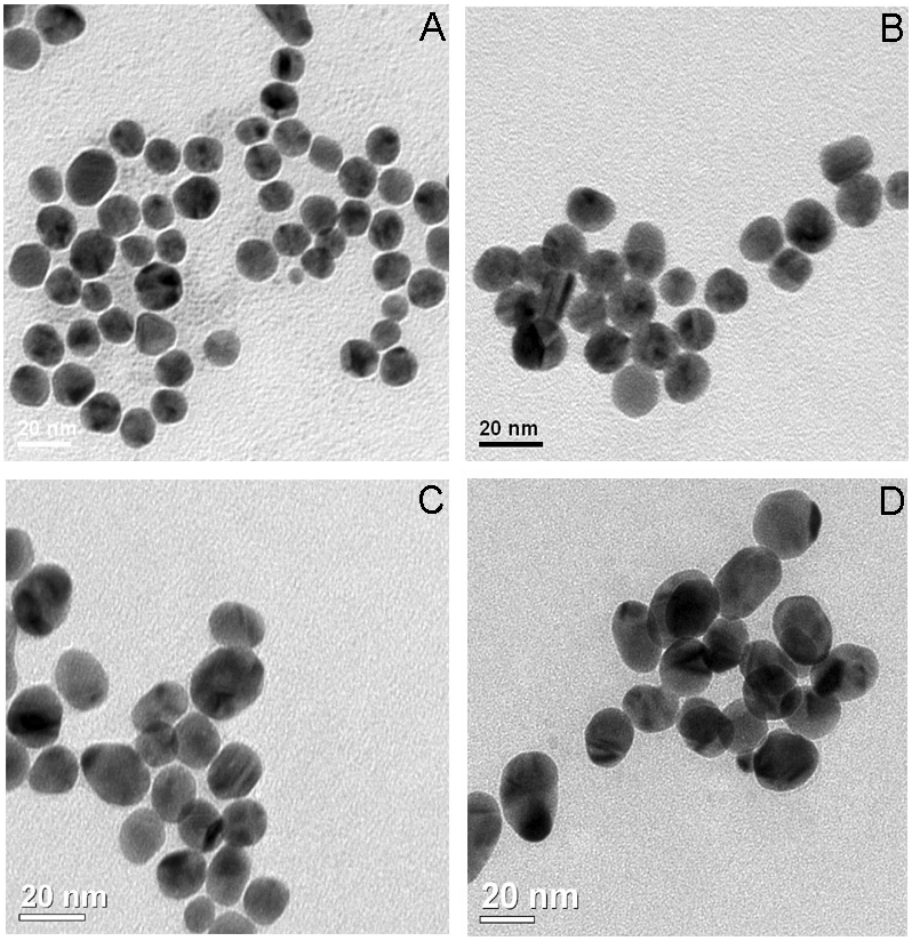

Figure 6.1 Transmission electron microscopy of different sized gold nanoparticles: **A:** 13 nm, **B**: 15 nm, **C**: 18 nm and **D**: 21 nm sized gold nanoparticles

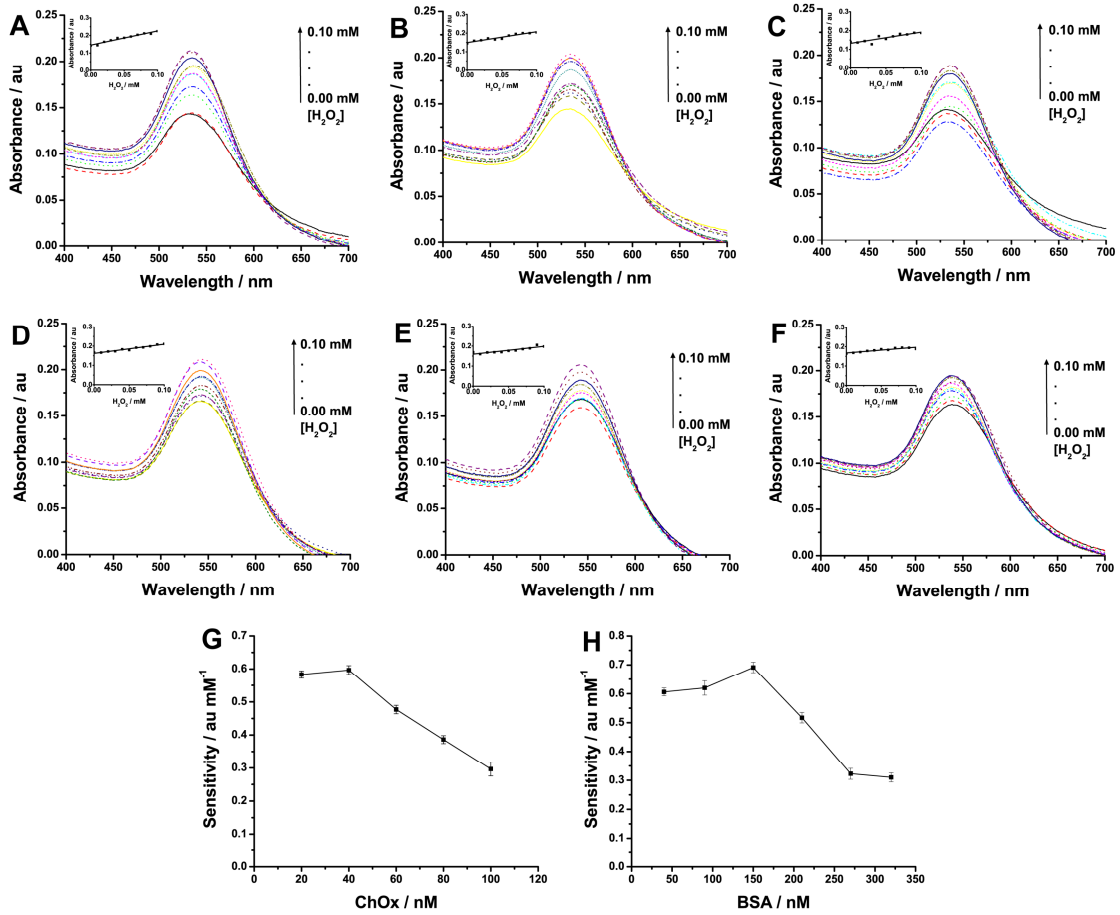

Figure 6.2 Seed mediated catalytic growth of gold nanoparticles:
Growth of AuNPs with H_2O_2, **A**: in the absence of ChOx, and in the presence of **B:** 20, **C**: 40, **D**; 60, **E**: 80 and **F**: 100 nM ChOx. Figure Insets (**A** to **F**): Response curves for the AuNPs growth with H_2O_2. Variation of sensitivity of AuNPs growth with different **G:** ChOx and **H**: BSA concentrations. Each datum point represents the average of the analysis of triplicate values (n =3), with the range indicated with error bars

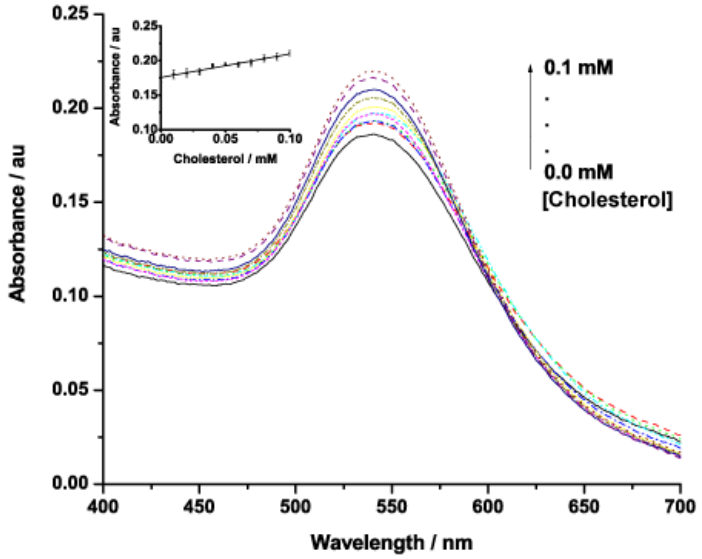

Figure 6.3 Growth of gold nanoparticles with ChOx (40 nM) and cholesterol: Figure Inset: Response curves for the AuNPs growth with ChOx and cholesterol

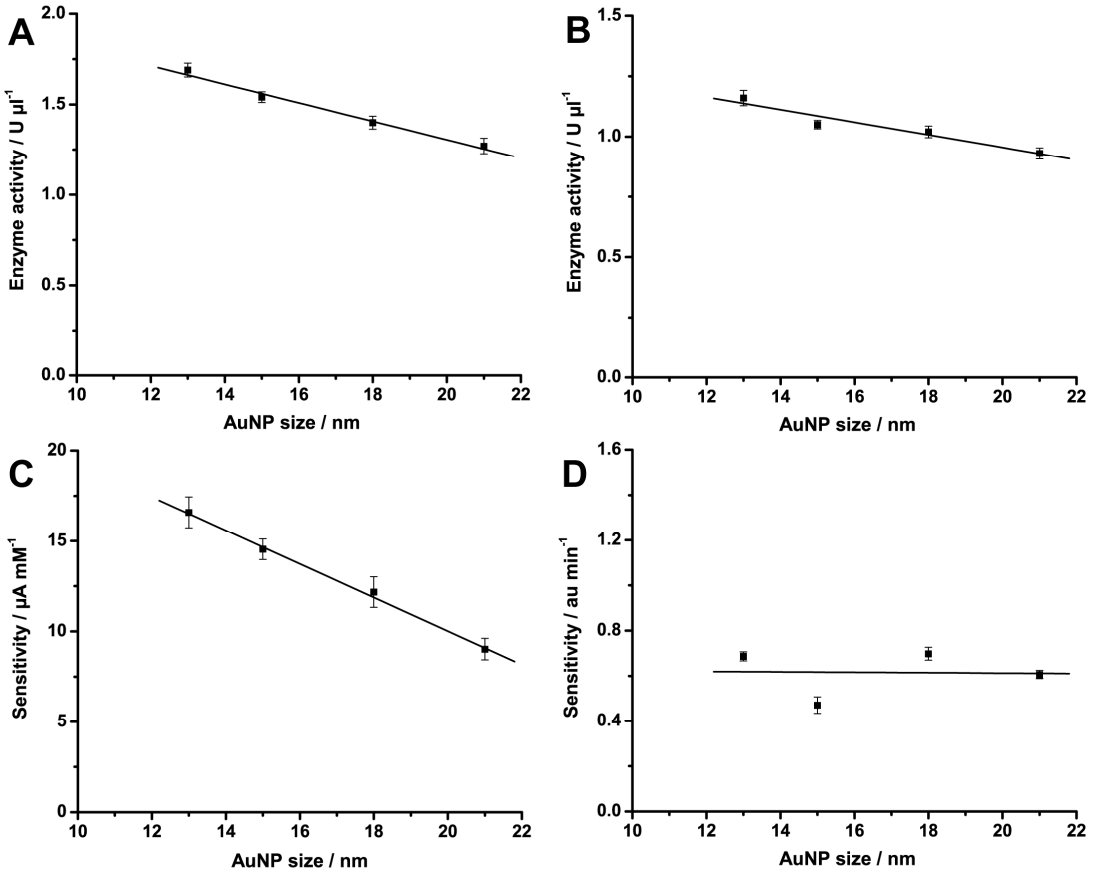

Figure 6.4 Effect of AuNPs size on their electrocatalytic and optocatalytic activities: Effect of AuNPs size on **A**: electrocatalytic activity of AuNPs with ChOx adsorbed on AuNPs, **B**: electrocatalytic activity of AuNPs with ChOx covalently attached on AuNPs, **C**: performance of gold nanoparticles based electrochemical biosensor, and **D**: performance of optical cholesterol biosensor. Each datum point represents the average of the analysis of triplicate values (n =3), with the range indicated with error bars

Conclusions and Scope for Future Work

Conclusions

The present investigation was intended to fabricate cholesterol biosensors with improved stability and sensitivity. For all the biosensor related studies, cholesterol oxidase (ChOx) from *Pseudomonas fluorescens* was used as the biorecognition element. Therefore, preliminary characterization of this *P. fluorescens* ChOx was done. This ChOx was found to be a ~57 kDa single subunit protein with reasonable kinetic parameters. The N-terminal sequencing of ChOx was done and the analysis of N-terminal sequence showed its similarity with the N-terminal sequence of ChOx protein from *Burkholderia cepacia*. The analysis of the ChOx catalyzed cholesterol oxidation product was also carried out and it was found that during the cholesterol catalysis, ChOx produces 6β-hydroperoxycholest-4-en-3-ne (HCEO) but not the cholest-4-en-3-one (CEO) as the final product. The N-terminal sequence analysis and product analysis showed that the ChOx protein from *Pseudomonas fluorescens* may have molecular similarities with that of *Burkholderia cepacia*.

The bioelectrode fabrication employed woven silk fiber (silk-mat) and nanomaterials (carbon nanotubes and gold nanoparticles) as immobilization matrices for ChOx. Silk-mat was demonstrated to be suitable matrix for the construction of oxygen electrode based cholesterol biosensor. The study revealed that the fibrous and porous morphology of the silk-mat provide an ideal microenvironment to the immobilized enzyme that results in good analytical performance with high stability ($t_{1/2}$, 13 months), sensitivity, reproducibility and good selectivity for cholesterol estimation. Although, the silk-mat based biosensor showed optimal characteristics, the real sample analysis could not be performed because of the fouling of silk-mat surface with serum proteins.

Apart from silk-mat, nanomaterials such as carbon nanotubes and gold nanoparticles have also been used as the immobilization matrices. Both these materials were found to enhance the current response of the fabricated bioelectrodes by increasing the electroactive surface area for higher enzyme loading, providing a biocompatible environment for the ChOx and improving the conductivity of the electrode surface. The use of nanomaterials reduced the overpotential which minimized the interference from other co-oxidizable compounds present in physiological samples. The bioelectrodes based on multiwalled carbon nanotubes and gold nanoparticles exhibited good response characteristics with a proper linearity, good sensitivity, high selectivity and high operational and storage stability. These bioelectrodes were also demonstrated to be efficiently used as an amperometric biosensor for the highly sensitive and selective determination of cholesterol in real samples. A comparison of the analytical properties of the bioelectrodes fabricated in our study with those of some other reported biosensors is shown below in a tabular form.

Biosensor configuration	Sensing element	Method of immobilization	Response parameters	References
PPy/Pt	ChOx	Entrapment	Linearity: 0.06 – 0.4 mM Detection limit: 14000 µM Sensitivity: 0.077 µA mM^{-1} Stability: ~ 98 % in 30 days	(Vidal et al. 2000)
Silica-sol gel-CHIT-MWCNTs	ChOx	Entrapment	Linearity: 0.004 - 0.7 mM Detection limit: 1 µM Sensitivity: 1.55 µA mM^{-1} Stability: ~ 11 % in15 days	(Tan et al. 2005)
FAD/BA/PQQ/Cysteamine (SAM)	ChOx	Reconstitution	Linearity: 0.07-1.25 mM Detection limit: 690 µM Sensitivity: 0.625 µA mM^{-1} Stability: ~20 % in 12 days	(Vidal et al. 2004a)
NiNP-CNTs	ChOx	Cross-linking	Linearity: 0.005 – 3 mM Detection limit: 1 µM Stability: 15 % in 1 month	(Yang et al. 2006b)
CNTs-PtNPs-CHIT	ChOx/ ChEt	Cross-linking	Linearity: 0.01 – 3 mM Detection limit: 5 µM Stability: 10 % in 1 week	(Yang et al. 2006c)
MWCNTs-AuNPs-CHIT-IL	ChOx	Entrapment	Linearity: 0.5 – 5 mM Sensitivity: 200 µA M^{-1} Stability: 5 % in 20 days	(Gopalan et al. 2009)
PtNPs-CNTs	ChOx	Entrapment	Linearity: 0.004 – 0.1 mM Stability: 5.7 % in 6 weeks	(Shi and Peng 2005)
SnO_2 NPs-CHIT	ChOx	Physisorption	Linearity: 0.26 –10.4 mM Detection limit: 130 µM Sensitivity: 1.33 µA/µM cm^2 Stability: 5 % in 4-6 weeks	(Ansari et al. 2009)
Silk-mat	**ChOx**	**Covalent attachment**	**Linearity: 0.02-0.09 mM** **Detection limit: 8.5 µM** **Sensitivity: 0.0313 µmol O_2 min^{-1}** **Stability: ~50 % in 13 months**	**Present work**
AuE-Nf-MWCNTs-ChOx-ChEt-Nf	**ChOx ChEt**	**Entrapment**	**Linearity: 0.080-0.645 mM** **Detection limit: 10 µM** **Sensitivity: 690.13 µA mM^{-1}** **Stability: ~10 % in 3 weeks**	**Present work**
AuE/dithiol/AuNPs/MUA/ChOx	**ChOx**	**Covalent attachment**	**Linearity: 0.04 –0.22 mM** **Detection limit: 34.6 µM** **Sensitivity: 9.02 µA mM^{-1}** **Stability: ~ 5 % in 1 month**	**Present work**

* Few values are normalized for making the units uniform for better comparison. The stability was reported as the decrease in biosensor response.

From the above comparison, we can observe that all of our fabricated bioelectrodes showed very high stabilities. The MWCNTs based bioelectrode showed a very high sensitivity of 690.13 µA mM^{-1}. The linear detection range for cholesterol with all the

electrodes was also found to be optimum. To conclude, the nanomaterial based bioelectrodes fabricated in our study have profound application potential for cholesterol estimation in real samples.

The spectrophotometric analysis of electronic coupling of gold nanoparticles and cholesterol oxidase showed that gold nanoparticles can act as electron transfer mediator for cholesterol oxidase and help in improving the current response of the bioelectrodes. The investigation on size-dependent catalytic properties of AuNPs showed that AuNPs of lower sizes have greater electron transfer abilities. The studies on electrocatalytic and optocatalytic activities of different sized AuNPs provide useful insight into the design of biosensors based on gold nanoparticles and the role that size of the NPs play in these studies. The findings have potential applications for the optimization of the AuNPs-protein complex for the analytical applications.

Scope for future work

The silk-mat is a commercially available low cost material and this may be a promising biocompatible biomaterial which could be useful for the future development of economic biosensors. In the present study, conventional biological oxygen monitor is used for fabricating the biosensor. In the future, the silk-mat-immobilized cholesterol oxidase may be used in the fabrication of cholesterol biosensor by assembling it with other modern electrochemical or optical transducers to overcome the problem caused by low O_2 diffusion due to fouling of electrode surface with serum proteins. Taking into account the good performance of the fabricated nanomaterials based bioelectrodes, the proposed novel fabrication methods are of great interest for the development of other highly sensitive and stable nanostructured biosensors. The elucidation of cholesterol oxidase

structure and mechanism of electron hopping from the redox center of ChOx to the electrode may help to optimize these nanomaterial based fabrication of bioelectrode for better performance. Further technological advancement of microelectronics and miniaturization may help in the development of current fabricated bioelectrodes to portable commercial cholesterol biosensors.

Bibliography

Ahmadalinezhad A, Chen A (2011) High-performance electrochemical biosensor for the detection of total cholesterol. Biosens Bioelectron 26:4508-13

Ahuja T, Mir IA, Kumar D, Rajesh (2007) Biomolecular immobilization on conducting polymers for biosensing applications. Biomaterials 28:791-805

Allain CC, Poon LS, Chan CS, Richmond W, Fu PC (1974) Enzymatic determination of total serum cholesterol. Clin Chem 20:470-5

Altman GH, Diaz F, Jakuba C, Calabro T, Horan RL, Chen J, Lu H, Richmond J, Kaplan DL (2003) Silk-based biomaterials. Biomaterials 24:401-16

Amine A, Mohammadi H, Bourais I, Palleschi G (2006) Enzyme inhibition-based biosensors for food safety and environmental monitoring. Biosens Bioelectron 21:1405-23

Ansari AA, Kaushik A, Solanki PR, Malhotra BD (2009) Electrochemical Cholesterol Sensor Based on Tin Oxide-Chitosan Nanobiocomposite Film. Electroanalysis 21:965-72

Antonini M, Ghisellini P, Paternolli C, Nicolini C (2004) Electrochemical study of the interaction between cytochrome P450sccK201E and cholesterol. Talanta 62:945-50

Aravamudhan S, Kumar A, Mohapatra S, Bhansali S (2007a) Sensitive estimation of total cholesterol in blood using Au nanowires based micro-fluidic platform. Biosens Bioelectron 22:2289-94

Aravamudhan S, Ramgir NS, Bhansali S (2007b) Electrochemical biosensor for targeted detection in blood using aligned nanowires. Sens Actuators B Chem 127:29-35

Arya SK, Datta M, Malhotra BD (2008) Recent advances in cholesterol biosensor. Biosens Bioelectron 23:1083-100

Arya SK, Datta M, Singh SP, Malhotra BD (2007a) Biosensor for total cholesterol estimation using N-(2-aminoethyl)-3-aminopropyltrimethoxysilane self-assembled monolayer. Anal Bioanal Chem 389:2235-42

Arya SK, Pandey P, Singh SP, Datta M, Malhotra BD (2007b) Dithiobissuccinimidyl propionate self assembled monolayer based cholesterol biosensor. Analyst 132:1005-9

Arya SK, Prusty AK, Singh SP, Solanki PR, Pandey MK, Datta M, Malhotra BD (2007c) Cholesterol biosensor based on N-(2-aminoethyl)-3-aminopropyl-trimethoxysilane self-assembled monolayer. Anal Biochem 363:210-8

Arya SK, Solanki PR, Datta M, Malhotra BD (2009) Recent advances in self-assembled monolayers based biomolecular electronic devices. Biosens Bioelectron 24:2810-7

Arya SK, Solanki PR, Singh RP, Pandey MK, Datta M, Malhotra BD (2006) Application of octadecanethiol self-assembled monolayer to cholesterol biosensor based on surface plasmon resonance technique. Talanta 69:918-26

Arya SK, Solanki PR, Singh SP, Kaneto K, Pandey MK, Datta M, Malhotra BD (2007d) Poly-(3-hexylthiophene) self-assembled monolayer based cholesterol biosensor using surface plasmon resonance technique. Biosens Bioelectron 22:2516-24

Asefa T, Duncan CT, Sharma KK (2009) Recent advances in nanostructured chemosensors and biosensors. Analyst 134:1980-90

Barik A, Solanki PR, Kaushik A, Ali A, Pandey MK, Kim CG, Malhotra BD (2010) Polyaniline-carboxymethyl cellulose nanocomposite for cholesterol detection. J Nanosci Nanotechnol 10:6479-88

Baron R, Zayats M, Willner I (2005) Dopamine-, L-DOPA-, adrenaline-, and noradrenaline-induced growth of Au nanoparticles: assays for the detection of neurotransmitters and of tyrosinase activity. Anal Chem 77:1566-71

Bartlett PN, Bradford VQ, Whitaker RG (1991) Enzyme electrode studies of glucose oxidase modified with a redox mediator. Talanta 38:57-63

Basu AK, Chattopadhyay P, Roychoudhuri U, Chakraborty R (2007) Development of cholesterol biosensor based on immobilized cholesterol esterase and cholesterol oxidase on oxygen electrode for the determination of total cholesterol in food samples. Bioelectrochemistry 70:375-9

Battaglini F, Bartlett PN, Wang JH (2000) Covalent attachment of osmium complexes to glucose oxidase and the application of the resulting modified enzyme in an enzyme switch responsive to glucose. Anal Chem 72:502-9

Baughman RH, Zakhidov AA, de Heer WA (2002) Carbon nanotubes--the route toward applications. Science 297:787-92

Benitez G, Vericat C, Tanco S, Remes Lenicov F, Castez MF, Vela ME, Salvarezza RC (2004) Role of surface heterogeneity and molecular interactions in the charge-transfer process through self-assembled thiolate monolayers on Au(111). Langmuir 20:5030-7

Besombes JL, Cosnier S, Labbe P (1997) Improvement of poly(amphiphilic pyrrole) enzyme electrodes via the incorporation of synthetic laponite-clay-nanoparticles. Talanta 44:2209-15

Bongiovanni C, Ferri T, Poscia A, Varalli M, Santucci R, Desideri A (2001) An electrochemical multienzymatic biosensor for determination of cholesterol. Bioelectrochemistry 54:17-22

Bradford MM (1976) A rapid and sensitive method for the quantitation of microgram quantities of protein utilizing the principle of protein-dye binding. Anal Biochem 72:248-54

Brahim S, Narinesingh D, Guiseppi-Elie A (2002) Bio-smart hydrogels: co-joined molecular recognition and signal transduction in biosensor fabrication and drug delivery. Biosens Bioelectron 17:973-81

Brewer SH, Glomm WR, Johnson MC, Knag MK, Franzen S (2005) Probing BSA binding to citrate-coated gold nanoparticles and surfaces. Langmuir 21:9303-7

Cao X, Ye Y, Liu S (2011) Gold nanoparticle-based signal amplification for biosensing. Anal Biochem 417:1-16

Carrara S, Shumyantseva VV, Archakov AI, Samori B (2008) Screen-printed electrodes based on carbon nanotubes and cytochrome P450scc for highly sensitive cholesterol biosensors. Biosens Bioelectron 24:148-50

Chaki NK, Vijayamohanan K (2002) Self-assembled monolayers as a tunable platform for biosensor applications. Biosens Bioelectron 17:1-12

Chatterjee S, Barbora L, Cameotra SS, Mahanta P, Goswami P (2009) Silk-fiber immobilized lipase-catalyzed hydrolysis of emulsified sunflower oil. Appl Biochem Biotechnol 157:593-600

Cheetham PS, Dunnill P, Lilly MD (1982) The characterization and interconversion of three forms of cholesterol oxidase extracted from Nocardia rhodochrous. Biochem J 201:515-21

Chen RJ, Choi HC, Bangsaruntip S, Yenilmez E, Tang X, Wang Q, Chang YL, Dai H (2004) An investigation of the mechanisms of electronic sensing of protein adsorption on carbon nanotube devices. J Am Chem Soc 126:1563-8

Chen XY, Li JR, Li XC, Jiang L (1998) A new step to the mechanism of the enhancement effect of gold nanoparticles on glucose oxidase. Biochem Biophys Res Commun 245:352-5

Chen Y, Flowers K, Calizo M, Bishnoi SW (2010) The role of protein binding in the poisoning of gold nanoparticle catalysts. Colloids Surf B Biointerfaces 76:241-7

Clark LC, Jr., Lyons C (1962) Electrode systems for continuous monitoring in cardiovascular surgery. Ann N Y Acad Sci 102:29-45

Crumbliss AL, Perine SC, Stonehuerner J, Tubergen KR, Zhao J, Henkens RW, O'Daly JP (1992) Colloidal gold as a biocompatible immobilization matrix suitable for the fabrication of enzyme electrodes by electrodeposition. Biotechnol Bioeng 40:483-90

Cuenya BR, Baeck SH, Jaramillo TF, McFarland EW (2003) Size- and support-dependent electronic and catalytic properties of Au0/Au3+ nanoparticles synthesized from block copolymer micelles. J Am Chem Soc 125:12928-34

Cui J, Kulagina NV, Michael AC (2001) Pharmacological evidence for the selectivity of in vivo signals obtained with enzyme-based electrochemical sensors. J Neurosci Methods 104:183-9

Demura M, Asakura T (1989) Immobilization of glucose oxidase with Bombyx mori silk fibroin by only stretching treatment and its application to glucose sensor. Biotechnol Bioeng 33:598-603

Devadoss A, Burgess JD (2004) Steady-state detection of cholesterol contained in the plasma membrane of a single cell using lipid bilayer-modified microelectrodes incorporating cholesterol oxidase. J Am Chem Soc 126:10214-5

Dhand C, Arya SK, Datta M, Malhotra BD (2008) Polyaniline-carbon nanotube composite film for cholesterol biosensor. Anal Biochem 383:194-9

Dhand C, Solanki PR, Pandey MK, Datta M, Malhotra BD (2010) Electrophoretically deposited polyaniline nanotubes based film for cholesterol detection. Electrophoresis 31:3754-62

D'Orazio P (2003) Biosensors in clinical chemistry. Clin Chim Acta 334:41-69

Doukyu N (2009) Characteristics and biotechnological applications of microbial cholesterol oxidases. Appl Microbiol Biotechnol 83:825-37

Doukyu N, Aono R (1998) Purification of Extracellular Cholesterol Oxidase with High Activity in the Presence of Organic Solvents from Pseudomonas sp. Strain ST-200. Appl Environ Microbiol 64:1929-32

Doukyu N, Aono R (1999) Two moles of O_2 consumption and one mole of H_2O_2 formation during cholesterol peroxidation with cholesterol oxidase from *Pseudomonas sp.* strain ST-200. Biochem J 341 (Pt 3):621-7

Doukyu N, Aono R (2001) Cloning, sequence analysis and expression of a gene encoding an organic solvent- and detergent-tolerant cholesterol oxidase of *Burkholderia cepacia* strain ST-200. Appl Microbiol Biotechnol 57:146-52

Doukyu N, Shibata K, Ogino H, Sagermann M (2008) Purification and characterization of *Chromobacterium sp.* DS-1 cholesterol oxidase with thermal, organic solvent, and detergent tolerance. Appl Microbiol Biotechnol 80:59-70

Eckenrode HM, Jen SH, Han J, Yeh AG, Dai HL (2005) Adsorption of a cationic dye molecule on polystyrene microspheres in colloids: effect of surface charge and composition probed by second harmonic generation. J Phys Chem B 109:4646-53

Feng JJ, Zhao G, Xu JJ, Chen HY (2005) Direct electrochemistry and electrocatalysis of heme proteins immobilized on gold nanoparticles stabilized by chitosan. Anal Biochem 342:280-6

Frens G (1973) Controlled nucleation for the regulation of the particle size in monodisperse gold suspensions. Nat Phys Sci 241:20-2

Fukuyama M, Miyake Y (1979) Purification and some properties of cholesterol oxidase from *Schizophyllum commune* with covalently bound flavin. J Biochem 85:1183-93

Ghosh SK, Pal A, Kundu S, Nath S, Pal T (2004) Fluorescence quenching of 1-methylaminopyrene near gold nanoparticles: size regime dependence of the small metallic particles. Chem Phys Lett 395:366-372

Gooding JJ, Erokhin P, Losic D, Yang W, Policarpio V, Liu J, Ho FM, Situmorang M, Hibbert DB, Shapter JG (2001) Parameters important in fabricating enzyme electrodes using self-assembled monolayers of alkanethiols. Anal Sci 17:3-9

Gopalan AI, Lee KP, Ragupathy D (2009) Development of a stable cholesterol biosensor based on multi-walled carbon nanotubes-gold nanoparticles composite covered with a layer of chitosan-room-temperature ionic liquid network. Biosens Bioelectron 24:2211-7

Goran JM, Lyon JL, Stevenson KJ (2011) Amperometric Detection of l-Lactate Using Nitrogen-Doped Carbon Nanotubes Modified with Lactate Oxidase. Anal Chem 83:8123-9

Grabarek Z, Gergely J (1990) Zero-length crosslinking procedure with the use of active esters. Anal Biochem 185:131-5

Grasset L, Cordier D, Ville A (1977) Woven silk as a carrier for the immobilization of enzymes. Biotechnol Bioeng 19:611-8

Guo S, Dong S (2009) Biomolecule-nanoparticle hybrids for electrochemical biosensors. Trends Anal Chem 28:96-109

Guo S, Wang E (2007) Synthesis and electrochemical applications of gold nanoparticles. Anal Chim Acta 598:181-92

He L, Lin D, Wang Y, Xiao Y, Che J (2011) Electroactive SWNT/PEGDA hybrid hydrogel coating for bio-electrode interface. Colloids Surf B Biointerfaces 87:273-9

Holtz JH, Asher SA (1997) Polymerized colloidal crystal hydrogel films as intelligent chemical sensing materials. Nature 389:829-32

Hussain F, Birch DJ, Pickup JC (2005) Glucose sensing based on the intrinsic fluorescence of sol-gel immobilized yeast hexokinase. Anal Biochem 339:137-43

Hyun S, Park TH (2011) Integration of biomolecules and nanomaterials: Towards highly selective and sensitive biosensors. Biotechnol J 6:1310-6

Iannello RM, Iacynych AM (1981) Immobilized enzyme chemically modified electrode as an amperometric sensor. Anal Chem 53:2090-5

Ishizaki T, Hirayama N, Shinkawa H, Nimi O, Murooka Y (1989) Nucleotide sequence of the gene for cholesterol oxidase from a *Streptomyces sp.* J Bacteriol 171:596-601

Jain PK, Lee KS, El-Sayed IH, El-Sayed MA (2006) Calculated absorption and scattering properties of gold nanoparticles of different size, shape, and composition: applications in biological imaging and biomedicine. J Phys Chem B 110:7238-48

Jena BK, Ghosh S, Bera R, Dey RS, Das AK, Raj CR (2010) Bioanalytical applications of Au nanoparticles. Recent Pat Nanotechnol 4:41-52

Kamei T, Takiguchi Y, Suzuki H, Matsuzaki M, Nakamura S (1978) Purification of 3beta-hydroxysteroid oxidase of *Streptomyces violascens* origin by affinity chromatography on cholesterol. Chem Pharm Bull (Tokyo) 26:2799-2804

Kaplan DL (1998) Fibrous proteins-silk as a model system. Polym Degrad Stab 59:25-32

Katz E, Willner I (2004) Integrated nanoparticle-biomolecule hybrid systems: synthesis, properties, and applications. Angew Chem Int Ed Engl 43:6042-108

Katz E, Willner I, Wang J (2004) Electroanalytical and bioelectroanalytical systems based on metal and semiconductor nanoparticles. Electroanalysis 16:19-44

Khan R, Kaushik A, Solanki PR, Ansari AA, Pandey MK, Malhotra BD (2008) Zinc oxide nanoparticles-chitosan composite film for cholesterol biosensor. Anal Chim Acta 616:207-13

Kim J, Grate JW, Wang P (2008) Nanobiocatalysis and its potential applications. Trends Biotechnol 26:639-46

Kouassi GK, Irudayaraj J, McCarty G (2005) Examination of Cholesterol oxidase attachment to magnetic nanoparticles. J Nanobiotechnology 3:1

Kowalski D, Schmuki P (2010) Polypyrrole self-organized nanopore arrays formed by controlled electropolymerization in TiO2 nanotube template. Chem Commun (Camb) 46:8585-7

Kreit J, Sampson NS (2009) Cholesterol oxidase: physiological functions. Febs J 276:6844-56

Kumar A, Pandey RR, Brantley B (2006) Tetraethylorthosilicate film modified with protein to fabricate cholesterol biosensor. Talanta 69:700-5

Kumar A, Rajesh, Chaubey A, Grover SK, Malhotra BD (2001) Immobilization of cholesterol oxidase and potassium ferricyanide on dodecylbenzene sulfonate ion-doped polypyrrole film. J Appl Polym Sci 82:3486-91

Laemmli UK (1970) Cleavage of structural proteins during the assembly of the head of bacteriophage T4. Nature 227:680-5

Laskey JG, Patterson P, Bilyeu K, Morris RO (2003) Rate enhancement of cytokinin oxidase/dehydrogenase using 2,6-dichloroindophenol as an electron acceptor. Plant Growth Regul 40:189-196

Laviron E (1974) Adsorption, autoinhibition and autocatalysis in polarography and in linear potential sweep voltammetry. J Electroanal Chem 52:355-93

Laviron E (1979) General expression of the linear potential sweep voltammogram in the case of diffusionless electrochemical systems. J Electroanal Chem 100:263-70

Law WT, Doshi S, McGeehan J, McGeehan S, Gibboni D, Nikolioukine Y, Keane R, Zheng J, Rao J, Ertingshausen G (1997) Whole-blood test for total cholesterol by a self-metering, self-timing disposable device with built-in quality control. Clin Chem 43:384-9

Lei CX, Hu SQ, Gao N, Shen GL, Yu RQ (2004) An amperometric hydrogen peroxide biosensor based on immobilizing horseradish peroxidase to a nano-Au monolayer supported by sol-gel derived carbon ceramic electrode. Bioelectrochemistry 65:33-9

Li D, He Q, Cui Y, Duan L, Li J (2007) Immobilization of glucose oxidase onto gold nanoparticles with enhanced thermostability. Biochem Biophys Res Commun 355:488-93

Li G, Liao JM, Hu GQ, Ma NZ, Wu PJ (2005) Study of carbon nanotube modified biosensor for monitoring total cholesterol in blood. Biosens Bioelectron 20:2140-4

Li YF, Liu ZM, Liu YL, Yang YH, Shen GL, Yu RQ (2006) A mediator-free phenol biosensor based on immobilizing tyrosinase to ZnO nanoparticles. Anal Biochem 349:33-40

Lim SH, Wei J, Lin J, Li Q, Kuayou J (2005) A glucose biosensor based on electrodeposition of palladium nanoparticles and glucose oxidase onto Nafion-solubilized carbon nanotube electrode. Biosens Bioelectron 20:2341-6

Lin CC, Yang MC (2003) Cholesterol oxidation using hollow fiber dialyzer immobilized with cholesterol oxidase: preparation and properties. Biotechnol Prog 19:361-4

Lin Y, Yantasee W, Wang J (2005) Carbon nanotubes (CNTs) for the development of electrochemical biosensors. Front Biosci 10:492-505

Liu X, Atwater M, Wang J, Huo Q (2007) Extinction coefficient of gold nanoparticles with different sizes and different capping ligands. Colloids Surf B Biointerfaces 58:3-7

Lu Q, Li CM (2008) One-step co-electropolymerized conducting polymer-protein composite film for direct electrochemistry-based biosensors. Biosens Bioelectron 24:773-8

Lu S, Wang X, Lu Q, Hu X, Uppal N, Omenetto FG, Kaplan DL (2009) Stabilization of enzymes in silk films. Biomacromolecules 10:1032-42

Luong JH, Male KB, Hrapovic S (2007) Carbon nanotube-based electrochemical biosensing platforms: fundamentals, applications, and future possibilities. Recent Pat Biotechnol 1:181-91

MacLachlan J, Wotherspoon AT, Ansell RO, Brooks CJ (2000) Cholesterol oxidase: sources, physical properties and analytical applications. J Steroid Biochem Mol Biol 72:169-95

Malhotra BD, Chaubey A (2003) Biosensors for clinical diagnosis industry. Sens Actuators B Chem 91:117-27

Malik V, Pundir CS (2002) Determination of total cholesterol in serum by cholesterol esterase and cholesterol oxidase immobilized and co-immobilized on to arylamine glass. Biotechnol Appl Biochem 35:191-7

Manesh KM, Kim HT, Santhosh P, Gopalan AI, Lee KP (2008) A novel glucose biosensor based on immobilization of glucose oxidase into multiwall carbon nanotubes-polyelectrolyte-loaded electrospun nanofibrous membrane. Biosens Bioelectron 23:771-9

Marazuela MD, Cuesta B, Moreno-Bondi MC, Quejido A (1997) Free cholesterol fiber-optic biosensor for serum samples with simplex optimization. Biosens Bioelectron 12:233-40

Matharu Z, Pandey P, Pandey MK, Gupta V, Malhotra BD (2009) Functionalized gold nanoparticles - octadecylamine hybrid langmuir-blodgett film for enzyme sensor. Electroanalysis 21:1587-96

Matharu Z, Sumana G, Arya SK, Singh SP, Gupta V, Malhotra BD (2007) Polyaniline Langmuir-Blodgett film based cholesterol biosensor. Langmuir 23:13188-92

Mi L, Zhang X, Yang W, Wang L, Huang Q, Fan C, Hu J (2009) Artificial nano-bio-complexes: effects of nanomaterials on biomolecular reactions and applications in biosensing and detection. J Nanosci Nanotechnol 9:2247-55

Minoura N, Tsukada M, Nagura M (1990) Physico-chemical properties of silk fibroin membrane as a biomaterial. Biomaterials 11:430-4

Molnar I, Hayashi N, Choi KP, Yamamoto H, Yamashita M, Murooka Y (1993) Bacterial cholesterol oxidases are able to act as flavoprotein-linked ketosteroid monooxygenases that catalyse the hydroxylation of cholesterol to 4-cholesten-6-ol-3-one. Mol Microbiol 7:419-28

Motonaka J, Faulkner LR (1993) Determination of cholesterol and cholesterol ester with novel enzyme microsensors. Anal Chem 65:3258-61

Muhammet SM, Cete S, Arslan F, Yasar A (2009) Amperometric cholesterol biosensors based on the electropolymerization of pyrrole and aniline in sulphuric Acid for the determination of cholesterol in serum. Artif Cells Blood Substit Immobil Biotechnol 37:273-8

Nakaminami T, Ito S, Kuwabata S, Yoneyama H (1999) Amperometric determination of total cholesterol at gold electrodes covalently modified with cholesterol oxidase and cholesterol esterase with use of thionin as an electron mediator. Anal Chem 71:1068-76

Nakaminami T, Kuwabata S, Yoneyama H (1997) Electrochemical oxidation of cholesterol catalyzed by cholesterol oxidase with use of an artificial electron mediator. Anal Chem 69:2367-72

Nambiar S, Yeow JT (2011) Conductive polymer-based sensors for biomedical applications. Biosens Bioelectron 26:1825-32

Nath N, Chilkoti A (2002) A colorimetric gold nanoparticle sensor to interrogate biomolecular interactions in real time on a surface. Anal Chem 74:504-9

Newman AR (1989) Measuring the fat of the land. Anal Chem 61:663A-664A

Niemeyer CM (2003) Functional hybrid devices of proteins and inorganic nanoparticles. Angew Chem Int Ed Engl 42:5796-800

Ohta T, Fujishiro K, Yamaguchi K, Tamura Y, Aisaka K, Uwajima T, Hasegawa M (1991) Sequence of gene choB encoding cholesterol oxidase of *Brevibacterium sterolicum*: comparison with choA of *Streptomyces sp.* SA-COO. Gene 103:93-6

Omodeo Sale F, Marchesini S, Fishman PH, Berra B (1984) A sensitive enzymatic assay for determination of cholesterol in lipid extracts. Anal Biochem 142:347-50

Ozsoz M, Erdem A, Ozkan D, Kara P, Karadeniz H, Meric B, Kerman K, Girousi S (2005) Allele-specific genotyping by using guanine and gold electrochemical oxidation signals. Bioelectrochemistry 67:199-203

Park BW, Yoon DY, Kim DS (2010) Recent progress in bio-sensing techniques with encapsulated enzymes. Biosens Bioelectron 26:1-10

Paternolli C, Antonini M, Ghisellini P, Nicolini C (2004) Recombinant cytochrome p450 immobilization for biosensor applications. Langmuir 20:11706-12

Pena N, Ruiz G, Reviejo AJ, Pingarron JM (2001) Graphite-teflon composite bienzyme electrodes for the determination of cholesterol in reversed micelles. Application to food samples. Anal Chem 73:1190-5

Pingarron JM, Yanez-Sedeno, P., Gonzalez-Cortes, A. (2008) Gold nanoparticle-based electrochemical biosensors. Electrochim Acta 53:5848-5866

Pollegioni L, Piubelli L, Molla G (2009) Cholesterol oxidase: biotechnological applications. Febs J 276:6857-70

Purcell JP, Greenplate JT, Jennings MG, Ryerse JS, Pershing JC, Sims SR, Prinsen MJ, Corbin DR, Tran M, Sammons RD, et al. (1993) Cholesterol oxidase: a potent insecticidal protein active against boll weevil larvae. Biochem Biophys Res Commun 196:1406-13

Ram MK, Bertoncello P, Ding H, Paddeu S, Nicolini C (2001) Cholesterol biosensors prepared by layer-by-layer technique. Biosens Bioelectron 16:849-56

Richmond W (1973) Preparation and properties of a cholesterol oxidase from Nocardia sp. and its application to the enzymatic assay of total cholesterol in serum. Clin Chem 19:1350-6

Roberts JG, Hamilton KL, Sombers LA (2011) Comparison of electrode materials for the detection of rapid hydrogen peroxide fluctuations using background-subtracted fast scan cyclic voltammetry. Analyst 136:3550-6

Rose G, Shipley MJ (1980) Plasma lipids and mortality: a source of error. Lancet 1:523-6

Roy S, Vedala H, Choi W (2006) Vertically aligned carbon nanotube probes for monitoring blood cholesterol. Nanotechnology 17:S14-8

Safavi A, Farjami F (2011) Electrodeposition of gold-platinum alloy nanoparticles on ionic liquid-chitosan composite film and its application in fabricating an amperometric cholesterol biosensor. Biosens Bioelectron 26:2547-52

Salinas E, Rivero V, Torriero AA, Benuzzi D, Sanz MI, Raba J (2006) Multienzymatic-rotating biosensor for total cholesterol determination in a FIA system. Talanta 70:244-50

Samanta D, Sarkar A (2011) Immobilization of bio-macromolecules on self-assembled monolayers: methods and sensor applications. Chem Soc Rev 40:2567-92

Sampson NS (2001) Dissection of a flavoenzyme active site: the reaction catalyzed by cholesterol oxidase. Antioxid Redox Signal 3:839-46

Sarma AK, Vatsyayan P, Goswami P, Minteer SD (2009) Recent advances in material science for developing enzyme electrodes. Biosens Bioelectron 24:2313-22

Scott RA, Lukehart CM (2007) Applications of physical methods to inorganic and bioinorganic chemistry, 10 edn. Hoboken, NJ: Wiley. 594 pp.

Shang L, Chen H, Deng L, Dong S (2008) Enhanced resonance light scattering based on biocatalytic growth of gold nanoparticles for biosensors design. Biosens Bioelectron 23:1180-4

Shi QC, Peng TZ (2005) A novel cholesterol oxidase biosensor based on pt-nanoparticle /carbon nanotube modified electrode. Clin Chem Lett 16:1081-4

Shobha Jeykumari DR, Sriman Narayanan S (2008) A novel nanobiocomposite based glucose biosensor using neutral red functionalized carbon nanotubes. Biosens Bioelectron 23:1404-11

Shreve OD, Heether, M.R. (1951) Infrared absorption spectra of some hydroperoxides, peroxides, and related compounds. Anal Chem 23:282-285

Shumyantseva V, Deluca G, Bulko T, Carrara S, Nicolini C, Usanov SA, Archakov A (2004) Cholesterol amperometric biosensor based on cytochrome P450scc. Biosens Bioelectron 19:971-6

Shumyantseva VV, Carrara S, Bavastrello V, Jason Riley D, Bulko TV, Skryabin KG, Archakov AI, Nicolini C (2005) Direct electron transfer between cytochrome P450scc and gold nanoparticles on screen-printed rhodium-graphite electrodes. Biosens Bioelectron 21:217-22

Singh S, Singhal R, Malhotra BD (2007) Immobilization of cholesterol esterase and cholesterol oxidase onto sol-gel films for application to cholesterol biosensor. Anal Chim Acta 582:335-43

Singh S, Solanki PR, Pandey MK, Malhotra BD (2006) Covalent immobilization of cholesterol esterase and cholesterol oxidase on polyaniline films for application to cholesterol biosensor. Anal Chim Acta 568:126-32

Situmorang M, Alexander PW, Hibbert DB (1999) Flow injection potentiometry for enzymatic assay of cholesterol with a tungsten electrode sensor. Talanta 49:639-49

Smith AG, Brooks CJ (1974) Application of cholesterol oxidase in the analysis of steroids. J Chromatogr 101:373-8

Smith AG, Brooks CJ (1975) Studies of the substrate specificity of cholesterol oxidase from *Nocardia erythropolis* in the oxidation of 3-hydroxy steroids. Biochem Soc Trans 3:675-7

Smith AG, Brooks CJ (1976) Cholesterol oxidases: properties and applications. J Steroid Biochem 7:705-13

Smith K, Silvernail NJ, Rodgers KR, Elgren TE, Castro M, Parker RM (2002) Sol-gel encapsulated horseradish peroxidase: a catalytic material for peroxidation. J Am Chem Soc 124:4247-52

Sojo M, Bru R, Lopez-Molina D, Garcia-Carmona F, Arguelles JC (1997) Cell-linked and extracellular cholesterol oxidase activities from *Rhodococcus erythropolis*. Isolation and physiological characterization. Appl Microbiol Biotechnol 47:583-9

Solanki PR, Arya SK, Nishimura Y, Iwamoto M, Malhotra BD (2007) Cholesterol biosensor based on amino-undecanethiol self-assembled monolayer using surface plasmon resonance technique. Langmuir 23:7398-403

Song MJ, Yun DH, Min NK, Hong SI (2007) Electrochemical biosensor array for liver diagnosis using silanization technique on nanoporous silicon electrode. J Biosci Bioeng 103:32-7

Staros JV, Wright RW, Swingle DM (1986) Enhancement by N-hydroxysulfosuccinimide of water-soluble carbodiimide-mediated coupling reactions. Anal Biochem 156:220-2

Sun W, Qin P, Zhao R, Jiao K (2010) Direct electrochemistry and electrocatalysis of hemoglobin on gold nanoparticle decorated carbon ionic liquid electrode. Talanta 80:2177-81

Tan X, Li M, Cai P, Luo L, Zou X (2005) An amperometric cholesterol biosensor based on multiwalled carbon nanotubes and organically modified sol-gel/chitosan hybrid composite film. Anal Biochem 337:111-20

Teng JI, Smith LL (1996) Sterol peroxidation by *Pseudomonas fluorescens* cholesterol oxidase. Steroids 61:627-33

Thanh NT, Rosenzweig Z (2002) Development of an aggregation-based immunoassay for anti-protein A using gold nanoparticles. Anal Chem 74:1624-8

Torabi SF, Khajeh K, Ghasempur S, Ghaemi N, Siadat SO (2007) Covalent attachment of cholesterol oxidase and horseradish peroxidase on perlite through silanization: activity, stability and co-immobilization. J Biotechnol 131:111-20

Trinder P, Webster D (1984) Determination of HDL-cholesterol using 2,4,6-tribromo-3-hydroxybenzoic acid with a commercial CHOD-PAP reagent. Ann Clin Biochem 21 (Pt 5):430-3

Tsai YC, Li SC, Chen JM (2005) Cast thin film biosensor design based on a Nafion backbone, a multiwalled carbon nanotube conduit, and a glucose oxidase function. Langmuir 21:3653-8

Tsunoyama H, Sakurai H, Negishi Y, Tsukuda T (2005) Size-specific catalytic activity of polymer-stabilized gold nanoclusters for aerobic alcohol oxidation in water. J Am Chem Soc 127:9374-5

Turfitt GE (1944a) Microbiological Agencies in the Degradation of Steroids: I. The Cholesterol-Decomposing Organisms of Soils. J Bacteriol 47:487-93

Turfitt GE (1944b) The microbiological degradation of steroids: 2. Oxidation of cholesterol by *Proactinomyces spp*. Biochem J 38:492-6

Turkevich J, Stevenson PC, Hillier J (1953) The formation of colloidal gold. J Phys Chem 57:670-3

Umar A, Rahman MM, Al-Hajry A, Hahn YB (2009) Highly-sensitive cholesterol biosensor based on well-crystallized flower-shaped ZnO nanostructures. Talanta 78:284-9

Updike SJ, Hicks GP (1967) The enzyme electrode. Nature 214:986-8

Vaddiraju S, Tomazos I, Burgess DJ, Jain FC, Papadimitrakopoulos F (2010) Emerging synergy between nanotechnology and implantable biosensors: a review. Biosens Bioelectron 25:1553-65

Vashist SK, Zheng D, Al-Rubeaan K, Luong JH, Sheu FS (2011) Advances in carbon nanotube based electrochemical sensors for bioanalytical applications. Biotechnol Adv 29:169-88

Vidal JC, Espuelas J, Castillo JR (2004a) Amperometric cholesterol biosensor based on in situ reconstituted cholesterol oxidase on an immobilized monolayer of flavin adenine dinucleotide cofactor. Anal Biochem 333:88-98

Vidal JC, Espuelas J, Garcia-Ruiz E, Castillo JR (2004b) Amperometric cholesterol biosensors based on the electropolymerization of pyrrole and the electrocatalytic effect of Prussian-Blue layers helped with self-assembled monolayers. Talanta 64:655-64

Vidal JC, Garcia E, Castillo JR (2002) Development of a platinized and ferrocene-mediated cholesterol amperometric biosensor based on electropolymerization of polypyrrole in a flow system. Anal Sci 18:537-42

Vidal JC, Garcia-Ruiz E, Castillo JR (2000) Strategies for the improvement of an amperometric cholesterol biosensor based on electropolymerization in flow systems: use of charge-transfer mediators and platinization of the electrode. J Pharm Biomed Anal 24:51-63

Vidal JC, Garcia-Ruiz E, Espuelas J, Aramendia T, Castillo JR (2003) Comparison of biosensors based on entrapment of cholesterol oxidase and cholesterol esterase in electropolymerized films of polypyrrole and diaminonaphthalene derivatives for amperometric determination of cholesterol. Anal Bioanal Chem 377:273-80

Vijayamohanan K, Aslam M (2001) Applications of self-assembled monolayers for biomolecular electronics. Appl Biochem Biotechnol 96:25-39

Vrielink A, Ghisla S (2009) Cholesterol oxidase: biochemistry and structural features. Febs J 276:6826-43

Wang J (2005) Nanomaterial-based electrochemical biosensors. Analyst 130:421-6

Wang J, Musameh M, Lin Y (2003) Solubilization of carbon nanotubes by Nafion toward the preparation of amperometric biosensors. J Am Chem Soc 125:2408-9

Wang S, Li S, Yu Y (2004) Immobilization of cholesterol oxidase on cellulose acetate membrane for free cholesterol biosensor development. Artif Cells Blood Substit Immobil Biotechnol 32:413-25

Wang Y, Liu L, Li M, Xu S, Gao F (2011) Multifunctional carbon nanotubes for direct electrochemistry of glucose oxidase and glucose bioassay. Biosens Bioelectron 30:107-11

Willner B, Katz E, Willner I (2006a) Electrical contacting of redox proteins by nanotechnological means. Curr Opin Biotechnol 17:589-96

Willner I, Baron R, Willner B (2006b) Growing metal nanoparticles by enzymes. Adv Mater 18:1109-1120

Willner I, Baron R, Willner B (2007a) Integrated nanoparticle-biomolecule systems for biosensing and bioelectronics. Biosens Bioelectron 22:1841-52

Willner I, Basnar B, Willner B (2007b) Nanoparticle-enzyme hybrid systems for nanobiotechnology. Febs J 274:302-9

Willner I, Katz E (2000) Integration of Layered Redox Proteins and Conductive Supports for Bioelectronic Applications. Angew Chem Int Ed Engl 39:1180-1218

Willner I, Willner B (2001) Biomaterials integrated with electronic elements: en route to bioelectronics. Trends Biotechnol 19:222-30

Willner I, Willner B (2010) Biomolecule-based nanomaterials and nanostructures. Nano Lett 10:3805-15

Willner I, Willner B, Katz E (2002) Functional biosensor systems via surface-nanoengineering of electronic elements. J Biotechnol 82:325-55

Willner I, Willner B, Katz E (2007c) Biomolecule-nanoparticle hybrid systems for bioelectronic applications. Bioelectrochemistry 70:2-11

Wink T, van Zuilen SJ, Bult A, van Bennkom WP (1997) Self-assembled monolayers for biosensors. Analyst 122:43R-50R

Wisitsoraat A, Sritongkham P, Karuwan C, Phokharatkul D, Maturos T, Tuantranont A (2010) Fast cholesterol detection using flow injection microfluidic device with functionalized carbon nanotubes based electrochemical sensor. Biosens Bioelectron 26:1514-20

Wong WW, Hachey DL, Clarke LL, Zhang S, Llaurador M, Pond WG (1994) An improved HPLC method to purify erythrocyte cholesterol for estimation of in vivo cholesterol synthesis using the deuterium method. Appl Radiat Isot 45:529-33

Wu XJ, Choi MM (2003) Hydrogel network entrapping cholesterol oxidase and octadecylsilica for optical biosensing in hydrophobic organic or aqueous micelle solvents. Anal Chem 75:4019-27

Xie W, Kong L, Kan M, Han D, Wang X, Zhang HM (2010) Introduction of gold nanoparticles into myoglobin-Nafion film for direct electrochemistry application. J Nanosci Nanotechnol 10:6720-4

Xu Z, Guo Z, Dong S (2005) Electrogenerated chemiluminescence biosensor with alcohol dehydrogenase and tris(2,2'-bipyridyl)ruthenium (II) immobilized in sol-gel hybrid material. Biosens Bioelectron 21:455-61

Yang M, Yang Y, Liu Y, Shen G, Yu R (2006a) Platinum nanoparticles-doped sol-gel/carbon nanotubes composite electrochemical sensors and biosensors. Biosens Bioelectron 21:1125-31

Yang M, Yang Y, Qu F, Lu Y, Shen G, Yu R (2006b) Attachment of nickel hexacyanoferrates nanoparticles on carbon nanotubes: Preparation, characterization and bioapplication. Anal Chim Acta 571:211-17

Yang M, Yang Y, Yang H, Shen G, Yu R (2006c) Layer-by-layer self-assembled multilayer films of carbon nanotubes and platinum nanoparticles with polyelectrolyte for the fabrication of biosensors. Biomaterials 27:246-55

Yao T, Takashima K (1998) Amperometric biosensor with a composite membrane of sol-gel derived enzyme film and electrochemically generated poly(1,2-diaminobenzene) film. Biosens Bioelectron 13:67-73

Yazdi MT, Zahraei M, Aghaepour K, Kamranpour N (2001) Purification and partial characterization of a cholesterol oxidase from Streptomyces fradiae. Enzyme Microb Technol 28:410-414

Yi X, Huang-Xian J, Hong-Yuan C (2000) Direct electrochemistry of horseradish peroxidase immobilized on a colloid/cysteamine-modified gold electrode. Anal Biochem 278:22-8

Zayats M, Baron R, Popov I, Willner I (2005) Biocatalytic growth of Au nanoparticles: from mechanistic aspects to biosensors design. Nano Lett 5:21-5

Zhang H, Lu H, Hu N (2006) Fabrication of electroactive layer-by-layer films of myoglobin with gold nanoparticles of different sizes. J Phys Chem B 110:2171-9

Zhang L, Jiang X, Wang E, Dong S (2005a) Attachment of gold nanoparticles to glassy carbon electrode and its application for the direct electrochemistry and electrocatalytic behavior of hemoglobin. Biosens Bioelectron 21:337-45

Zhang S, Wang N, Yu H, Niu Y, Sun C (2005b) Covalent attachment of glucose oxidase to an Au electrode modified with gold nanoparticles for use as glucose biosensor. Bioelectrochemistry 67:15-22

Zhao S, Zhang K, Bai Y, Yang W, Sun C (2006) Glucose oxidase/colloidal gold nanoparticles immobilized in Nafion film on glassy carbon electrode: Direct electron transfer and electrocatalysis. Bioelectrochemistry 69:158-63

Zhou N, Wang J, Chen T, Yu Z, Li G (2006) Enlargement of gold nanoparticles on the surface of a self-assembled monolayer modified electrode: a mode in biosensor design. Anal Chem 78:5227-30

Zicha J, Kunes J, Devynck MA (1999) Abnormalities of membrane function and lipid metabolism in hypertension: a review. Am J Hypertens 12:315-31

List of Publications

Publications in referred journals

1. **Urmila Saxena**, Pranab Goswami (2010) Silk Mat as Bio-matrix for the Immobilization of Cholesterol Oxidase, *Appl Biochem Biotechnol* 162, 1122.

2. **Urmila Saxena**, Madhuri Das, Seraj Ahmed, Lepakshi Barbora, Mala Borthakur, Anil Verma, Utpal Bora, Pranab Goswami (2011) Multiwalled carbon nanotube-based bi-enzyme electrode for total cholesterol estimation in human serum. *J Exp Nanosci* 6, 84.

3. **Urmila Saxena**, Mitun Charkraborty, Pranab Goswami (2011) Covalent immobilization of cholesterol oxidase on self-assembled gold nanoparticles for highly sensitive amperometric detection of cholesterol in real samples. *Biosens Bioelectron* 26, 3037.

4. **Urmila Saxena** and Pranab Goswami (2012) Electrical and optical properties of gold nanoparticles: applications in gold nanoparticles-cholesterol oxidase integrated systems for cholesterol sensing. *J Nanopart Res* 14, 813.

Abstracts published in conferences

1. **Urmila Saxena** and Pranab Goswami, Development of cholesterol biosensor based on immobilized cholesterol oxidase on silk fiber. 1st International Society Biotechnology Conference, 2008, Gangtok, Sikkim, 28-30 December, 2008. Page no. 15.

2. **Urmila Saxena**, Madhuri Das, Seraj Ahmed and Pranab Goswami, An amperometric cholesterol biosensor based on multiwalled carbon nanotube-nafion-cholesterol oxidase-cholesterol esterase nanobiocomposite. International Conference on Advanced Nanomaterials and Nanotechnology, 2009, IIT Guwahati, Guwahati, Assam, 9-11 December, 2009. Abstract no. E-134.

3. **Urmila Saxena**, Mitun Chakraborty and Pranab Goswami, Gold nanoparticle based cholesterol biosensor. International Conference on Frontiers in Biological Sciences (InCoFIBS-2010), National Institute of Technology Rourkela, 1st to 3rd October 2010. P-139. **(Adjudged as best paper in a category)**.

4. **Urmila Saxena** and Pranab Goswami, Nanomaterials as the electroactive interface for direct electron transfer between redox center of enzyme and electrode in developing cholesterol biosensor. 4th Annual Advances in Biodetection and Biosensors Conference, Hamburg, Germany, 30th June to 1st July, 2011. P-159.